UNIVERSITY OF WARMIA AND MAZURY IN OLSZTYN

Technical Sciences

19(1) 2016

PUBLISHER UWM

OLSZTYN 2016

The Technical Sciences is indexed and abstracted in BazTech (http://baztech.icm.edu.pl) and in IC Journal Master List (http://journals.indexcopernicus.com)

The Journal is available in electronic form on the web sites
http://www.uwm.edu.pl/techsci (subpage Issues)
http://wydawnictwo.uwm.edu.pl (subpage Czytelnia)

The electronic edition is the primary version of the Journal

PL ISSN 1505-4675
e-ISNN 2083-4527

Address
ul. Jana Heweliusza 14
10-718 Olsztyn-Kortowo, Poland
tel.: +48 89 523 36 61
fax: +48 89 523 34 38
e-mail: wydawca@uwm.edu.pl

Ark. wyd. 7,8, ark. druk. 6,5, nakład 85 egz.
Druk – Zakład Poligraficzny UWM w Olsztynie
zam. nr 240

Contents

Biosystem Engineering

Civil Engineering

Geodesy and Cartography

Information Technology

Mechanical Engineering

Technical Sciences, 2016, 19(1), 5–16

UNIWERSYTET WARMIŃSKO-MAZURSKI W OLSZTYNIE

Quarterly peer-reviewed scientific journal
ISSN 1505-4675
e-ISSN 2083-4527
TECHNICAL SCIENCES
Homepage: www.uwm.edu.pl/techsci/

CORRELATIONS BETWEEN GERMINATION CAPACITY AND SELECTED PHYSICAL PROPERTIES OF PERENNIAL RYEGRASS CV. MAJA SEEDS

Zdzisław Kaliniewicz, Krzysztof Jadwisieńczak, Beata Jadwisieńczak, Łukasz Potkaj

Department of Heavy Duty Machines and Research Methodology
University of Warmia and Mazury in Olsztyn

Received 7 November 2015; accepted 5 January 2016; available online 15 January 2016.

Key words: seeds, physical parameters, germination rate index, correlation.

Abstract

Perennial ryegrass is one of the most valuable pasture grasses. The species is recommended for sodding various types of land in Poland due to its fast growth and the ability to produce large numbers of vegetative shoots. Seedling emergence and biomass yield are largely determined by seed quality. This study analyzes the correlations between the basic physical properties of seeds of perennial ryegrass cv. Maja and their germination capacity. The basic dimensions (length, width and thickness) and mass of each of the 150 seeds were determined, and their arithmetic mean diameter, geometric mean diameter, aspect ratio, sphericity index and density were calculated. The seeds were germinated for 14 days, and the results were recorded daily, which enabled to determine germination time for each seed. The relationships between the evaluated parameters were determined by the Student's *t*-test for independent samples and correlation analysis. The analyzed physical properties of seeds had no significant effect on the germination rate index. Germinated and non-germinated seeds differed significantly in width, length and arithmetic mean diameter, but they should not be sorted based on their plumpness to improve the quality of seed material because it could lead to a high loss of viable seeds.

Symbols:

C_g – germination capacity, %,
D_a – arithmetic mean diameter, mm,
D_g – geometric mean diameter, mm,
m – seed mass, mg

Correspondence: Zdzisław Kaliniewicz, Katedra Maszyn Roboczych i Metodologii Badań, Uniwersytet Warmińsko-Mazurski, ul. Oczapowskiego 11/B112, 10-719 Olsztyn, phone: 48 89 523 39 34, e-mail: zdzislaw.kaliniewicz@uwm.edu.pl

R – aspect ratio, %,
T, W, L – seed thickness, width and length, mm,
T_n – time required to produce a healthy germ, days,
T_o – duration of germination test, days,
W_g – germination rate index,
V_g – germinative energy, %,
ρ – seed density, g·cm^{-3},
Φ – sphericity index, %.

Introduction

Grasses belong to the group of wind-pollinated flowering plants. They are highly valued for their environmental significance, and they are an important economic commodity. Grasses are ubiquitous plants that shape the natural landscape. Grasses and forests are abundant sources of biomass which accumulates solar energy and lowers carbon dioxide levels in ambient air. Grasses constitute cheap and nutritious fodder material, in particular for ruminants, and they are indispensable in the production of milk and meat (BARYŁA, KULIK 2005, PROŃCZUK 2005, MOORBY et al. 2006, HOEKSTRA et al. 2007, SURMEN et al. 2013).

Perennial ryegrass (*Lolium perenne* L.), also known as English ryegrass, is one of the most valuable species of pasture grasses. It is a common wildlife species in Poland which is also used in pastures and meadows. Perennial ryegrass is a highly competitive species that dominates over other plants and leads to their elimination under supportive conditions (BARYŁA, KULIK 2005, 2006, 2013, GILLILAND et al. 2011). It thrives in localities with full sun exposure and fertile mineral soils. The species is sensitive to environmental stressors, and its growth is stilted in response to summer droughts and freezing temperatures in winter, but it is capable of resilient regrowth when unfavorable conditions subside. Perennial ryegrass initiates growth in early spring and grows back easily after harvest or grazing. The species is resistant to trampling and nibbling by animals, and it is capable of utilizing manure nitrogen, which is why it is highly recommended for pastures (KULIK et al. 2004, BUMANE, ADAMOVICS 2006, MOORBY et al. 2006, HOEKSTRA et al. 2007, BARYŁA, KULIK 2013, SURMEN et al. 2013).

Perennial ryegrass is widely used to seed lawns that play various roles, including ecological, sanitary, recreational and esthetic (PROŃCZUK 2005, PROŃCZUK, PROŃCZUK 2008, JANKOWSKI et al. 2010, 2012). The key features that determine the suitability of perennial ryegrass for sodding are fast growth and the ability to produce large numbers of vegetative shoots (HARKOT, POWROŹNIK 2010, STARCZEWSKI, AFFEK-STARCZEWSKA 2011, CARVALHO et al. 2013).

Perennial ryegrass is also widely grown for seeds. Seed yield ranges from 225 to 2500 kg ha^{-1}, depending on variety, soil type, soil fertility, fertilization and crop protection regimes, and, most importantly, climate (SZCZEPANEK 2005, BUMANE, ADAMOVICS 2006, NIZAM 2009, ROLSTON et al. 2009, POP et al. 2010, DIMITROVA, KATOVA 2011, CHYNOWETH et al. 2012). Ryegrass seeds are husked kernels, 5–7 mm in length. In Poland, the species ripens in early July when its seeds turn brown-grey and have to be harvested before they fall to the ground (ELGERSMA et al. 1988). Seeds are usually harvested in two stages: the first-cut is left in the field to dry, after which it is threshed in a combine harvested equipped with a pick-up attachment.

There is a general scarcity of published data about the range of changes in the physical properties of grass seeds and the relationships between those parameters. Such information is required for designing and modeling seed sowing, harvesting, transport, cleaning, sorting and storage processes (HEBDA, MICEK 2007, BOAC et al. 2010, KALKAN, KARA 2011, MARKOWSKI et al. 2010, 2013, SOLOGUBIK et al. 2013). The results of laboratory and field experiments performed on other plant species (MUT, AKAY 2010, HOJJAT 2011, NIK et al. 2011, SADEGHI et al. 2011, AHIRWAR 2012, AMIN, BRINIS 2013) indicate that germinative energy and germination capacity are influenced by seed dimensions and seed mass because larger and heavier seeds produce more abundant and denser stands, which contributes to a higher yield. Therefore, an attempt was made in the present experiment to investigate the influence of the mass and geometric properties of grass seeds on germination efficiency.

The aim of this study was to determine the correlations between the basic physical properties of perennial ryegrass seeds and their germination capacity, which are vital parameters for planning and developing seed separation processes.

Materials and Methods

The experimental material comprised seeds of tetraploid perennial ryegrass cv. Maja. The seeds were grown on soils of 4a, 4b and 5 complex in an organic plantation covering an area of 3.75 ha in the Region of Podlasie. The plantation was started in the first 10 days of April 2013 by sowing 38 kg ha^{-1} seeds in soil subjected to various cultivation measures after fall tillage. Manure fertilizer was applied at 40 t ha^{-1} immediately before fall tillage. In October 2013, the field was fertilized with slurry at 10 000 l ha^{-1} after harvest. In spring 2014, the turf was harrowed to stimulate grass tillering and to eliminate weeds. Seeds were harvested in two stages in the first 10 days of September 2014: cut grass was left to dry in the field, after which it was threshed in a combine harvester equipped with a pick-up attachment. Seed yield was determined at 660 kg ha^{-1}. Seed samples of approximately 1 kg were collected, and their physical properties and germination capacity were determined in the Agricultural Analytical Laboratory of the Faculty of Technical Sciences at the University of Warmia and Mazury in Olsztyn. The relative moisture content of seeds was determined at 12.7% with the use of the MAX 5-/WH halogen moisture analyzer (Radwag Radom, Poland).

Batches of 150 seeds each were separated from seed samples by the survey sampling method (GREŃ 1984). The length and width of each seed were determined with the use of the MWM 2325 laboratory microscope (PZO Warszawa, Poland) to the nearest 0.02 mm (one measurement covered two micrometer readings with 0.01 mm resolution), and seed thickness was measured with a dial thickness gauge with 0.01 mm resolution. The measurements were performed in accordance with the methodology described by KALINIEWICZ et al. (2011). Seed weight was determined on the WAA 100/C/2 weighing scales (Radwag Radom, Poland) with 0.1 mg resolution.

Based on the number of seeds in each batch, standard error for the evaluated physical parameters did not exceed: 0.2 mm for seed length, 0.1 mm for seed width and thickness, and 0.2 mg for seed mass.

In the second stage of the experiment, measured data were used to calculate the following parameters for every seed:

– arithmetic and geometric mean diameters, aspect ratio and sphericity index (MOHSENIN 1986):

$$D_a = \frac{T + W + L}{3} \tag{1}$$

$$D_g = (T \cdot W \cdot L)^{\frac{1}{3}} \tag{2}$$

$$R = \frac{W}{L} \times 100 \tag{3}$$

$$\Phi = \frac{(T \cdot W \cdot L)^{\frac{1}{3}}}{L} \times 100 \tag{4}$$

– density (on the assumption that seeds had an ellipsoid shape):

$$\rho = \frac{6 \times m}{\pi \times T \times W \times L} \tag{5}$$

– germination rate index (Kaliniewicz et al. 2015):

$$W_g = \frac{T_o + 1 - T_n}{T_o + 1} \tag{6}$$

In the germination test, perennial ryegrass seeds were placed in a container lined with moistened filter paper and covered with a glass lid. Evaporated water was supplemented daily with a sprinkler, and filter paper was kept moist throughout the experiment. The test was carried out at a temperature of approximately 25°C under exposure to natural light. Germination progress was monitored daily between 8 a.m. and 9 a.m. Seeds that produced a sprout with a minimum length of 75% seed length were classified as germinated. Observations were continued for 14 days (from 23 May to 6 June). Germinative energy V_g and germination capacity C_g were determined based on the ratio of the number of seeds that had germinated in 7 and 14 days (*International Rules for Seed Testing* 2004) to the number of seeds in the analyzed sample.

The results were processed with the use of Statistica PL v. 12.5 application at a significance level of α=0.05. Differences in the physical properties of germinated and non-germinated seeds were determined by the Student's t-test for independent samples, and the relationships between those parameters were evaluated by linear correlation analysis (Rabiej 2012).

Results and Discussion

The physical properties of perennial ryegrass seeds are presented in Table 1. The coefficient of variation ranged from approximately 9% (arithmetic mean diameter) to 94% (germination rate index). Relatively high variation was observed for seed thickness (23%), seed mass (37%) and seed density (25%). Seed thickness was determined in the range of 0.25 to 1.05 mm, seed width – 1.11 to 2.02 mm, and seed length – 4.87 to 8.95 mm. Mean length and mass data indicate that the analyzed seeds were longer (by around 20%) and lighter (by around 10%) than the seeds of perennial ryegrass cv. Bastion grown in Switzerland and examined by Wagner et al. (2001). The seeds analyzed in this study were similar to seeds of tetraploid varieties in terms of average mass and were significantly heavier than the seeds of diploid varieties examined by Pop et al. (2010). They were also 29% heavier than the seeds of perennial ryegrass cv. Veja from Lithuania (Šlepetys 2001), 24% and 30% heavier than the seeds of perennial ryegrass cv. Grasslands Nui and cv. Grasslands Samson, respectively, from New Zealand (Rolston et al. 2005). The above findings indicate that the seeds of perennial ryegrass cv. Maja are similar to seeds of other tetraploid varieties in terms of plumpness. The seeds of the analyzed species were similar in length to the seeds of yellow lupine cv. Mister (SADOWSKA, ŻABIŃSKI 2011), and were similar in thickness to psyllium (AHMADI et al. 2012) and parsnip seeds (KALINIEWICZ et al. 2014). The aspect ratio of perennial ryegrass seeds was determined in the range of 16.42% to 28.43%.

Table 1
Statistical distribution of the physical properties and calculated parameters of perennial ryegrass seeds

Physical property/ parameter	Value			Standard deviation
	minimum	maximum	mean	
T [mm]	0.25	1.05	0.69	0.158
W [mm]	1.11	2.02	1.46	0.182
L [mm]	4.87	8.95	6.90	0.717
m [mg]	0.8	5.9	3.02	1.117
D_a [mm]	2.21	3.68	3.02	0.276
D_g [mm]	1.27	2.33	1.89	0.195
R [%]	16.42	28.43	21.33	2.661
Φ [%]	20.78	36.58	27.59	2.862
ρ [g cm^{-3}]	0.273	1.410	0.827	0.206
W_g [–]	0	0.733	0.209	0.176

The germination test revealed that perennial ryegrass seeds were characterized by very low germinative energy (V_g=11.33%), but relatively high germination capacity (C_g=93.33%). The germination capacity of the analyzed perennial ryegrass seeds exceeded 80% (acceptable germination level), and it was comparable with the values reported by WAGNER et al. (2001) and GRYGIERZEC et al. (2015) for other perennial ryegrass cultivars. However, their germinative energy was approximately 55 percentage points lower than that noted by JODEŁKA et al. (2003) in cv. Ovation. An analysis of seed germination rates (Fig. 1) demonstrated that the first seeds began to germinate already on day 4 of the germination test, but more than 45% of seeds germinated only at the end of the trial on day 13. The above could be attributed to the fact that the husk has a high percentage of total seed mass (ELGERSMA et al. 1988), and it forms an insulation layer that prevents water from reaching the interior of the seed.

The results of the Student's t-test for independent samples (Fig. 2) suggest that germinated and non-germinated seeds differed significantly only in width, length and, consequently, arithmetic mean diameter. In view of those parameters, germinated seeds were somewhat smaller than non-germinated seeds. However, a detailed analysis revealed that perennial ryegrass seeds should not be sorted based on the above attributes. All seed fractions had a high percentage of germinated seeds, therefore, the separation process would lead to a high loss of viable seeds without eliminating non-germinated seeds from the sorted product. Despite an absence of statistically significant differences, germinated seeds were characterized by higher thickness, mass, sphericity index and density, and by lower geometric mean diameter and aspect ratio in comparison with non-germinated seeds.

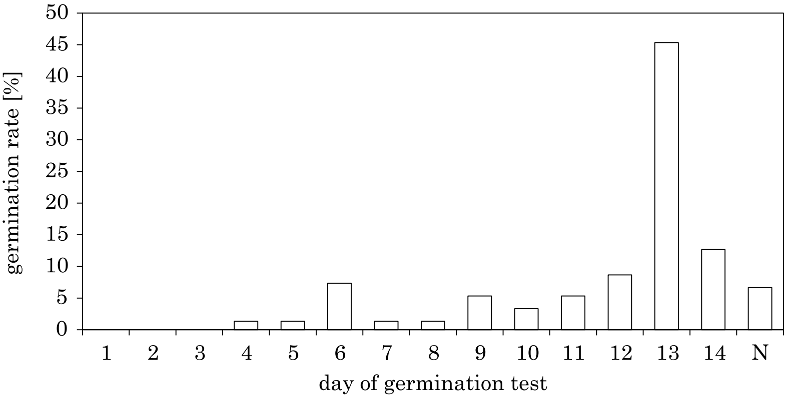

Fig. 1. Germination percentage of perennial ryegrass seeds: N – non-germinated seeds

The strength of linear relationships between selected physical properties of perennial ryegrass seeds is presented in Table 2. Statistically significant correlations between the analyzed parameters were noted in the majority of cases (28 out of 45). The most highly correlated parameters were seed length and arithmetic mean diameter, and in the group of attributes that can be potentially used in separation processes – seed thickness and seed mass. Those results indicate that perennial ryegrass seeds would be most effectively separated with the use of mesh screens with longitudinal openings. The germination rate index was not significantly correlated with any of the evaluated physical properties, which suggests that the analyzed attributes cannot be used to improve the emergence time of perennial ryegrass seedlings. This observation is confirmed by the values of the germination rate index before and after seed samples were divided into three thickness groups of nearly identical size (Fig. 3). The use of mesh screens with longitudinal openings would effectively separate seeds that differ in average mass, but it would not contribute to their germination uniformity. For this reason, the germination efficiency of perennial ryegrass seeds can be improved with the use of chemical, physical and physiological methods, such as seed dressing, soaking in selected chemical solutions, conditioning, irradiation and electromagnetic field stimulation (DANNEBERGER et al. 1992, SCHOPFER et al. 2001, PODLEŚNY 2004, LYNIKIENE et al. 2006, MUSZYŃSKI, GŁADYSZEWSKA 2008, GRZESIK et al. 2012).

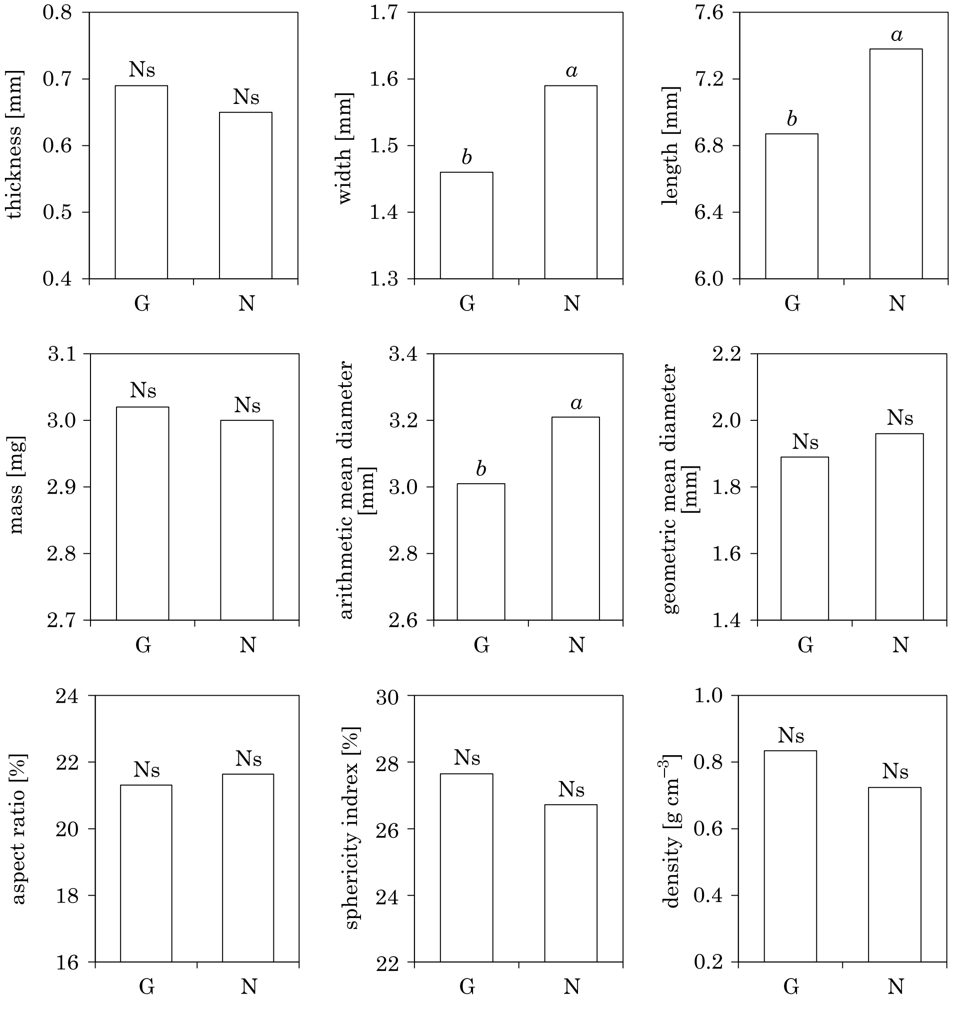

Fig. 2. Significance of differences between the physical properties and calculated parameters of perennial ryegrass seeds: G – germinated seeds, N – non-germinated seeds; *a* and *b* – statistically significant differences, Ns – not significant

Table 2
Coefficients of linear correlation between the physical properties and calculated parameters of perennial ryegrass seeds

Physical property/ parameter	*T*	*W*	*L*	*m*	D_a	D_g	*R*	*Φ*	*ρ*
W	-0.056	1							
Lc	0.021	**0.422**	1						
m	**0.778**	**0.168**	**0.204**	1					
D_a	**0.197**	**0.575**	**0.964**	**0.363**	1				
D_g	**0.785**	**0.472**	**0.528**	**0.761**	**0.711**	1			
R	-0.060	**0.627**	**-0.431**	0.001	**-0.248**	0.027	1		
Φ	**0.772**	0.041	**-0.502**	**0.548**	**-0.278**	**0.462**	**0.486**	1	
ρ	**0.235**	**-0.381**	**-0.335**	**0.562**	**-0.329**	-0.090	-0.090	**0.273**	1
W_g	0.106	-0.092	-0.071	0.102	-0.062	-0.041	-0.041	0.092	0.159

The bold font indicates that the value of the correlation coefficient is higher than the critical value of 0.166.

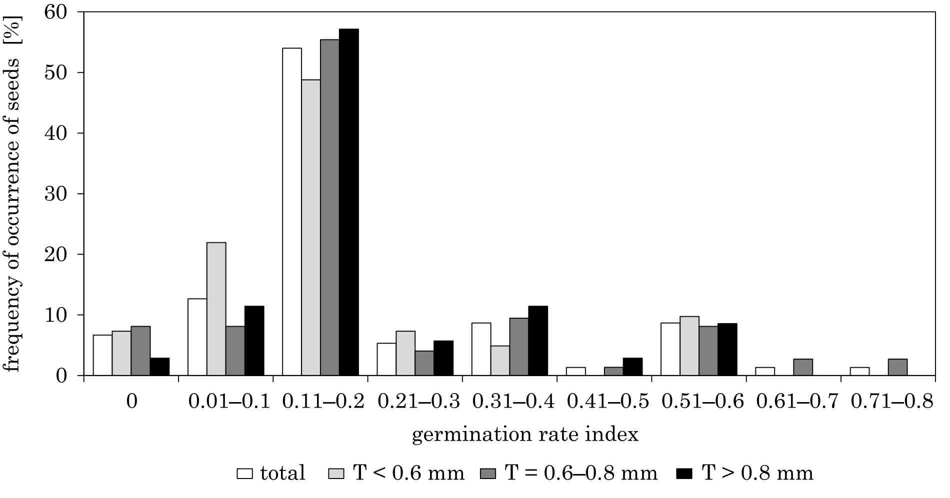

Fig. 3. Germination rate index calculated based on the thickness of perennial ryegrass seeds

Conclusions

1. The analyzed seeds of perennial ryegrass cv. Maja are characterized by very low germinative energy of 11.33%, but relatively high germination capacity of 93.33%. The majority of seeds germinate on day 13 of the germination test.

2. The examined physical properties of seeds, including length, width, thickness, arithmetic mean diameter, geometric mean diameter, aspect ratio, sphericity index and seed density, do not exert a significant influence of the germination rate index. Therefore, seeds should not be separated based on their plumpness as it would not improve the uniformity of seedling emergence.

3. In comparison with non-germinated seeds, germinated seeds are characterized by higher thickness, mass, sphericity index and density, and by lower width, length, arithmetic mean diameter, geometric mean diameter and aspect ratio. Despite those differences, there is no need to eliminate non-germinated seeds from the seed material because it could lead to a significant loss of high-quality seeds.

References

AHIRWAR J.R. 2012. *Effect of seed size and weight on seed germination of Alangium lamarckii, Akola, India*. Research Journal of Recent Sciences, 1: 320–322.

AHMADI R., KALBASI-ASHTARI A., GHARIBZAHEDI S.M.T. 2012. *Physical properties of psyllium seed*. International Agrophysics, 26: 91–93. http://dx.doi.org/10.2478/v10247-012-0013-y.

AMIN C., BRINIS L. 2013. *Effect of seed size on germination and establishment of vigorous seedlings in durum wheat (Triticum durum Desf.)*. Advances in Environmental Biology, 7(1): 77–81.

BARYŁA R., KULIK M. 2005. *Yielding and species composition of sward of chosen pasture mixtures in diverse soil conditions*. Acta Scientiarum Polonarum, Agricultura, 4(2): 17–28 (article in Polish with an abstract in English).

BARYŁA R., KULIK M. 2006. *Persistence and stability of different cultivars of Lolium perenne L. in pasture and meadow sward on peat-muck soils*. Acta Scientiarum Polonarum, Agricultura, 5(2): 5–13 (article in Polish with an abstract in English).

BARYŁA R., KULIK M.A. 2013. *Assessment of the usefulness of selected Lolium perenne L. cultivars for pasture mixtures on peat-muck soils*. Annales Universitatis Mariae Curie-Skłodowska, Lublin, Polonia, LXVIII(2): 12–23 (article in Polish with an abstract in English).

BOAC J.M., CASADA M.E., MAGHIRANG R.G., HARNER III J.P. 2010. *Material and interaction properties of selected grains and oilseeds for modeling discrete particles*. Transactions of the ASABE, 53(4): 1201–1216. http://handle.nal.usda.gov/10113/44454.

BUMANE S., ADAMOVICS A. 2006. *Influence of fertilization rates on Lolium perenne sward photosynthethic characteristics and seed field*. Grassland Science in Europe, 11: 116–118.

CARVALHO A., NABAIS C., ROILOA S.R., RODRÍGUEZ-ECHEVERRÍA S. 2013. *Revegetation of abandoned copper mines: the role of seed banks and soil amendments*. Web Ecology, 13: 69–77. http://dx.doi.org/10.5194/we-13-69-2013.

CHYNOWETH R.J., ROLSTON M.P., MCCLOY B.L. 2012. *Irrigation management of perennial ryegrass (Lolium perenne) seed crops*. Agronomy New Zealand, 42: 77–85.

DANNEBERGER T.K., MCDONALD M.B. JR., GERON C.A., KUMARI P. 1992. *Rate of germination and seedling growth of perennial ryegrass seed following osmoconditioning*. Hortscience, 27(1): 28–30.

DIMITROVA T., KATOVA A. 2011. *Selectivity of some herbicides to perennial ryegrass (Lolium perenne L.), grown for seed production*. Pesticides Phytomedicine, 26(2): 129–134. http://dx.doi.org/10.2298/PIF1102129D.

ELGERSMA A., LEEUWANGH J.E., WILMS H.J. 1988. *Abscission and seed shattering in perennial ryegrass (Lolium perenne L.)*. Euphytica, 39(3) 51–57.

GILLILAND T.J., HENNESSY D., GRIFFITH V. 2011. *Studies into the dynamics of perennial ryegrass (Lolium perenne L.) seed mixtures*. Irish Journal of Agricultural and Food Research, 50: 99–112.

GREŃ J. 1984. *Statystyka matematyczna. Modele i zadania*. PWN, Warszawa.

GRYGIERZEC B., KILIMEK-KOPYRA A., MUSIAŁ K., VOZÁR L., KOWÁR P. 2015. *Comparison of selected cultivars of perennial ryegrass in Green fodder cultivation*. Part I. Fragmenta Agronomica, 32(1): 28–40 (article in Polish with an abstract in English).

GRZESIK M., JANAS R., GÓRNIK K., ROMANOWSKA-DUDA Z. 2012. *Biological and physical methods of seed production and processing*. Journal of Research and Applications in Agricultural Engineering, 57(3): 147–152 (article in Polish with an abstract in English).

HARKOT W., POWROŹNIK M. 2010. *Reakcja wybranych gazonowych odmian Lolium perenne na pogodowe czynniki stresowe w okresie początkowego wzrostu i rozwoju*. Łąkarstwo w Polsce, 13: 65–75 (article in Polish with an abstract in English).

HEBDA T., MICEK P. 2007. *Geometric features of grain for selected corn varieties*. Inżynieria Rolnicza, 5(93): 187–193 (article in Polish with an abstract in English).

HOEKSTRA N.J., STRUIK P.C., LANTINGA E.A., SCHULTE R.P.O. 2007. *Chemical composition of lamina and sheath of Lolium perenne as affected by herbage management*. NJAS – Wageningen Journal of Life Sciences, 55(1): 55–73. http://dx.doi.org/10.1016/S1573-5214(07)80004-2.

HOJJAT S.S. 2011. *Effects of size on germination and seedling growth of some Lentil genotypes (Lens culinaris Medik.)*. International Journal of Agriculture and Crop Sciences, 3(1): 1–5.

International Rules for Seed Testing. 2004. International Seed Testing Association, Zurich.

JANKOWSKI K., CZELUŚCIŃSKI W., JANKOWSKA J., CIEPIELA G.A. 2010. *Effect of aquagel on the initial development of turfgrasses and their aesthetical value.* Journal of Research and Applications in Agriculture Engineering, 55(2): 36–41 (article in Polish with an abstract in English).

JANKOWSKI K., SOSNOWSKI J., JANKOWSKA J., KOWALCZYK R. 2012. *Impact of hydrogel and kind of soil cover on the compactness of turf lawns*. Inżynieria Ekologiczna, 30: 249–256 (article in Polish with an abstract in English).

JODEŁKA J., JANKOWSKI K., CIEPIELA G.A. 2003. *The allelopathic influence of hawkweed (Hieracium pilosella L.) on initial growth of meadow grass (Lolium perenne L.) and red fescue (Festuca rubra L.)*. Biuletyn Instytutu Hodowli i Aklimatyzacji Roślin, 225: 353–358.

KALINIEWICZ Z., JADWISIEŃCZAK K., CHOSZCZ D., KOLANKOWSKA E., PRZYWITOWSKI M., ŚLIWIŃSKI D. 2014. *Interdependence between germination ability and the selected properties of parsnip seeds (Pastinaca sativa L.)*. Inżynieria Rolnicza, 1(149): 39–50 (article in Polish with an abstract in English).

KALINIEWICZ Z., JADWISIEŃCZAK K., MARKOWSKI P., CHOSZCZ D., KOLANKOWSKA E. 2015. *Correlations between the germination capacity and selected physical properties of cultivated radish seeds*. Zemdirbyste-Agriculture, 102(2): 217–222. http://dx.doi.org/10.13080/z-a.2015.102.028.

KALINIEWICZ Z., GRABOWSKI A., LISZEWSKI A., FURA S. 2011. *Analysis of correlations between selected physical attributes of Scots pine seeds*. Technical Sciences, 14(1): 13–22.

KALKAN F., KARA M. 2011. *Handling, frictional and technological properties of wheat as affected by moisture content and cultivar*. Powder Technology, 213: 116–122. http://dx.doi.org/10.1016/j.powtec.2011.07.015.

KULIK M., BARYŁA R., LIPIŃSKA H. 2004. *Winterhardiness of Lolium perenne in pasture and meadow swards on peat-muck soil*. Acta Scientiarum Polonorum, Agricultura, 3(2): 215–220 (article in Polish with an abstract in English).

LYNIKIENE S., POZELIENE A., RUTKAUSKAS G. 2006. *Influence of corona discharge field on seed viability and dynamics of germination*. International Agrophysics, 20: 195–200.

MARKOWSKI M., MAJEWSKA K., KWIATKOWSKI D., MALKOWSKI M., BURDYLO G. 2010. *Selected geometric and mechanical properties of barley (Hordeum Vulgare L.) grain*. International Journal of Food Properties, 13: 890–903. http://dx.doi.org/10.1080/10942910902908888.

MARKOWSKI M., ŻUK-GOŁASZEWSKA K., KWIATKOWSKI D. 2013. *Influence of variety on selected physical and mechanical properties of wheat*. Industrial Crops and Product, 47: 113–117. http://dx.doi.org/10.1016/j.indcrop.2013.02.024.

MOHSENIN N.N. 1986. *Physical properties of plant and animal materials*. Gordon and Breach Science Public, New York.

MOORBY J.M., EVANS R.T., SCOLLAN N.D., MACRAE J.C., THEODOROU M.K. 2006. *Increased concentration of water-soluble carbohydrate in perennial ryegrass (Lolium perenne L.). Evaluation in dairy cows in early lactation*. Grass and Forage Science, 61: 52–59. http://dx.doi.org/10.1111/j.1365-2494.2006.00507.x.

MUSZYŃSKI S., GŁADYSZEWSKA B. 2008. *Representation of He-Ne laser irradiation effect on radish seeds with selected germination indices*. International Agrophysics, 22: 151–157.

MUT Z., AKAY H. 2010. *Effect of seed size and drought stress on germination and seedling growth of naked oat (Avena sativa L.)*. Bulgarian Journal of Agricultural Science, 16(4): 459–467.

NIK M.M., BABAEIAN M., TAVASSOL A. 2011. *Effect of seed size and genotype on germination characteristic and seed nutrient content of wheat*. Scientific Research and Essays, 6(9): 2019–2025. DOI: 10.5897/SRE11.621.

NIZAM Y. 2009. *Effect of nitrogen fertilization on seed yield and some plant characteristics of perennial ryegrass (Lolium perenne L.)*. Journal of Tekirdag Agricultural Faculty, 6(2): 111–120.

PODLEŚNY J. 2004. *The effect of magnetic stimulation of seeds on growth, development and yielding of crops*. Acta Agrophysica, 4(2): 459–473 (article in Polish with an abstract in English).

POP M.R., SAND C., BARBU H., BALAN M., GRUSEA A., BOERIU H., POPA A. 2010. *Correlations between productivity elements in Lolium perenne L. species for new varieties resistant to drought*. Analele Universităţii din Oradea – Fascicula Biologie, XVII(1): 183–185.

PROŃCZUK M. 2005. *Grass endophytes – importance, incidence and methods for detection. Literature review*. Biuletyn Instytutu Hodowli i Aklimatyzacji Roślin, 235: 297–309 (article in Polish with an abstract in English).

PROŃCZUK S., PROŃCZUK M. 2008. *Evaluation of the response of perennial ryegrass (Lolium perenne L.) cultivars to temporary shading in turf maintenance*. Biuletyn Instytutu Hodowli i Aklimatyzacji Roślin, 248: 135–145 (article in Polish with an abstract in English).

RABIEJ M. 2012. *Statystyka z programem Statistica*. Helion, Gliwice.

ROLSTON M.P., MCCLOY B.L., HARVEY I.C., CHYNOWETH R.W. 2009. *Ryegrass (Lolium perenne) seed yield response to fungicides: a summary of 12 years of field research*. New Zealand Plant Protection, 62: 343–348.

ROLSTON M.P., ARCHIE W.J., RUMBALL W. 2005. *Branched inflorescence perennial ryegrass (Lolium perenne L.) – seed yield evaluated in field trials and response to nitrogen and trinexapac-ethyl plant growth regulator*. New Zealand Journal of Agricultural Research, 48(1): 87–92. http://dx.doi.org/10.1080/00288233.2005.9513635.

SADEGHI H., KHAZAEI F., SHEIDAEI S., YARI L. 2011. *Effect of seed size on seed germination behavior of safflower (Carthamus tinctorius L.)*. ARPN Journal of Agricultural and Biological Science, 6(4): 5–8.

SADOWSKA U., ŻABIŃSKI A. 2011. *Influence of mixed sowing of yellow lupine with gymnosperm barley on the selected physical properties of seed*. Inżynieria Rolnicza, 6(131): 187–195 (article in Polish with an abstract in English).

SCHOPFER P., PLACHY C., FRAHRY G. 2001. *Release of reactive oxygen intermediates (superoxide radicals, hydrogen peroxide, and hydroxyl radicals) and peroxidase in germination radish seeds controlled by light, gibberellin, and abscisic acid*. Plant Physiology, 125: 1591–1602. http://dx.doi.org/10.1104/pp.125.4.1591.

SOLOGUBIK C.A., CAMPAÑONE L.A., PAGANO A.M., GELY M.C. 2013. *Effect of moisture content on some physical properties of barley*. Industrial Crops and Products, 43: 762–767. http://dx.doi.org/10.1016/j.indcrop.2012.08.019.

STARCZEWSKI K., AFFEK-STARCZEWSKA A. 2011. *Compactness assessment of selected perennial ryegrass cultivars in lawn turfs*. Fragmenta Agronomica, 28(4): 70–76 (article in Polish with an abstract in English).

SURMEN M., YAVUZ T., ALBAYRAK S., CANKAYA N. 2013. *Forage yield and quality of perennial ryegrass (Lolium perenne L.) lines in the black sea coastal area of Turkey*. Turkish Journal of Field Crops, 18(1): 40–45.

SZCZEPANEK M. 2005. *Stability of Lolium perenne L. cultivated for seed in relation to methods of sowing and row spacing*. Acta Scientiarum Polonarum, Agricultura, 4(2): 101–112 (article in Polish with an abstract in English).

ŠLEPETYS J. 2001. *Changes in the chemical composition of grass seed and stem during the period of ripening*. Biologija, 2: 57–61.

WAGNER J., LÜSCHER A., HILLEBRAND C., KOBALD B., SPITALER N., LARCHER W. 2001. *Sexual reproduction of Lolium perenne L. and Trifolium repens L. under free air CO_2 enrichment (FACE) at two levels of nitrogen application*. Plant, Cell and Environment, 24: 957–965. http://dx.doi.org/10.1046/j.1365-3040.2001.00740.x.

Technical Sciences, 2016, 19(1), 17–26

Quarterly peer-reviewed scientific journal
ISSN 1505-4675
e-ISSN 2083-4527
TECHNICAL SCIENCES
Homepage: www.uwm.edu.pl/techsci/

INFLUENCE OF MOISTURE ON EXTERNAL FRICTION COEFFICIENT AND BASIC PHYSICAL PROPERTIES OF ASTORIA VARIETY WHEAT GRAIN

***Agnieszka Markowska*[1], *Małgorzata Warechowska*[1], *Józef Warechowski*[2]**

[1] Chair of Foundations of Safety
[2] Chair of Process Engineering and Equipment
University of Warmia and Mazury in Olsztyn

Received 28 July 2015; accepted 31 December 2015; available on line 2 January 2016.

Key words: wheat grain, angle of repose, tilting box method, moisture content, coefficient of external friction.

Abstract

This paper analyzed the effect of moisture content on selected physical properties of Astoria variety wheat grain using six levels of grain moisture content (14%, 16%, 18%, 20%, 22% and 24%). The following were determined for each level of moisture content: angle of repose, static angle of repose (SAR), bulk density and thousand kernel weight. The friction coefficients for four different construction materials (CEF) were also determined: acid-resistant steel, wear-resistant steel, plastic (PPLD) and rubber. It was found that an increasing moisture content in grains was accompanied by an increase in the thousand kernel weight, angle of repose, SAR, as well as the CEF against each of the surfaces used in the study. The highest value of the CEF was recorded for a rubber surface (0.782) and the smallest was for a polypropylene surface (0.443). The highest values of the angle of repose and the SAR were recorded for the grain with the highest moisture content: 37.15^{o} and 39.44^{o}, respectively. An increase in the moisture content in kernels reduced their bulk density from 79.870 $kg \cdot hl^{-1}$ (moisture content: 14%) to 68.783 $kg \cdot hl^{-1}$ (moisture content 24%).

Symbols

M – moisture content,
BD – bulk density [$kg \cdot hl^{-3}$],
TKW – thousand kernel weight [g],
μ – coefficient of externalfriction,
α – tilt angle [deg].

Correspondence: Agnieszka Markowska, Katedra Podstaw Bezpieczeństwa, ul. Jana Heweliusza 10, 10-719 Olsztyn, phone: 48 89 524 56 12, e-mail: agnieszka.markowska@uwm.edu.pl

Introduction

Understanding the interaction between biological material and the parts of a machine used for its processing lies at the foundation of the proper design of process installations (KUSIŃSKA 2001, MARKOWSKI et al. 2006). Cereals are of considerable importance in this regard, with wheat being one of the most commonly-grown crops. It accounts for about 29% of the total cereal production output, along with rice (28%) and maize (27%) (DENDY, DOBRASZCZYK 2001). Wheat is also the dominant cereal in Poland. The majority of global wheat production (75% ÷ 78%) is used in food production. Between 16% and 17% is used in industry and the rest is used as reproduction material (PSAROUDAKI 2007).

Physical properties depend on the species and variety, climate conditions, agrotechnical measures and moisture content (AL-MAHASNEHAND RABABAH 2007, MARKOWSKI et al. 2013, WARECHOWSKA et al. 2013). Moisture content in grain considerably affects its physical conditions (TABATABAEEFAR 2003, LASKOWSKI et al. 2005, KARIMI et al. 2009).

Understanding moisture content in grain is very important to engineers designing machines for grain harvesting and pre-processing, because there is sometimes a need to harvest grain with a high moisture content (DRESZER et al. 1998). The basic physical properties of grain are of particular importance, including bulk density, tapped density, angle of repose and static angle of repose (LEE, HERRMANN 1993, SPANDONIDIS, SPYROU 2013). Knowledge of these values is necessary to properly design such devices as: hoppers, intermediate containers and transport devices (KUSIŃSKA 2001, ZOU, BRUSEWITZ 2002). The external friction of grain mass is of particular importance. It is present in all processes to which grain is subjected. A high inconstancy in the value of the coefficient of the friction of bulk materials of plant origin often affects the operation that is being carried out (HORABIK, ŁUKASZUK 2000). Friction is an important factor affecting the course and outcome of processes of transport, storage, cleaning and sorting. Reliable information about its value is necessary in designing agricultural machines and processes (KRAM 2006). The range of friction coefficient values is very wide due to the diversity of materials of plant origin and their physical conditions. The external friction of one material may vary by several hundred percent (KRAM 2006).The aim of the study was to determine the relationships between the main physical properties and the coefficient of external friction of wheat grain and moisture content.

Materials and Methods

Astoria variety winter wheat grain (obtained from the AGRO-PLON Elżbieta Woycicka seed station in Ostróda, Poland) was used as the study material. The grain sample (approx. 18 kg) was cleaned before the measurements. The moisture content in the grain was determined by drying, in accordance with the Polish Standard PN-EN ISO 712:2009. The initial moisture content was 13.87%. The measurements were conducted at 6 levels of moisture content (M) (14%, 16%, 18%, 20%, 22% and 24%). In order to reach the desired moisture content, the grain was humidified in tightly-closed containers with a pre-calculated amount of distilled water. The moisture content was stabilized for 72 hours at 20±2°C and the grain was periodically stirred during the humidification process. Subsequently, the following physical properties of wheat grain were determined:

– static angle of repose (SAR) as per US 3940997 A (the tilting box method);

– angle of repose (AR) as per PN -65/Z-04005;

– bulk density as per PN 73/R-74007;

– thousand kernel weight (TKW) – with the use of an electronic grain counter (LN S 50A, UNITRA CEMI) and a WPE 120 Radwag (PN68/R-74017) electronic scale;

– coefficient of external friction (CEF) – a device with a tilting plate covered with a material of a friction pair (HORABIK et al. 2002).

The grain external friction was determined using four different construction materials, frequently applied in the construction of transporters and containers. These included:

– acid-resistant steel (1.4404);

– wear-resistant steel (1.0562);

– plastic (PPLD);

– rubber – the transport surface of a conveyor belt (a commercial product).

A knob was used to steadily increase the inclination angle of the plate, whose surface was made of the material of a friction pair. When the grain sample started to slide, the angle was read out from the scale of the device. The coefficient of friction was calculated using the formula (SHARMA et al. 2011):

$$\mu = \mathrm{tg}(\alpha) \tag{1}$$

The results were then analyzed statistically. The basic statistical parameters were determined and an analysis of variance was conducted in order to determine how they depend on the moisture content in the material. The statistical calculations were performed with STATISTICA® for Windows v. 10 (StatSoft Inc.). Hypotheses were tested at the level of significance of $p = 0.05$.

Results and Discussion

Table 1 shows the results of measurements of the thousand kernel weight (TKW) and bulk density of Astoria variety wheat grain. The TKW with a moisture content of 14% was 49.69 g and it increased with increasing moisture content. The same tendency was observed by KUSIŃSKA et al. (2010). The TKWat the highest moisture content (24%) was 54.55 g. The TKW at a moisture content between 14–18% did not differ significantly. A similar relationship was observed for moisture content between 20–24%.

Table 1
Thousand kernel weight and bulk density of Astoria wheat grain at different moisture contents

M [%]	TKW [g]				BD [kg · hl^{-1}]			
	$\bar{x}$	min.	max	S	$\bar{x}$	min.	max	S
14*	49.699^{a}	48.333	50.386	0.778	79.870^{a}	79.724	80.057	0.100
16*	49.924^{a}	49.157	50.922	0.653	77.027^{b}	76.810	77.355	0.196
18*	50.957^{ac}	49.251	52.223	1.126	75.322^{c}	74.926	75.584	0.205
20*	52.810^{bc}	50.147	55.980	2.200	74.024^{d}	73.335	75.171	0.440
22*	53.895^{b}	53.092	55.636	1.015	70.938^{e}	70.438	71.391	0.302
24*	54.554^{b}	53.389	57.229	1.549	68.783^{f}	68.265	69.500	0.371

$\bar{x}$ – average value, S – standard deviation;
* averages marked with the same letters in a column do not differ statistically at p = 0.05 (homogenous group)

The measurement results for grain bulk density showed that a 2% change in the moisture content significantly changes density (Tab. 1). The highest bulk density was measured for grain with a moisture content of 14% (79.870 kg · hl^{-1}). Grain humidification steadily decreased its bulk density. The results obtained in the measurements corroborate the findings of TABATABAEEFAR (2003), who found an increase in the moisture content in grain reduced its bulk density.

KOBUS et al. (2010) examined the physical properties of triticale grain and found that the AR and SAR increased with increasing moisture content. The current study found similar relationships – the largest AR and SAR were observed for material with the highest moisture content (Tab. 2). ZOU and BRUSEWITZ (2002) showed that SAR is even lower than AR. In this study, we found that the above relationship occurs when the grain has a moisture content of less than 22%. At the highest grain moisture content (22–24%), the SAR values were lower than AR. This may indicate a decisive change physical mechanism of friction. As with bulk density, a 2% change in moisture content caused a statistically significant change in the SAR across the entire range of moisture content values under study. The AR changed significantly across nearly the entire moisture content range under study. Only at the highest grain moisture content (22–24%) did the AR change slightly (while the general tendency was maintained) and its values formed a homogeneous group.

Table 2
The angle of repose and the static angle of repose for Astoria wheat grain with different moisture contents

M [%]	Static angle of repose [°]				Angle of repose [°]			
	$\bar{x}$	min.	max	S	$\bar{x}$	min.	max	S
14	28.2^{a}	27.8	28.5	0.238	30.8^{b}	30.5	31.6	0.392
16	29.8^{b}	29.2	30.6	0.514	31.8^{c}	31.2	32.4	0.335
18	30.6^{c}	30.3	30.9	0.179	34.1^{d}	32.8	34.6	0.584
20	32.6^{d}	32.1	33.3	0.314	35.1^{e}	34.1	35.5	0.563
22	38.0^{e}	37.2	38.8	0.525	36.9^{a}	36.5	37.6	0.477
24	39.4^{f}	38.7	40.0	0.488	37.2^{a}	36.5	37.6	0.411

$\bar{x}$ – average value, S – standard deviation;
* averages marked with the same letters in a column do not differ statistically at p = 0.05 (homogenous group)

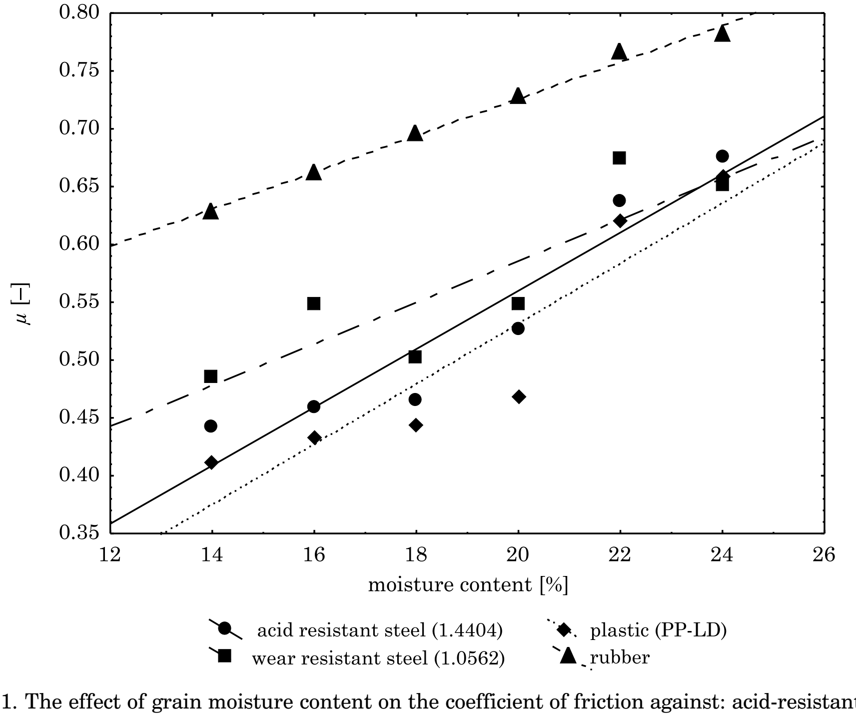

Fig. 1. The effect of grain moisture content on the coefficient of friction against: acid-resistant steel (1.4404), wear-resistant steel (1.0562), plastic (PPLD) and rubber

Kram (2006) found that the CEF of grain against different materials changed along with different grain moisture contents. This relationship was confirmed for each friction pair under study. The weakest friction interactions occurred between grains of Astoria wheat and a PPLD board (Fig. 1). Slightly stronger friction was present between the wheat grains and a stainless steel plate (1.4404).

As with the other friction pairs, the CEF of grain against a sheet of wear-resistant steel (1.0562) increased with increasing moisture content in grain. However, another variability was observed, which could not be explained on the basis of this experiment. The highest CEF was observed between grain and rubber, which is the standard working surface in belt conveyors.

The study also found that the CEF of Astoria wheat grains against each of the surfaces under study increased with increasing moisture content. The changes in the CEF values between grain and rubber (Fig. 1) were smaller than in the other friction pairs. According to the literature data, a change in the grain moisture content does not greatly affect the CEF between grain and a wooden surface (Kram 2006). The effect of changing moisture content on the CEF between grain and steel sheets and a polypropylene surface was similar (and was greater than for rubber). The results of a regression analysis for each of the physical features are shown in Figs. 2–5.

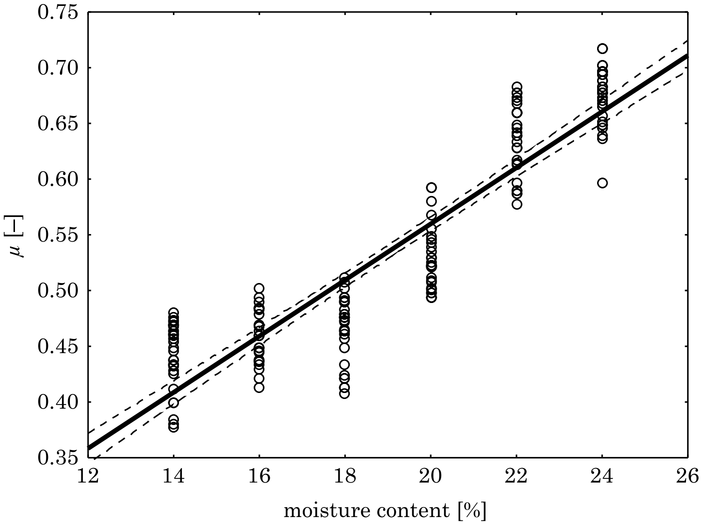

Fig. 2. The effect of grain moisture content on the friction of grain against an acid-resistant steel surface (1.4404)

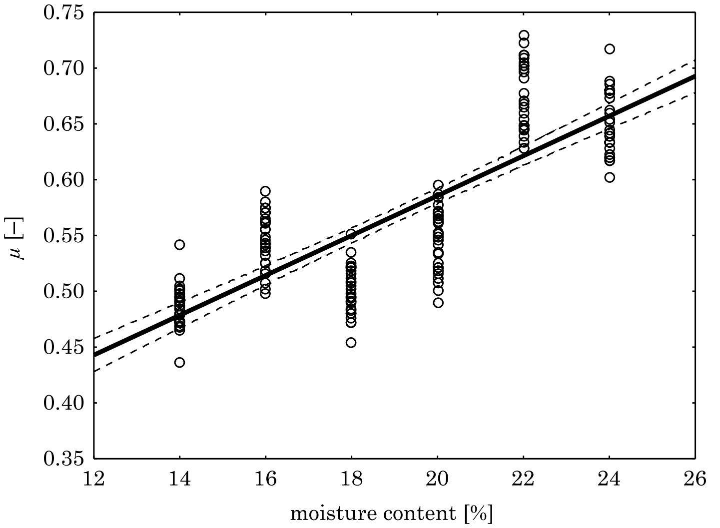

Fig. 3. The effect of grain moisture content on the friction of grain against awe ar-resistant steel surface (1.0562)

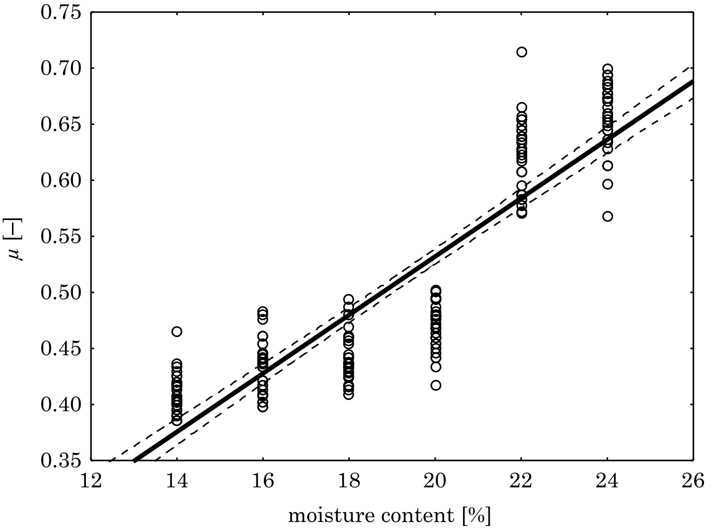

Fig. 4. The effect of grain moisture content on the friction of grain against a plastic surface (PPLD)

The equations describing the relationship between the CEF Astoria variety wheat grains and other surfaces are presented in Table 3. It also contains the correlation coefficients for each of the equations. The linear correlation coefficient between the grain moisture content and the CEF was high for each of the friction pairs under study. Its values were above 0.800, with a level of significance of p<0.0503.

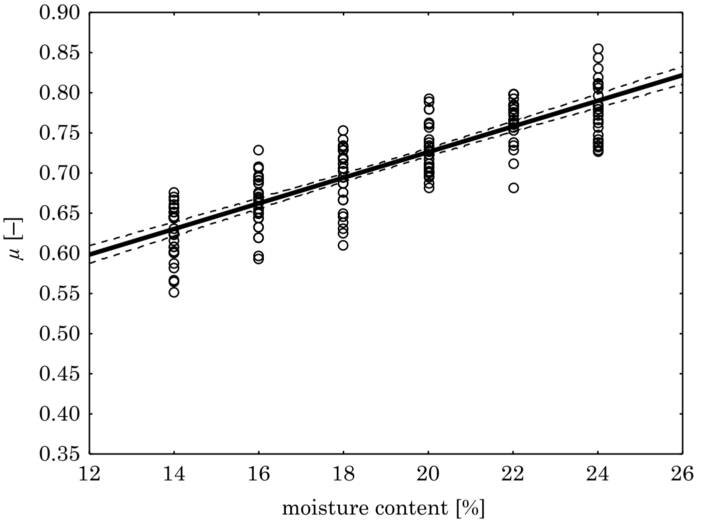

Fig. 5. The effect of grain moisture content on the friction of grain against a rubber surface

Table 3

The relationship between coefficient of friction of Astoria variety wheat grain against construction materials and moisture content

Material of the friction pair	Regression equation	Correlation coefficient for the adopted equation of regression
PPLD	$\mu = 0.011 + 0.026 \cdot \mathrm{M}$	$r = 0.893$
Steel 1.0562	$\mu = 0.229 + 0.018 \cdot \mathrm{M}$	$r = 0.811$
Steel 1.4404	$\mu = 0.056 + 0.025 \cdot \mathrm{M}$	$r = 0.905$
Rubber	$\mu = 0.407 + 0.016 \cdot \mathrm{M}$	$r = 0.855$

Coefficients of correlation statistically significant at $p < 0.0503$

The regression equation coefficients indicate that grain moisture affects the CEF of PPLD the most – over 95% of the value of the coefficient is associated with the moisture content (Fig. 1 and Tab. 3). The effect of grain moisture is two times greater than if in a pair of friction is molded plastic (KARIMI et al. 2009). The value of the intercept in the reported studies is 3 times smaller than in the case of pressed plastic obtained by KARIMI et al. (2009).

The grain moisture content affects the CEF against a rubber surface to the least extent (Fig. 5). In this case, the constant (0.407) which is part of the regression function, accounts for over 50% of the value (Tab. 3). Among the studied friction pairs, an increase in grain moisture had the least impact on CEF for wheat-rubber.

This is an advantage when considering that rubber is used as a standard working surface for conveyor belts. A slightly different friction correlation function for the friction of different wheat varieties of grain against a rubber surface was obtained by KRAM (2006). Compared to the plywood friction coefficient (KARIMI et al. 2009), rubber improved the friction pair for wheat grains. Moreover, CEF with plywood, when compared to rubber, was less dependent on grain moisture changes.

If steel is used as the friction surface, a change in moisture content from 14% to 24% increases the CEF by 37% for 1.0562 steel (Fig. 3) and 62% for 1.4404 acid-resistant steel (Fig. 2). For 1.4404 steel, the change in grain moisture had a 30% greater effect than galvanized steel friction (KARIMI et al. 2009). The value of the intercept in the correlational equation was three times smaller than that obtained for galvanized steel. The effect of changes in grain moisture on the coefficient of friction against 1.0562 steel is the same as in the case of galvanized steel (KARIMI et al. 2009) but the intercept values are greater than 0.05.

Conclusions

The coefficients of friction against rubber are significantly higher than those of grain against steel sheets or polypropylene, regardless of grain moisture content and they change the least with changing moisture content. The CEF of Astoria variety winter wheat increases in a linear manner with increasing grain moisture content. The thousand kernel weight, the angle of repose and the static angle of repose increase with an increasing moisture content in Astoria wheat grain. An increase in the moisture content in Astoria variety winter wheat results in a decrease in its bulk density.

References

AL-MAHASNEH M.A., RABABAH T.M. 2007. *Effect of moisture content on some physical properties of green wheat.* Journal of Food Engineering, 79: 1467–1473.

DENDY D.A., DOBRASZCZYK B.J. 2001. *Cereals and cereal products. Chemistry and technology*. Aspen Publishers, Inc. Gaithersburg, Maryland, p. 13.

DRESZER K., GIEROBA J., ROSZKOWSKI A. 1998. *Kombajnowy zbiór zbóż.* IBMER, Warszawa.

HORABIK J., ŁUKASZUK J. 2000. *Pomiar kąta tarcia wewnętrznego ziarna pszenicy metodą trójosiowego ściskania*. Acta Agrophysica, 37: 39–50.

HORABIK J., RUSINEK R., MOLENDA M., STASIAK M. 2002. *Wpływ wybranych parametrów na właściwości cierne ziarna.* Technica Agraria, 1(2): 81–87.

KARIMI M., KHEIRALIPOUR K., TABATABAEEFAR A., KHOUBAKHT G.M., NADERI M., HEIDARBEIGI K. 2009. *The effect of moisture content on physical properties of Wheat.* Pakistan Journal of Nutrition, 8(1): 90–95.

KOBUS Z., GUZ T., KUSIŃSKA E., NADULSKI R., OSZCZAK Z. 2010. *Wpływ wilgotności na wybrane właściwości fizyczne pszenżyta odmiany Pawo*. Inżynieria Rolnicza, 3 (121): 61–67.

KRAM B.B. 2006. *Badania współczynnika tarcia zewnętrznego ziarna zbóż w funkcji wilgotności*. Inżynieria Rolnicza, 3(78): 175–182.

KUSIŃSKA E. 2001. *Wpływ przechowywania na właściwości fizyczne ziarna owsa*. Acta Agrophysica, 58: 105–114.

KUSIŃSKA E., KOBUS Z., NADULSKI R. 2010. *Wpływ wilgotności na właściwości fizyczne i geometryczne ziarna żyta odmiany słowiańskie*. Inżynieria Rolnicza, 4(122): 151–156.

LASKOWSKI J., ŁYSIAK G., SKONECKI S. 2005. *Mechanical properties of granular agro-materials and food powders for industrial practice*. Part II. *Material properties for grinding and agglomeration*. Institute of Agrophysics PAS, Lublin, p. 29, 30.

LEE J., HERRMANN H.J. 1993. *Angle of repose and angle of marginal stability: molecular dynamics of granular particles*. Journal of Physics, A, Mathematical and General, 2(26): 373–383.

MARKOWSKI M., KONOPKA I., CYDZIK R., KOZIROK W. 2006. *The effect of air temperature on the kinetics of drying and the quality of dried malting barley*. Annual Review of Agricultural Engineering, 5(1): 41–49.

MARKOWSKI M., ŻUK-GOŁASZEWSKA K., KWIATKOWSKI D. 2013. *Influence of variety on selected physical and mechanical properties of wheat*. Industrial Crops and Products, 47: 113–117.

PSAROUDAKI A. 2007. *An extensive survey of the impact of tropospheric ozone on the biochemical properties of edible plants*. WSEAS Transactions on Environment and Development, 3(6): 99–110.

SHARMA V., DAS L., PRADHAN R.C., NAIK S.N., BHATNAGAR N., KUREEL R.S. 2011. *Physical properties of tung seed: an industrial oil yielding crop*. Industrial Crops and Products, 33(2): 440–444.

SPANDONIDIS C.C., SPYROU K.J. 2013. *Micro-scale modeling of excited granular ship cargos: A numerical approach*. Ocean Engineering, 74: 22–36.

TABATABAEEFAR A. 2003. *Moisture-dependent physical properties of wheat*. Int. Agrophysics, 17: 207–211.

WARECHOWSKA M., WARECHOWSKI J., MARKOWSKA A. 2013. *Interrelations between selected physical and technological properties of wheat grain*. Technical Sciences, 16(4): 281–290.

ZOU Y., BRUSEWITZ G.H. 2002. *Flowability of uncompacted marigold powder as affected by moisture content*. Journal of Food Engineering, 55: 165–171.

Technical Sciences, 2016, 19(1), 27–39

Quarterly peer-reviewed scientific journal
ISSN 1505-4675
e-ISSN 2083-4527
TECHNICAL SCIENCES
Homepage: www.uwm.edu.pl/techsci/

THE ENVIRONMENTAL MANAGEMENT SYSTEM IN A BUILDING COMPANY IN THE ASPECT OF THE REQUIREMENTS OF THE PN-EN ISO 14001:2015-09 STANDARD

***Jolanta Harasymiuk*[1], *Natalia Ciak*[1], *Beata Ferek*[1], *Andrzej Rudziński*[1], *Jan Tyburski*[2], *Lucyna Korona*[3]**

[1] Department of Building Engineering, Faculty of Geodesy, Geospatial and Civil Engineering
[2] Foreign Language Studies, English Language Section,
University of Warmia and Mazury in Olsztyn
[3] Department of Architecture, Construction and Spatial Economy,
University of Economy in Bydgoszcz

Received 3 September 2015; accepted 28 December 2015; available on line 2 January 2016.

Key words: environmental management system, PN-EN ISO 14001:2015-09, process approach, building enterprise.

Abstract

The article presents the environmental management system in a building company from the process perspective which meets the requirements of the international ISO 14001 standard. A new issue of this document from September 2015 introduced essentials changes in the attitude of building the system, its structure and in ways of documentation. The article is to precede an attempt of working out the criteria and parameters of the effectiveness of the assumed structure of processes, which will be a subject of next article. In the first part of the article, the justification for using the process approach in building the environmental management system was depicted – the modern concept which determines the effectiveness of action. The second part presents the theoretical model of the process structure of the environmental management system, which when adopted to the needs of a given building company may become a basis for the preparation of an effective system in practice.

Correspondence: Jolanta Harasymiuk, Zakład Inżynierii Materiałów i Procesów Budowlanych, Uniwersytet Warmińsko-Mazurski, ul. J. Heweliusza 4, 10-724 Olsztyn, phone: 48 89 523 47 27, e-mail: jolanta.harasymiuk@uwm.edu.pl

Introduction

One of the challenges faced by modern building practice is a system based approach to the issue of sustainable development, understood as a legal requirement and a necessity in a civil society. The practical realization of this concept should not only be restricted to the design of eco-friendly and energy saving buildings, but it should also involve a change of attitude of building companies in regards to environmental care. The tool, which fosters the limitation of the influence of processes and products used by a building company on the environment, and which rationalizes the utilization of environmental resources and its advantages, which is the environmental management system based on the requirements of the international ISO 14001 standard.

The problem of the creation of an environmental system in a building company has not been described sufficiently. In the literature on the issue, there are only general points, such as e.g. the formal requirements for environmental management systems in production organizations (EJDYS et al. 2012, ŁADOŃSKI et al. 2005, URBANIAK 2004), the development of the environmental management system and the stages of its introducing (LISOWSKA-MIESZKOWSKA 2007, ŁUCZKA-BAKUŁA 2009, MATUSZAK-FLEJSZMAN 2011, MISZTAL, JASIULEWICZ-KACZMAREK 2014, NIEMIEC et al. 2012). There is also a shortage of publications enabling to work out the practical aspects of an environmental management system. At the same time the specific operational features of a building company bring the realization that the undertaking is more difficult than in the case of industrial enterprises. From the analysis of the present state of best practices organizational external conditions have an adverse impact on this realization (instability of legal and financial environment of building companies, low profitability of building production, etc.) and internal conditions (the lack of engagement of the company's CEOs in introducing a system and making it work, the low motivation of the mid-level managerial staff to undertake tasks exceeding the scope of past duties). The difficulties to correctly interpret the requirements of the ISO 14001 standard are frequent occurrences in building companies.

Characteristics of the process approach in creating the environment management system

The environmental management system issues from the quality management system[1]. In the literature on the subject, there are numerous definitions

[1] Because of the popularity of the ISO standards of the 9000 series it was decided to implant this concept in the sphere of environment protection in businesses.

of the system. According to the authors, it may be described as an intentionally designed and organized material, information and energy system, which is applied by a building company, and is used to make products and achieve the environmental goals which the firm is obliged to meet.

The basis of building the system may constitute the international standard, defining the necessary requirements to be met by the system and being a reference document in the process of its certification. In September 2015 the third edition of the standard was issued, which introduced important changes of the concept, as compared to its earlier publications (1996, 2004).

The foundation of the PN-EN ISO 14001:2015-09 standard is a model using the cycle of organized activities „Plan-Do-Check-Act" (PDCA), in which special duties connected with supporting of the environmental management in an organization are attributed to the CEOs (JASIULEWICZ-KACZMAREK, MISZTAL 2014). On the basis of a model of the system shown in Figure 1, which is very general and assumes that it should fit an organization of any kind and size, a building business ought to work out its own environmental system.

From the qualitative research done by the authors on real systems and according to (JASIULEWICZ-KACZMAREK, DROŻYNER 2013), it can be concluded that the effectiveness of the operations of the system depends on the method used in its design. In accordance with the process approach, which is recommended in the PN-EN ISO 14001:2015-09, mandatory in the Polish version of ISO 9001 standard 2008 and its amendments or the modern concepts of Total quality management (TQM), each organization, among them also a building enterprise, is a set of processes. According to the PN-EN ISO 14001:2015-09 standard, the process should be understood as a succession of interrelated or interacting activities which transforms inputs into outputs. The elements of the input can be constituted by e.g. the requirements of the investor determined in the offer query or in the contract and an attached documentation, legal requirements stated in the building standards and building law, work objects, binding principles of procedures in the course of a processor financial resources for its realization. The elements of an output can consist of: products of a building company (expenditure and/or organizational documentation of construction, building work, object elements, the entire object or a set of objects of a given building task, environmentally-adverse waste materials).

According to the authors, the process approach should be understood as an identification and linkage of all the key processes for the realization of products of building enterprises, and their inclusion into the environmental management system.

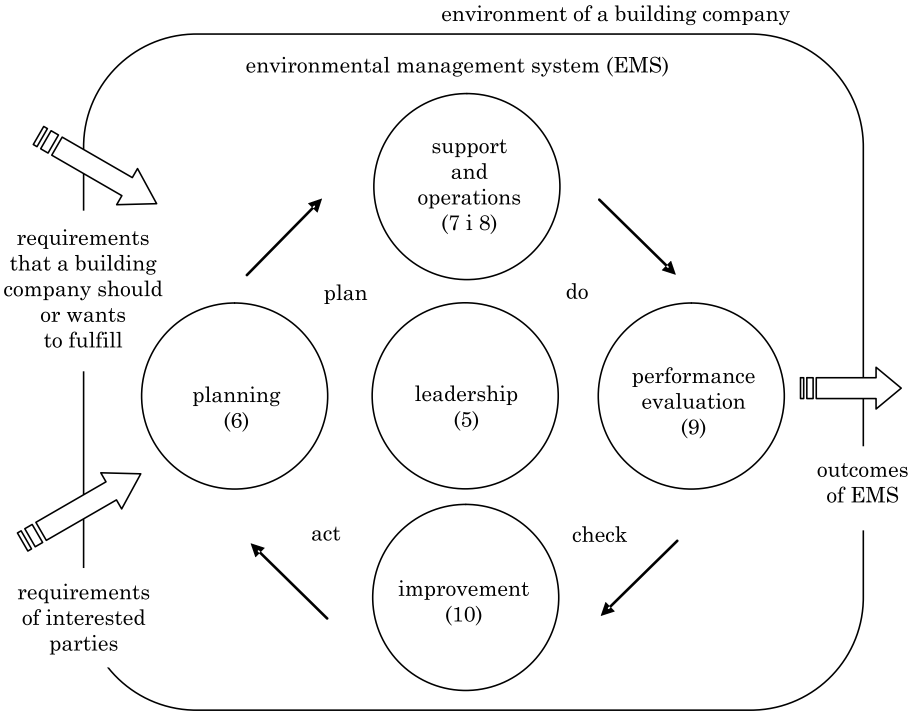

Fig. 1. The model of the environmental management system based on the Deming's cycle „Plan-Do--Check-Act"
Source: elaborated by the authors on the basis of PN-EN ISO 14001:2015-09.

All the processes to be planned according to all the requirements of the ISO 14001 standard applicable to this process, each process to have determined goals, and the effectiveness of its realization is to be monitored. Additionally, the amended ISO 14001 standard [ISO 14001 Revision ...] emphasizes the need for process planning with the consideration of threats and opportunities for the realization of the enterprise's business goals (FAHMI, GREENWOOD 2015, ZYMONIK et al. 2013).

A general model of the environment management system in a building company

A general model of the system was prepared for a medium-sized private enterprises, whose objective of operations is realization of building work and buildings objects.

The structure of the environmental management system is made up of processes and relations between them. A set of processes should embrace all essential processes on different levels of the hierarchy, because omitting some of them may result in dysfunction of the entire system (KARAPETROVIC 2002). A set of relations between processes should determine their order and mutual influence. In the structure of processes (Fig. 2), the following groups of processes may be distinguished: basic, auxiliary, managerial and maintaining the system of environmental management.

As the main processes are considered those indirectly connected to the realization of building tasks, creating so-called added value for an enterprises. These are processes conventionally called PP-1 – Obtaining an offer and signing a contract, PP-2 – Preparation of building activities and PP-3 – Realization of building activities with regard to the needs of environment protection. Each of these above-mentioned processes is a complex process, in which together with the activities characteristic for building operation, these which are required by the ISO 14001 standard are realized.

The PP-1 is a succession of interconnected activities which aim at obtaining an offer/order for construction works and at concluding a contract, which realization will fulfill the expectations of the customer (an investor, a general contractor) and will observe the regulations, as well as will prove advantageous for the enterprises.

The PP-2 process encompasses all the planned activities which are indispensable to create adequate conditions for completion of construction works.

The activity required in the course of the PP-1 and PP-2 processes from the viewpoint of the needs of the environmental system is identification and review of the requirements of environment protection, accompanying the realization of the planned building work. The following points should be registered by an authorized person: national and local environmental regulations, the investor's requirements as well as those of co-operators and other parties involved.

The nation-wide requirements are defined by parliamentary acts, decrees and instructions on environment protection which are passed by the Polish parliament, issued by the Cabinet and ministers. The local requirements may be given by resolutions, ordinances or decisions issued by local authorities (e.g. through a local land use planning, decisions of constructing conditions and terrain use, decisions permitting the felling of trees' and bushes', etc). The investor's requirements may be determined in a contract or a report on the impact of the undertaking on the environment. The requirements connected to the scope and form of environmental documentation may be also determined by a general contractor who is responsible for the entirety of work on a building site. All the identified requirements must be reviewed with the goal of elimination of possible discrepancies between the recognized requirements

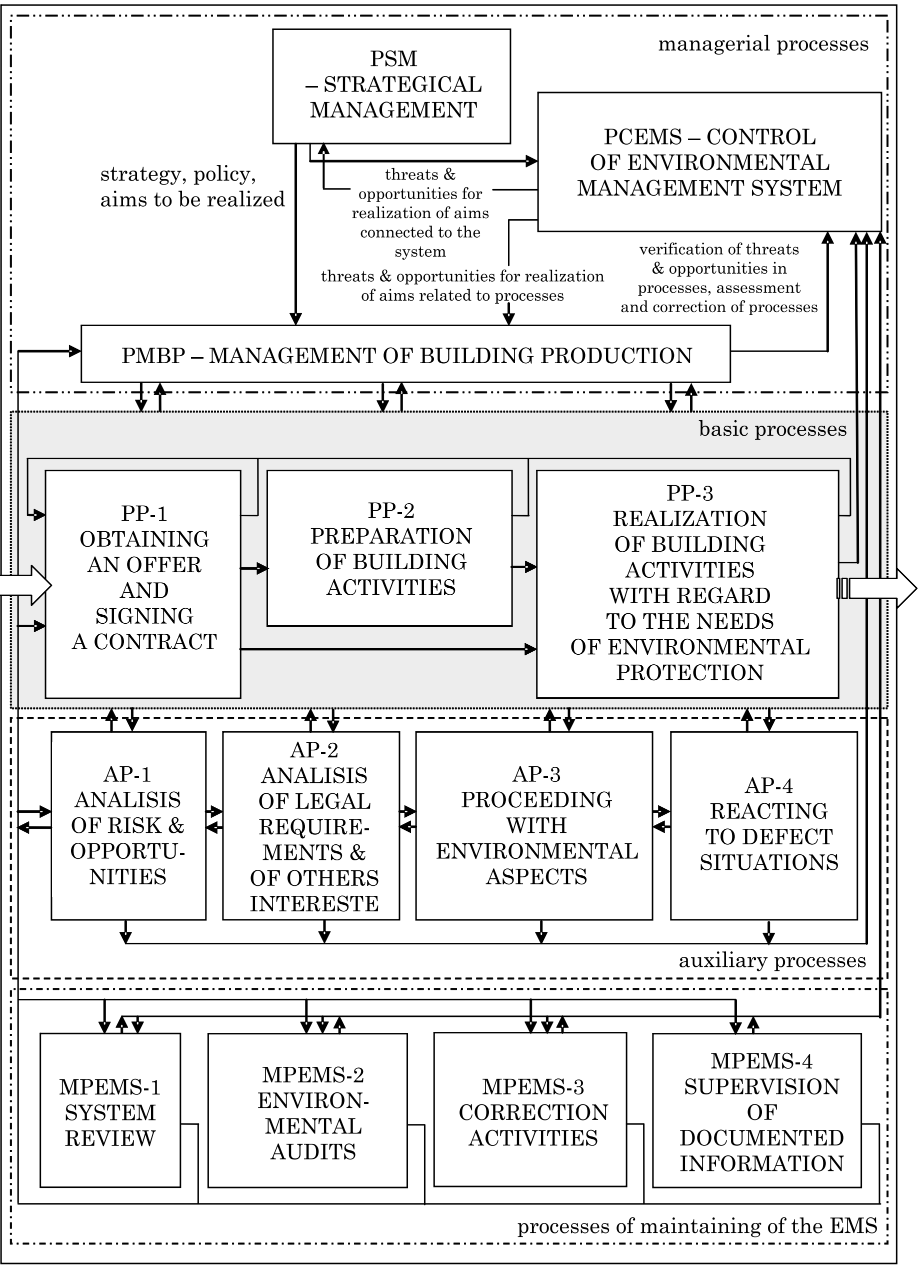

Fig. 2. A general model of the structure of processes in the environmental management system of a building enterprise
Source: elaborated by the authors.

on the preparation stage of building activities, and those determined earlier (on the stage of signing a contract or accepting an offer of building work). According to the assumed course of the PG-2 process, prior to the initiation of a new building activity, the environmental aspects (referred to in the literature also as environmental problems)[2] should be determined, which issues from an adopted organization and technology of realization of building work. Building activities may impact on the environment in many ways. The potential environmental outcomes are among other things: soil contamination, ground water pollution, noise, vibrations and offensive smells, usage of electrical energy, of water and natural raw materials, water, air, road and street contamination by the means of transport working on a building site, damage or the destruction of trees and shrubs. A register of environmental aspects for new building activities should be using the earlier prepared enterprise aspect register. For the aspects which lack in the register, identification cards of new environmental aspects should be worked out. A specimen of an exemplary card assigning environmental aspects to the processes being realized on a building site, on working operation or technological measures, is shown in Figure 3. The prepared criteria may apply to: legal and interested parties' requirements, costs, threats/opportunities for the principal activity of an enterprise, etc. An example of a form of the assessment of the significance of environmental aspects is shown in Table 1.

The PP-3 process – Realization of building activities with consideration of the requirements of environmental protection is a succession of organizational and technical actions, which are indispensable for the fulfillment of the requirements that are set by the binding contract, the design documentation and legal regulations. The process encompasses these actions:

a) specific for the building trade, and among these:

– organizing of operational management staff of building work,

– initiating activities issuing from the project documentation and work schedule,

– organizing of work for teams and gangs performing the building work,

– distribution of means of production,

– supervision of work done,

– technical inspection and acceptance of work,

– accounts settlement of the work done,

– the final acceptance of the building task, taking over of work/a building in a guarantee service;

b) required by the formalized system of environmental management, and among these:

[2] An environmental aspect – an element of activities of a building enterprises or its products, which may mutually react with the environment.

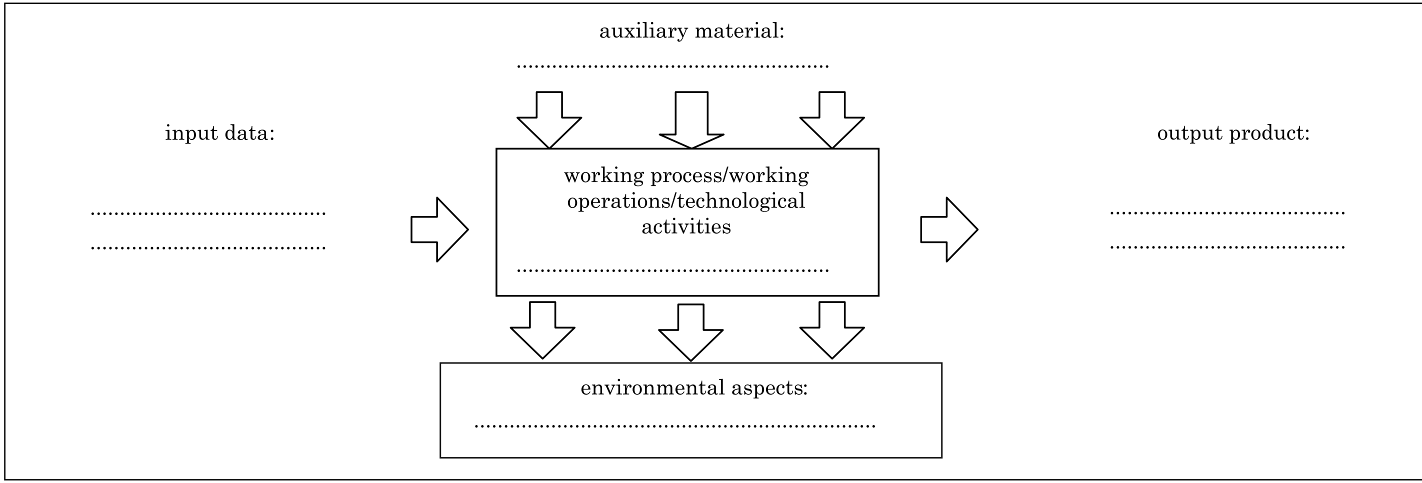

Fig. 3. An example of a card for identification of environmental aspects

Source: the authors own studies.

Table 1

An example of a form for registration and assessment of envionmental aspects

No	Environmental aspect	Working process/ working operation/ technological activity connected with the aspect	Impact of the aspect for environment	Criteria of aspect assessment					Assessment of the aspect (product significance)	Actions taken
				legal requirements	opinion of the interested parties	costs	occurence of break-down situation	opportunities for the building enterprise connected with the aspect		
1	2	3	4	5	6	7	8	9	10	11

Source: the authors own studies.

– review of environment requirements connected to the building work,

– recognition of new processes/operations or technological activities, which occurred during the construction works, and preparing for them identification cards as well as an assessment of environmental aspects,

– preparing an instruction of operational activities, which require particular principles of proceeding,

– signing a contract on using the environment (e.g. picking up building waste material – unless the investor was made obliged by the contract to take the responsibilities of producer of these waste materials on drawing water, on removing sewers, on supplying electrical energy and heat, etc.),

– giving over to the subcontractors of specialized work information materials on the environmental management system,

– organizing trainings for workers and subcontractors on the principles of the system operation and on the proceeding in the case of break-downs,

– controlling of observation of the instruction on operational actions and of the realization of the elaborated environmental programmes.

Among the processes, which support the functioning of the main ones in the environmental management system of a building enterprise can be distinguished:

1. AP-1 – Analisis of risks and opportunities. The process relies on an systematic approach to avoiding of losses (through: identification, assessment and determining possible variants of handling risk) and on taking an opportunity of advantageous situations for a company.

2. AP-2 – Proceeding with environmental aspects. This process encompasses a succession of correlated activities, such as: recognition of environmental aspects connected to enterprise's activities in the past and its present activities (among these, the aspects related to: the processes performed directly on a building site and to the auxiliary processes, which though not connected to the building work itself, but without which the performance of the work would not be possible or would not fulfill the technical requirements), preparation of an enterprise-wide list of identified environmental aspects, making an assessment of their significance according to the settled criteria, preparation of a list of essential environmental aspects[3] and informing the employees involved in the realization of enterprise's processes about them, bringing up to date of lists according to the needs – before the introduction of the following items: new technologies, new operational techniques and before each new building work, monitoring of significant environmental aspects.

[3] An essential aspect – an aspect recognized according to the criteria used in an enterprise as essentially effecting the environment.

3. AP-3 – Identification of legal requirements and of others. This process encompasses a succession of correlated activities, consisting of recognition and registration of all the environmental requirements connected to the enterprise operation and to the realized building work, with a special consideration for requirements of the interested parties.

4. AP-4 – Reaction to the break-down situation[4]. This process encompasses a succession of activities, such as: recognition of a potential break-down situation, working out of an instruction of proceeding in a break-down situation and submitting them for checking or validation by an authorized person(s) or institution (Fire Brigade, Environmental Protection Inspector), conducting instructional training at the workplace for the workers and the subcontractors of any specialized work, making a periodical evaluation of workers' preparation for a defect situation through doing practical exercises under simulated conditions, and the verification of actions on procedures after an occurrence of accidents or break-down situations.

The main processes, except for the mutual correlation ensuring the flow of information, must be linked with the process of management of a set of all the simultaneously planned and realized offers for building work. This process may be conventionally called PMBP – Management of building production. It encompasses activities related to the distribution of tasks and resources, to the assessment of their realization and usage, as well as to the undertaking of preventive action, eliminating sources of potential problems.

The second of the management processes, conventionally called PSM – Strategic management encompasses all the systematic activities related to: the determination of strategy and environmental policy, the management of development undertakings and changes issuing form the adopted strategy, the acceptance of accepted goals for the processes and the en tire enterprises as well as the settlement of principles of assessment of their realization.

Apart from the above-mentioned management processes, one more process should be distinguished, which is related to the managerial staff of the highest rank in the structure of processes of the environmental management system. This is a PCEMS – Control of the environmental management system. Its aim is to ensure an effective operation of the system in such a way so that an environmental policy will be realized. This process encompasses activities related to: identification and recommendation to appropriate people of threats and opportunities connected with system/business goals/ processes as well as establishing the proceeding principles in the course of processes and formalization of these principles.

[4] A break-down situation – a sudden event, which caused a serious threat to the environment (e.g. a leakage of oil derivate substance to the soil).

The processes of maintaining of the environment al management system consist of:

1. MPEMS-1 – Review of the environmental management system. This process embraces a succession of activities related to the assessment of the consistence of the operations of the environment al management system with the requirements of the ISO 14001 standard. It also assesses the consistence of legal regulations, as well as of the requirements of the parties involved and the own requirements of a building enterprise.
2. MPEMS-2 – Audits of the environmental management system. This process may be described as a succession of activities embracing: planning, conducting and reporting of the effects of audits realized in an enterprise and on building sites, which are to verify whether the activities related to environment protection and their results are in accordance with the planned ones.
3. MPEMS-3 – Correction activities. This process can be described as a succession of activities encompassing: initiation and realization by authorized people of correction activities of detected internal discrepancies (in products of a building enterprises or the environment al management system) and an external (problems with subcontractors of specialized work, or suppliers of building materials), making notes of each activity and making its review in order to assess the results obtained.
4. MPEMS-4 – Supervision of documented information. This process embraces a succession of activities aiming at up-to-date character of required documents both in the seat of an enterprises and on building site (among which: environmental policy and aims, building standards, legal regulations on environment protection, operational instructions, etc.) and storing appropriate documentation for a determined period of time (contracts' reviews and other documents which form basis of realization of building work, audit reports, certificates confirming conduction environmental training, etc.).

The enumerated processes may be described in the form of documented procedures, but it is not an absolute requirement. The PN-EN ISO 14001:2015-09 standard recommends to focus the documentation of the environmental management system on the results of activities grouped in processes, and not on the description of these processes (POCHYLUK 2015).

Summary

In order to satisfy the increasing requirements of customers, building enterprises must be ready for the necessity of extending their management systems by use of new thematic scopes. With the progressing degradation of the environment and with the increased care of it, only the appropriately prepared environmental management system may present a trump card while obtaining orders [offers], in which the attitude of a building contractor towards environmental protection is considered.

The use of process approach in working – out of an environmental system increases the probability of its effectiveness on the condition of a suitable division of activities of a building company into appropriate processes.

Presented general model of the environmental management system fulfills the requirements of the PN-EN ISO 14001:2015-09 standard and it is also compatible with the PN-EN ISO 9001:2015-10 one, which make it easier to integrate both the environmental and the quality management systems.

The prepared model focuses on improvement of results in environment protection and on reducing the risk of doing a business in building companies, which should be reflected in an increase of interest in introduction of the environmental system to practice in their activities. The model may be used to preparation of a formalized and non-formalized environmental system in a given case in a medium-sized private building company. After an appropriate expansion of auxiliary and managerial processes, the model may be applied to prepare the system in a big company. The presented model of the environmental system eliminates the most frequent disadvantage of the formalized solutions, in which the role of documentation is over-emphasized.

References

EJDYS J., KOBYLIŃSKA U., LULEWICZ-SAS A. 2012. *Zintegrowane systemy zarządzania jakością środowiskiem i bezpieczeństwem pracy*. Oficyna Wydawnicza Politechniki Białostockiej, Białystok.

FAHMI D., GREENWOOD L. 2015. *Environmental Management System Risks and Opportunities: A Case Study in Pertamina Geothermal Energy Area Kamojang*. Proceedings World Geothermal Congress 2015 Melbourne, Australia, 19–25 April 2015, p. 11–13.

GALEAZZO A., KLASSEN R.D. 2015. *Organizational context and the implementation of environmental and social practices: what are the linkages to manufacturing strategy?* Journal of Cleaner Production, 108: 158–168.

JASIULEWICZ-KACZMAREK M., DROŻYNER P. 2013. *The Role of Maintenance in Reducing the Negative Impact of a Business on the Environment*. In: *Sustainability Appraisal: Quantitative Methods and Mathematical Techniques for Environmental Performance Evaluation*. Eds. M.G. Erechtchoukova, P.A. Khaiter, P. Golinska. EcoProduction, Springer-Verlag Berlin Heidelberg, p. 142–166.

JASIULEWICZ-KACZMAREK M., MISZTAL A. 2014. *Projektowanie i integracja systemów zarządzania projakościowego*. Wydawnictwo Politechniki Poznańskiej, Poznań.

KARAPETROVIC S. 2002. *Strategies for the integration of management system and standards*. The TQM Magazine, 14(1): 61–67.

LISOWSKA-MIESZKOWSKA E. 2007. *Systemy zarządzania środowiskowego – rozwój i funkcjonowanie w Polsce*. Czasopismo Ochrona Środowiska i Zasobów Naturalnych, 30: 5–24.

ŁUCZKA-BAKUŁA W. 2009. *Skutki systemu zarządzania środowiskowego według normy ISO 14001 i EMAS*. Roczniki Ekonomiczne Kujawsko-Pomorskiej Szkoły Wyższej w Bydgoszczy, 2: 111–123, http://www.kpsw.edu.pl/menu/pobierz/RE2/7Luczka.pdf (access: 15.07.2015).

Matuszak-Flejszman A. 2011. *Factors for improving Environmental Management Systems in Polish Companies According ISO 14001*. Polish Journal of Environmental Study, 20(3): 709–718.

Misztal A., Jasiulewicz-Kaczmarek M. 2014. *Environmental issues of the corporate social responsibility*. Management, 18(1): 58–70.

Niemiec W., Pacana A., Niemiec O. 2012. *Wybrane instrumenty ochrony środowiska*. Oficyna Wydawnicza Politechniki Rzeszowskiej, Rzeszów.

PN-EN ISO 14001:2015-09. Environmental management systems – Requirements with guidance for use.

PN-EN ISO 9001:2015-10. Quality management systems – Requirements.

Pochyluk R. 2015. *Nowa norma ISO 14001:2015. Czas na zmiany*. Online: http://eko-net.pl/aktualnosci/news/n-b/1/n-n/nowa-norma-iso-140012015-czas-na-zmiany.html (access: 8.10.2015).

Ładoński W., Szołtysek K., Grzesiak E., Kwaśnik J., Lesiów T., Żychiewicz A. 2005. *Zarządzanie jakością*. Część 1. *Systemy jakości w organizacji*. Wydawnictwo Akademii Ekonomicznej im. Oskara Langego we Wrocławiu, Wrocław.

Urbaniak M. 2004. *Zarządzanie jakością. Teoria i praktyka*. Centrum Doradztwa i Informacji Difin sp. z o. o., Warszawa.

Seidel M., Seidel R., Tedford D., Cross R., Wait L., Hämmerle E. 2009. *Overcoming Barriers to Implementing Environmentally Benign Manufacturing Practices: Strategic Tools for SMEs*. Environmental Quality Management, 18(3): 37–55.

Zymonik Z., Hamrol A., Grudowski P. 2013. *Zarządzanie jakością i bezpieczeństwem*, Polskie Wydawnictwo Ekonomiczne, Warszawa.

Technical Sciences, 2016, 19(1), 41–58

Quarterly peer-reviewed scientific journal
ISSN 1505-4675
e-ISSN 2083-4527
TECHNICAL SCIENCES
Homepage: www.uwm.edu.pl/techsci/

ASSESSMENT OF THERMAL COMFORT IN A LECTURE HALL WITH THE APPLICATION OF INSTRUMENTS FOR COMPUTATIONAL FLUID DYNAMICS

Aldona Skotnicka-Siepsiak

Institute of Building Engineering
University of Warmia and Mazury in Olsztyn

Received 21 April 2015; accepted 19 January 2016; available online 20 January 2016.

Key words: thermal comfort, air division, air conditioning.

Abstract

The examinations presented in this article aim at illustrating some possibilities of applying instruments for computational fluid dynamics to assess thermal comfort on the example of a lecture hall in the building of the Institute of Building Engineering at the University of Warmia and Mazury in Olsztyn. The obtained results have been subjected to an analysis according to the guidelines provided in the PN-EN ISO 7730:2006 norm. For the air heating system used in the hall, the distributions of velocity, temperature, as well as the PMV and PDD indices have been subjected to an analysis, with a particular focus on the optimal temperature of the air inflow.

Introduction

Thermal comfort is defined as state of satisfaction with thermal conditions of the surroundings (FANGER 1974). The main assumptions to ensure the conditions of thermal comfort are:

– a will to satisfy the need to feel content with the present thermal conditions;

– obtaining optimal conditions for proper efficiency of work.

Correspondence: Aldona Skotnicka-Siepsiak, Zakład Budownictwa Ogólnego i Fizyki Budowli, ul. Jana Heweliusza 4, 10-724 Olsztyn, phone: 48 89 5234576, e-mail: aldona.skotnicka-siepsiak@uwm.edu.pl

The subject literature distinguishes three different approaches to thermal comfort assessment (ŚLIWOWSKI 2000):

– physical – viewing the human organism in a way similar to a heat-generating and working machine;

– psychological – where the thermal comfort assessment is based on responses provided by people in questionnaires and tests;

– physiological – applying the research methods based on direct or indirect human calorimetry. Those are not very useful in thermo-neutral conditions and in small changes of metabolism, which are difficult to measure.

When assessing thermal comfort, various scale types may be applied, e.g. the Bedford scale, the ASHRAE thermal sensation scale, the Predicted Mean Vote (PMV), the assessment of subjective thermal sensation, or the assessment of local thermal discomfort (CHLUDZIŃSKA 2010).

Such a multitude of systems for thermal comfort assessment and various approaches to the problem reported in the subject literature create a need to systematize the methodology of classification and assessment for thermal conditions. To do so, some norms may be referred to and a particular attention should be paid to the PN-EN ISO 7730:2006 norm: *Ergonomics of the Thermal Environment – Analytical Determination and Interpretation of Thermal Comfort Using Calculation of the PMV and PPD Indices and Local Thermal Comfort Criteria*, as well as to the PN-EN 15251:2012 norm: *Indoor Environmental Input Parameters for Design and Assessment of Energy Performance of Buildings Addressing Indoor Air Quality, Thermal Environment, Lighting and Acoustics*.

This article is an attempt to assess the thermal comfort of a lecture hall in the building of the Institute of Building Engineering at the University of Warmia and Mazury, located at ul. Heweliusza 4 in Olsztyn, based on simulations performed with the use of the commercial FloVENT package that applies computational fluid dynamics (CFD). The examinations have been carried out for a design study and are an example of the correctness and efficiency assessment for the proposed conceptual solutions.

The choice Flovent package was due to the fact, that it is a software especially dedicated to the engineering issues involved in the design and optimization of heating, ventilating and air conditioning (HVAC) systems. FloVENT predicts 3D airflow, heat transfer, contamination distribution and comfort indices in and around buildings. All those parameters can be analyze in both forced and free convection ventilated systems under laminar or turbulent flow conditions. FloVENT solvers are based on Finite Volume method. (FloVent User Guide, Software Version 10.1).

Many researchers have studied the human comfort in indoor environments (RUPP et al. 2015). Different thermal comfort approaches can be found in literature: the rational (heat-balance approach) or adaptive approach (DJONGYANG et al. 2010). The impact of different factors for thermal comfort sensation can be analysed as well (FRONTCZAK, WARGOCKI 2011). The problem of human thermal comfort in the built environment becomes increasingly crucial in the face of extending time of human residing in buildings. Experimental investigation of that issue including not only research in climate chambers or in semi-controlled environments but also in the real buildings. During last 50 years CFD has been increasingly used for room air distribution and thermal comfort subject (NIELSEN 2015). Publication dedicated to the standard office room can be given as an example of numerical studies (YONGSON et al. 2007). The k-epsilon and Reynolds stress models for turbulence flow were used for the analysis of temperature and velocity distribution. What is more, to achieve the maximum comfort for the occupant, the different locations of the air conditioner blower were analyzed. For an office room, the verification of a numerical model for airflow and heat transfer were made (STAMOU, KATSIRIS 2006). The experimental results were compared with the results of the standard k-ε, the RNG k-e model and the laminar model. As a main conclusion authors has proved, that all the tested turbulent models predict correctly the main qualitative features of the air movement and the temperature distribution. Numerical and experimental investigation related to large space building can be found in many articles; case of patient hall of a hospital building (WANG et al. 2014), theatre (KAVGIC et al. 2008) or lecture hall (MUHIELDEEN et al. 2015).

Classification of the Internal Climate Quality

The PN-EN ISO 7730:2006 norm provides recommended parameters for thermal comfort together with a division into categories of thermal environment:

– Category A – characterized by a high level of the expected microclimatic conditions and the highest percentage of satisfied people;

– Category B – characterizes objects of an average quality level of the expected microclimatic conditions and an average percentage of satisfied people;

– Category C – objects of moderate, yet acceptable, quality level of the expected microclimatic for a minimal number of people.

The PN-EN 15251: 2012 norm provides an analogical division applying the category marking: I, II, and III. It also introduces category IV including objects that do not fall into any of the former three categories. That category should be accepted only for a part of a year. The objects in Category IV are characterized

Table 1

Categories of thermal comfort according to PN-EN ISO 7730:2006:
Ergonomics of the Thermal Environment – Analytical Determination and Interpretation of Thermal Comfort Using Calculation of the PMV and PPD Indices and Local Thermal Comfort Criteria

Category	Thermal Neutrality		Local Discomfort			
	PPD [%]	PMV	DR [%]	PD [%]		
				warm or cold floors	vertical air temperature	asymmetric thermal radiation
A	<6	-0.2 < PMV < +0.2	< 10	<3	<10	<5
B	<10	-0.5 < PMV < +0.5	<20	<5	<10	<5
C	<15	-0.7 < PMV < +0.7	<30	<10	<15	<10

by the values PPD > 15, PMV < -0.7, or PMV > +0.7. The provided PMV (Predicted Mean Vote) index makes it possible to predict thermal sensations for any combinations of energy expenditure, clothing, and four thermal environmental parameters (air temperature, mean radiant temperature, air velocity, and air humidity) (FANGER 1974). The assessment of thermal sensation is performed with the application of a seven-degree scale, with the following values: +3, +2, +1, 0, -1, -2, and -3 where the notes mirror the sensations respectively: hot, warm, slightly warm, neutral, slightly cool, cool, and cold.

The PMV index is calculated according to formula 1 (PN-EN ISO 7730:2006):

$$\left\{\begin{matrix} \mathrm{PMV} = (0{,}303 \cdot e^{-0{,}036 \cdot M} + 0{,}028) \cdot \\ (M-W) - 3{,}05 \cdot 10^{-3} \cdot [5733 - 6{,}99 \cdot (M-W) - p_a] - 0{,}42 \cdot [M-W) - 58{,}15 \\ -1{,}7 \cdot 10^{-5} \cdot M \cdot (5{,}867 - p_a) - 0{,}0014 \cdot M \cdot (35 - t_a) \\ -3{,}96 \cdot 10^{-8} \cdot f_{cl} \cdot [(t_{cl} + 273)^4 - (\bar{t}_r + 273)^4] - f_{cl} \cdot h_c \cdot (t_{cl} - t_a) \end{matrix}\right\} \quad (1)$$

where, when considering the recommended interval of values:

M – metabolic rate, $\left[\frac{\mathrm{W}}{\mathrm{m}^2}\right] = 0{,}8 \div 4{,}0$ [met],

W – external work, $\left[\frac{\mathrm{W}}{\mathrm{m}^2}\right]$,

I_{cl} – thermal insulation of the clothing $I_{cl} = 0 \div 0{,}310 \left[\frac{\mathrm{m}^2 \cdot \mathrm{K}}{\mathrm{W}}\right] = 0{,}0 \div 2{,}0$ [clo]

f_{cl} – ratio of the surface area of the clothed body to the surface area of the nude body,

t_a – air temperature $t_a = 10 \div 30$ [°C],

$\bar{t}_r$ – mean radiant temperature $\bar{t}_r = 10 \div 40$ [°C],

v_{ar} – relative air velocity $v_{ar} = 0 \div 1 \left[\frac{\mathrm{m}}{\mathrm{s}}\right]$,
p_a – partial water vapour pressure $p_a = 0 \div 2700$ [Pa],
h_c – convective heat transfer coefficient $\left[\frac{\mathrm{W}}{\mathrm{m}^2 \cdot \mathrm{K}}\right]$,
t_{cl} – clothing surface temperature [°C].

The above index identifies the predicted mean assessment of thermal comfort by a large group of people who have been influenced by the defined combination of changeable parameters of their environment. The PMV provides information on a general degree of discomfort for the whole studied group; however, the thermal sensations of people subjected to the same changeable factors in such a group are varied. Thus, the PPD (Predicted Percentage Dissatisfied) index may be applied as an assessment tool as it determines a share of people who are not satisfied with the environmental conditions. Participants who have given the notes: -2 (cool), -3 (cold), +2 (warm), or +3 (hot) are considered to be dissatisfied. The PPD index is calculated according to formula 2 (PN-EN ISO 7730:2006):

$$\mathrm{PPD} = 100 - 95 \cdot e^{-(0{,}03353 \cdot \mathrm{PMV}^4 - 0{,}2179 \cdot \mathrm{PMV}^2)} \tag{2}$$

The PPD index may be presented as a function of the PMV parameter (Fig. 1). The curve is characterized by its symmetry to the value of PMV = 0. The curve minimum is located on the level of 5% of the dissatisfied at the mean environmental assessment equal to zero.

The draught rating (DR) value may also be used as an assessment parameter for it presents a percentage of people dissatisfied with the velocity of air passing around the body and is calculated according to dependency 3 (PN-EN ISO 7730:2006):

$$\mathrm{DR} = (34 - t_{a,l}) \cdot (\bar{v}_{a,l} - 0{,}05)^{0{,}62} \cdot (0{,}37 \cdot \bar{v}_{a,l} \cdot Tu + 3{,}14) \tag{3}$$

where:
$t_{a,l}$ – air temperature $t_a = 120 \div 26$ [°C],
$\bar{v}_{a,l}$ – air velocity, if $\bar{v}_{a,l} < 0{,}05 \left[\frac{\mathrm{m}}{\mathrm{s}}\right]$, it is accepted that $\bar{v}_{a,l} = 0{,}05 \left[\frac{\mathrm{m}}{\mathrm{s}}\right]$,
Tu – turbulence intensity $Tu = 10\% \div 60\%$.

If the final value of DR > 100% is obtained, the value of DR = 100% is accepted.

The norm (PN-EN ISO 7730:2006) provides also the PD (percent of dissatisfied) index as an assessing parameter as it reflects a percentage of people dissatisfied with the difference between the temperatures at the levels of their feet and their heads. It is calculated according to the formula:

$$PD = \frac{100}{1 + e^{(5,76 - 0,856 \cdot \Delta t_{a,v})}} \tag{4}$$

The above formula should be applied if the $\Delta t_{a,v}$ value of a thermal difference between the levels of the feet and the head does not exceed 8°C.

The Analysed Object

A computational simulation based on the assumptions of the computational fluid dynamics (CFD) has been carried out for a lecture hall in the building of the Institute of Building Engineering at the University of Warmia and Mazury in Olsztyn, situated at ul. Heweliusza 4. The study has been performed with the use of the commercial FloVENT application by Mentor Graphics.

The floor space of the hall is 239.9 m^2 and it capable of holding 224 people. The room is designed to contain mechanical air conditioning with cooling that is aimed at:

– providing a required amount of hygienic air for people;
– leading out excessive thermal gains from people in summertime;
– air heating.

The computational simulations have been carried out for the situation reflecting the assumptions of the design for wintertime (external temperature according to PN-EN 12831 is -22°C) and they aimed at verifying the parameters of thermal comfort (operative temperature, mean air velocity, PMV and PPD indices) and assessing the efficiency of the air heating system. The main focus was to assess the state of thermal organism as a whole.

According to the design assumptions, the amount of the air inflow and outflow is the same and is 9,000 m^3/h. The design assumes that in order to maintain the required internal temperature at 20°C in the empty room, the air inflow into the room in wintertime should be at the temperature of 23°C. When using the lecture hall, the temperature of the air inflow is to change according to the number of people in the room and the temperature of the external air.

The outlet in the room has been designed to use of seventy-two KNP-al.-P grids, sized 255×125, located under the students' chairs in the central part of the hall. The air inflow takes place in the frontal part of the hall, over the lecturer's podium (using three symmetrically placed NWP 355 rotational-centrifugal air inlets, the efficiency of each: 600 m^3/h) and in ten DUK-V 400 nozzles, the efficiency of each: 720 m^3/h, located alongside the external rear wall with windows.

The computational model of the described room has been presented in Figure 1. The inlets and outlets have been marked red. The construction of the acoustic ceiling has been marked light yellow.

Under the lecture hall, there are technical rooms with the temperature of 15°C. The internal wall is made of a partition situated behind the lecturer's back and, partially (about a half of the length), by a vertical wall to the right from the speaking person. The temperature on the other side of those partitions is 20°C. The remaining partitions are external. The values of heat transfer coefficients for particular constructional partitions have been accepted according to the architectonical project (*Projekt budowlany budynku Wydziału Nauk Technicznych UWM w Olsztynie*, 2008). At the back of the hall, there is technical space for multimedia services in the lecture hall as well as one external wall, in which windows are mounted.

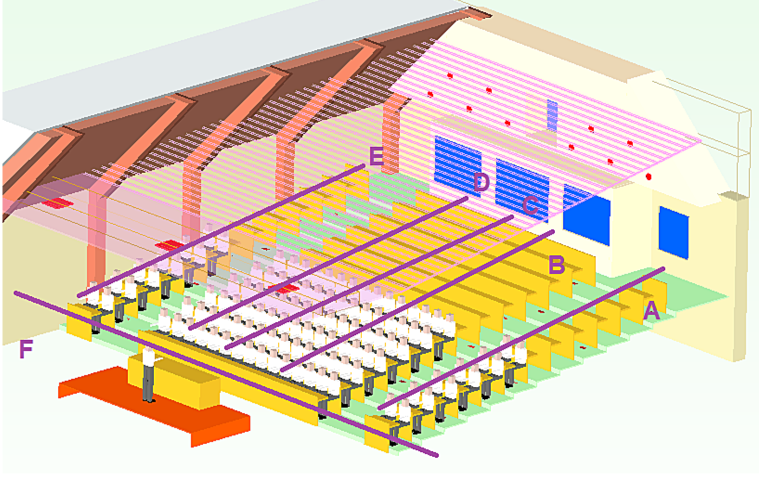

Fig. 1. Computational model of the analysed room – the half-full room case

The computational studies included two cases: when the hall is completely full and when it is filled in 50%. There is a plenty of possibilities, in which 112 people can take seats in the examined area. Because of technical CFD method limitation (steady state solution) and time needed to complete one simulation, the most popular case, when people are seating in the first rows, was analysed. Each part of the mannequin body in the model was the source of heat. Total heat amount is equal for each person 119 W. Due to the number of people in the room, the temperature of the air inflow has been changing, however, its amount has not. A grid with number of 6,860,000 cells has been used in both cases. The k-ε turbulence model has been applied to the calculations.

Although, the research are prepared in 3D, the results for this article are presented in the form of two-dimensional planes with specified location or for more precise analysis of numerical values, in a six measure lines (Fig. 1). The first five measure lines are situated in the audience area. They start at the location of the lowest seats for students in the hall and end at the backrests of the last seats, located at the highest position. The parameters have been analysed for the height of about 1.5 m above the floor. When looking with the direction of the lecturer's sight, line A is located in the mid-width a two-person row of seats situated on the right from the aisle. Analogically, line E is in the mid-width of a two-person row of seat situated on the left (along the external wall). Measure line C is located in the axis of symmetry of the hall, in the mid-width of a 14-person row of seats. Measuring lines B and D are placed symmetrically, to the left and to the right to line C, in the distance of about 2 m from it (in 1/4 and in 3/4 of the width of the central 14-person row of seats). Measure line F is located across the lecture hall (in the central part of the lecturer's podium), at the height of about 1.5 m from it.

Results of the Simulations

The first of basic questions to arise when analysing the results is the relevance of the conditioned air amount accepted in the assumptions of the design. The PN-EN 15251:200 norm defines the way to identify a conditioned airflow according to formula 5:

$$q_{tot} = n \cdot q_p + A \cdot q_B \tag{5}$$

where:

n – number of people in the room,

q_p – airflow per person $\left[\frac{1}{\mathrm{s}}, \text{person}\right]$,

A – room surface [m^2],

q_B – airflow for building emissions pollutions $\left[\frac{1}{\mathrm{s}}, \mathrm{m}^2\right]$.

When assuming that the room is characterized by a low level of pollution, the conditioned airflow must be no less than 2,480 $\frac{1}{\mathrm{s}}$ to comply with the requirements of Category I. With the assumed amount of 9,000 m^3/h, the above requirement is met.

According to the PN-EN ISO 7730:2006 norm, the designing criteria for the analysis of temperature distribution describe the optimal operative temperature as 22°C for the heating season. For objects in Category *A*, the accepted deviation is ±1°C, for objects in Category *B* it is ±2°C, and for object in Category *C*, the temperature deviation may be ±3°C. The FloVENT application makes it possible to separately analyse the environment temperature and the mean radiant temperature in the room.

The results presented in Figure 2 allow for a clear observation of a decrease in the environment temperature (*a*) and the mean radiant temperature (*b*) along the internal partitions (yellow and green areas). The walls of the technical space at the end of the lecture hall are marked grey. Presented in the figure is also a fragment of the external area (temperature: -22°C, navy blue) alongside the external wall with windows.

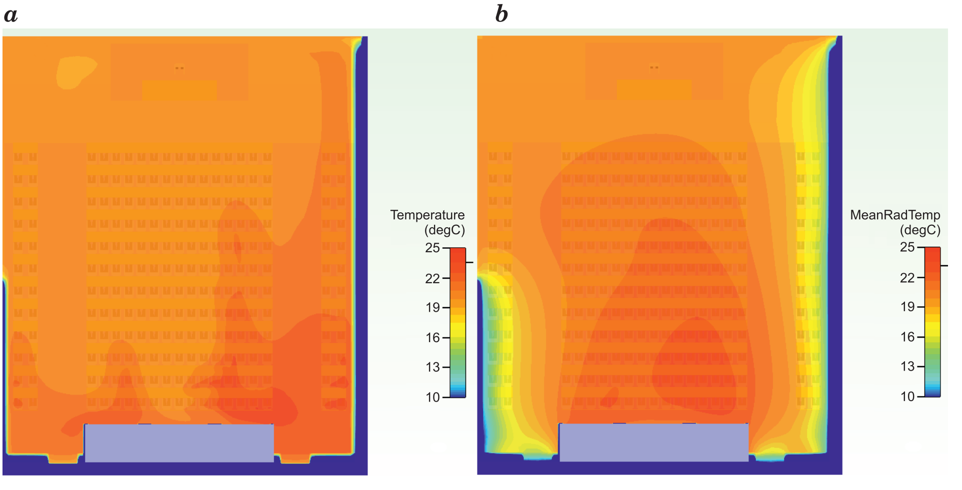

Fig. 2. The environment temperature (*a*) and the mean radiant temperature (*b*) – the results for the room filled with students in 100%, bird's eye view, distribution in a plane about 1.5 m over the floor for the highest-located seats

The operative temperature is what humans experience thermally in a space. The operative temperature is defined as a uniform temperature of a radiantly black enclosure in which an occupant would exchange the same amount of heat by radiation and convection as in the actual non uniform environment. It's expressed as the dependency between the environment temperature (t_a) and the mean radiant temperature (t_r), has been calculated for the room according to guidelines of the PN-EN ISO 7726 norm: *Ergonomics of the Thermal Environment – Instruments for Measuring Physical Quantities* based on the formula 6:

$$t_o = \frac{h_c t_a + h_r t_r}{h_c + h_r} \tag{6}$$

where:

h_r – radiative heat transfer coefficient – 4.6 $\left[\frac{\mathrm{W}}{\mathrm{m^2K}}\right]$,

h_c – convective heat transfer coefficient – 50.0 $\left[\frac{\mathrm{W}}{\mathrm{m^2K}}\right]$.

An analysis of the operative temperature distribution for the fully filled room (Fig. 3) has shown that its mean value is 21.38°C. This makes it very close to the normative optimal value. A closer look at the local distribution of the parameter makes it possible to identify areas with the largest diversification. As for measure lines *B*, *C*, and *D*, in the central part of the audience, the criteria defined in Category *B* of the norm are met. Line *D* is located in the area characterized by the highest operative temperature values that locally are coming close to almost 24°C. It may also be noticed that in the frontal area of the lecture hall, near the lecturer's podium, a lower operative temperature occurs – reaching about 20°C (measuring line *F*). This results from the fact that this area is used by a lecturer only; hence thermal gains from humans are lower. A negative influence of the low mean radiant temperature, resulting from the closeness of the external partitions, is visible in the area that is wholly covered by measure line *E*, partially (for the distance below 5.5 m a wall separates the hall from a heated corridor) by the measure line *A*, and in the section of about 3 m by the measure line *F*. The lowest recorded value of the operative temperature is 19.09°C.

For the computational case in which a partial load of the lecture hall has been analysed (students seated in the front rows – the distance below 5.5 m), the mean value of the operative temperature is 21.42°C (Fig. 4). Similarly as in the case of Figure 3, a negative influence of the neighbouring external partitions is visible (measure lines *A*, *E*, and *F*). It is even more visible and falls down to the minimal value of 18.84°C. What is noteworthy is a very visible influence of thermal gains from people in the central part of the hall (measure lines *B*, *C*, and *D*). The increase to about 24°C in the zone of the students seated in places that are the most far away from the lecturer's podium is also noticeable.

Obtaining the presented level of temperature distribution requires an inflow of conditioned air at the temperature of 18.6°C for the maximum number of students in the lecture hall and at the temperature of 21.0°C for the half-full room.

As for the maximum mean airflow velocity, the PN-EN ISO 7730:2006 norm indicates that the value should not exceed 0.10 m/s for rooms in

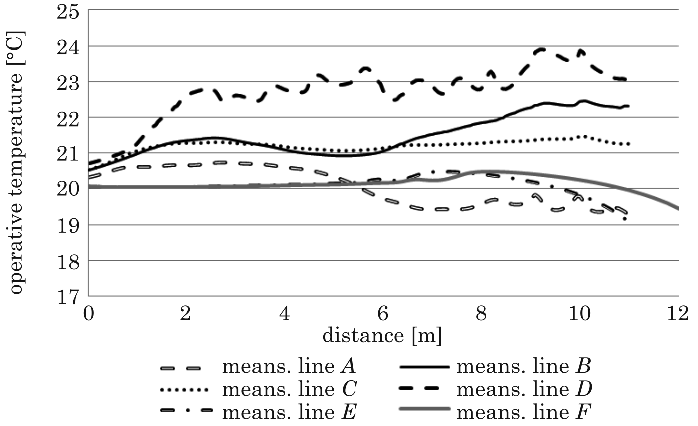

Fig. 3. The distribution of the operative temperature in the analysed measure lines – the full room case

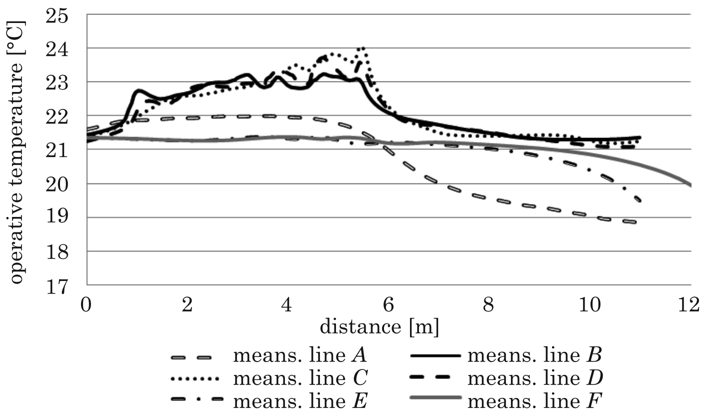

Fig. 4. The distribution of the operative temperature in the analysed measure lines – the half-full room case

Category *A*, 0.16 m/s for Category *B*, and the threshold value of 0.21 m/s is accepted for Category *C*.

An analysis of the results for the case in which the room is filled in 100% (Fig. 5) reveals that maximum mean airflow velocities significantly exceed the normative level of values for rooms in Category *C*. Locally, the recorded maximum velocity value is 0.46 m/s and in a huge majority of the results its level is above 0.21 m/s. Measure line *A* is an exception here, as its recorded maximum velocity value is 0.17 m/s.

When considering the design case in which the room is filled in 50% (Fig. 6), it is visible that the distribution of velocities in the studied area where measure line *A* is located is analogical to the case in which the room is filled in 100%.

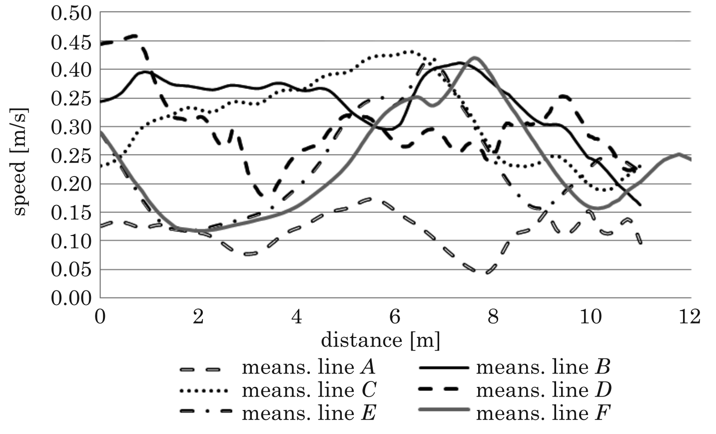

Fig. 5. The distribution of the mean airflow velocity in the analysed measure lines – the full room case

In the front rows of the audience, much higher (about two times) values of the mean airflow velocity occur than in the part of the hall that is not filled with people (the distance no higher than 5.5 m for lines $B \div E$). This poses the question whether in the proposed system of conditioned air division (the air outflow by grids mounted in the steps under the students' chairs) those are the location of chair seats, their opened worktops, and students sitting on the chairs that play key roles in the way the air flows.

Figure 7 reflects the results of the distribution for the mean airflow velocity when there are no people in the hall and the seats and worktops are closed. A maximal limitation of elements that may disturb the airflow results in a significant decrease of velocity. As for the case of extreme measure lines (*A* and *E*) in the audience area, as well as for the results in the frontal area of the hall where the lecturer's podium is placed (measure line *F*), the mean velocity value is 0.09 m/s. Locally, in the first row, included into measuring line *A*, some maximum velocity values of 0.18 m/s have been recorded. Measure lines *B*, *C*, and *D*, which run along the central area of the audience, are of totally different characteristics. In the distance of about 3.5 m (the third row), the maximum values of the mean airflow velocity have been reached at the level of about 0.27 m/s. There is a decrease in the velocity visible for the higher rows, down to the levels of about 0.02 m/s near the last rows at the technical space of the lecture hall.

An analysis of the PMV and PPD indices has been performed with the assumption that the metabolic rate of the people in the hall is 70 W/m^2 and the value of thermal insulation for daily wear clothing is 0.110 (m^{2}K)/W (PN-EN ISO 7730:2006). Figure 8, presented below, reflects the distribution of the PMV parameter in the central area of the hall, in a vertical plane.

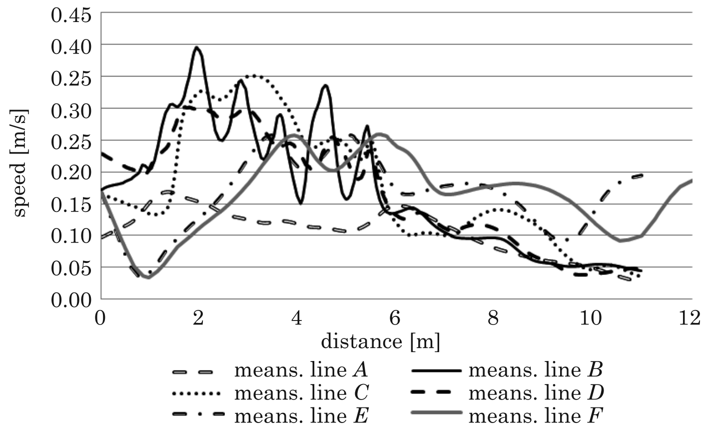

Fig. 6. The distribution of the mean airflow velocity in the analysed measure lines – the half-full room case

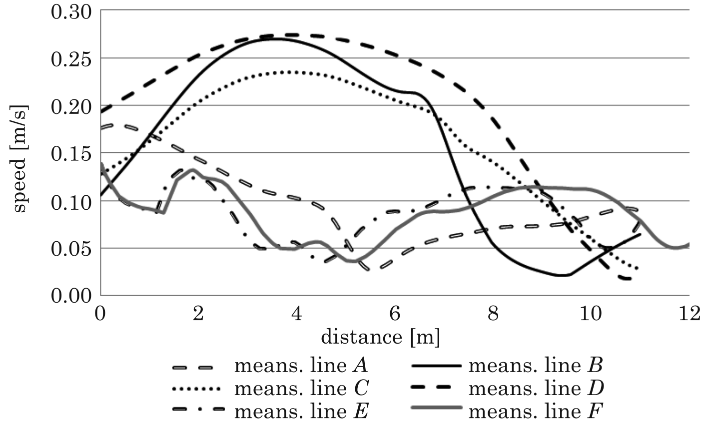

Fig. 7. The distribution of the mean airflow velocity in the analysed measure lines – the case with no people in the room

In the case of the maximal load of the hall, the mean value of the PMV indices is -0.43 while in the case of loading the room with students partially, the mean PMV value is -0.26. There is a clearly visible trend to decrease the value of the parameter in the areas characterized by the lowest values of the mean radiant temperature. As for loading the room with students completely, the minimum PMV value is -0.87 and it has been recorded at the edge of measure line *E*. As for the case of seats in the hall taken in half, the minimum value of the PMV indices is -0.75 and it is also located by the lowest row in the area of line *E*. The highest values of the indices (for both cases) have been noticed in the central area of the hall, by the highest rows that are character-

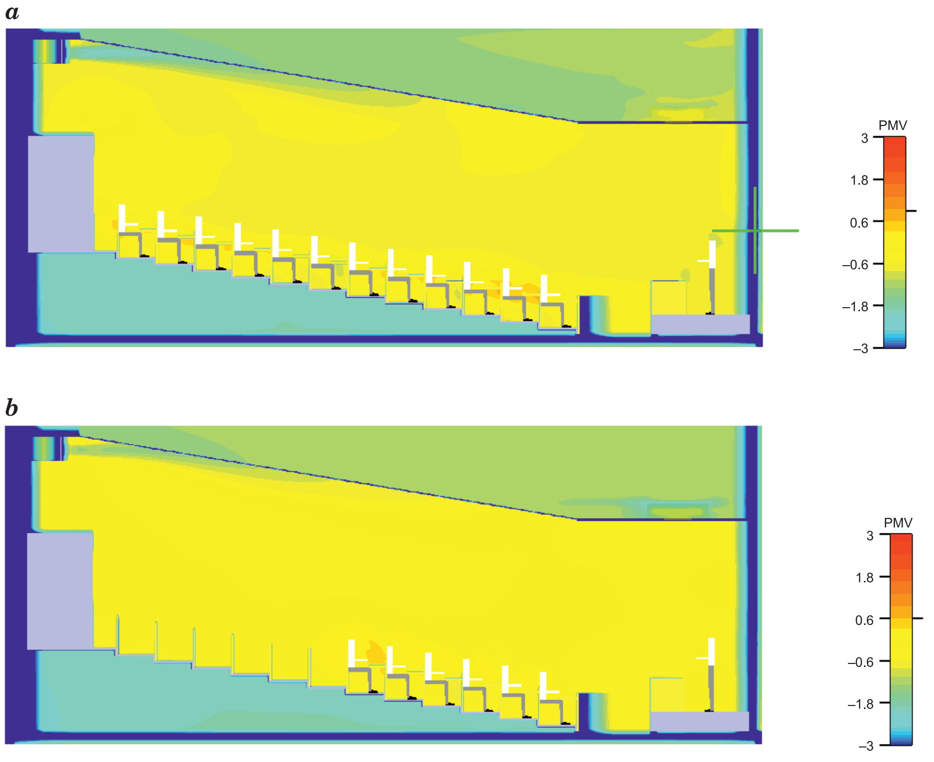

Fig. 8. The value of the PMV index in a vertical plane, in the axis of symmetry of the lecturer's hall: *a* – the room filled in 100%, *b* – the room filled in 50%

ized by the lowest airflow velocities. The maximum PMV value is 0.07 for case (*a*) and 0.15 for case (*b*).

An analysis of the PPD indices indicates that as for the case of 100% load of the lecture hall, the mean PPD value is 10.21; however, in the case of using the seats in the hall by the students in 50%, the value is at the level of 7.10. In both design cases, the minimum values of the PPD indices are about 5.00. As for case (*a*), the maximum values are PPD=20.90, in the zone of the highest rows in the area of measure line E. When half of the seats are taken by students in the front rows, the highest levels of the PPD indices, at the level of about 16.95, have been recorded in measure lines *A* and *B* that run along the walls in the area of the highest rows.

Table 2, presented below, contains a summary of the obtained results for the parameters of local discomfort. The criteria for rooms in Category *C* are met for the discussed design case in which 100% of seats in the hall are used. An analysis of the case in which a half of the seats is taken by students

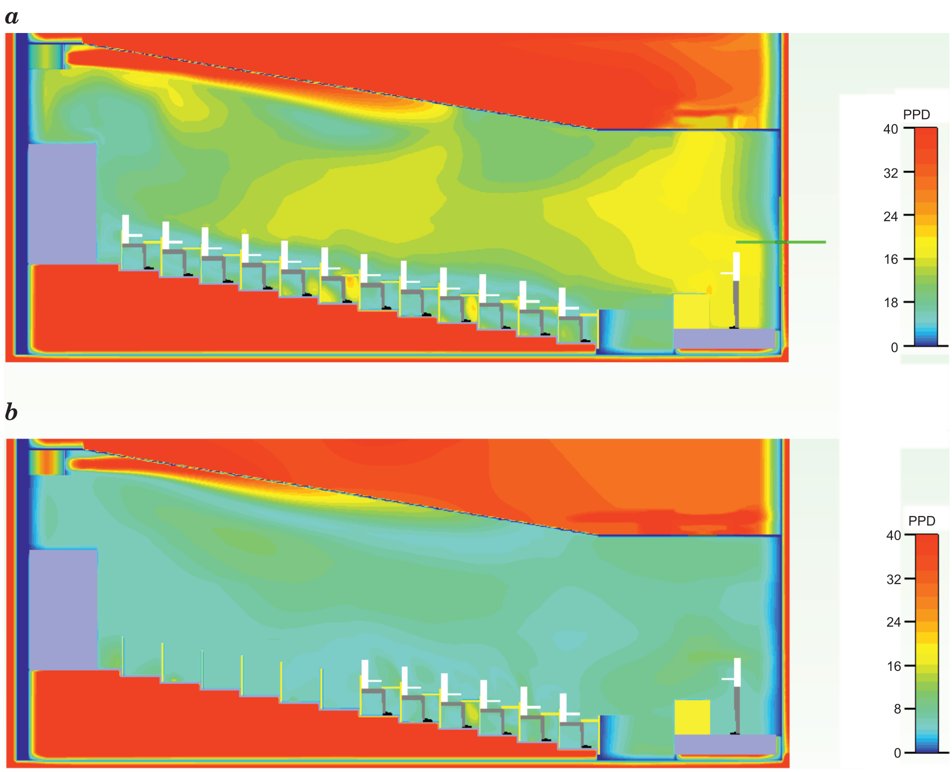

Fig. 9. The value of the PPD index in a vertical plane, in the axis of symmetry of the lecturer's hall: *a* – the room filled in 100%, *b* – the room filled in 50%

Table 2

The discomfort parameters for the analysed model

Specification	DR		PD	
	mean	maximum	mean	maximum
The lecture hall illed in 100%	15.12	24.53	0.67	5.32
The lecture hall filled in 50%	8.01	19.14	0.44	2.84

indicates that, maximally, about 3% of the users may express their dissatisfaction with the vertical temperature difference between the levels of their feet and their heads, however, about 10% of the users may complain about a discomfort caused by air drafts.

Conclusions

The obtained results of the analyses indicate that, according to the PN-EN ISO 7730:2006 norm, the requirements for Categories $A \div C$ are met in the studied room. The conducted computational simulations show that its concept of leading the conditioned air should be reanalysed at the design stage. In the proposed system, taking seats by students and opening the worktops significantly disturbs the airflow between the inlets and outlets. Maintaining a proper airflow velocity is not going to be possible even if adjusting the air inflow temperature to the thermal requirements is ensured by the measuring and driving sub-system in the automated system of air heating (the air temperature depending on the temperature of the air outflow and the external air). In the discussed cases, the analysis of PMV and PPD indices distribution has been presented for the air inflow temperature selected by the method of successive approximations.

It should be remembered, however, that methods of computational fluid dynamics have got their limitations. The presented analyses reflect situations that are deprived of dynamics. None of the elements in the model has changed its parameters and location in time. Also, the external parameters outside the lecture hall and location of people in the room have both been considered as unchangeable. Moreover, the presented study does not include an analysis of humidity distribution. However, CFD models should be validated and in optimal case, compared with experimental investigation of the distributions of velocity, temperature and PMV and PDD indices.

The example of the analysis presented in this article includes the designing phase for an object. It provides a possibility to verify its correctness of conceptual assumptions and to avoid mistakes that may turn out to be severe and their removal may be very time-and-money-consuming or, in some cases, just impossible.

Comment

Analyzed lecture hall is part of a new building. Initial version of the following article was being prepared while the object was still not in use. At present, the object is fully used. On 14 January 2016 among users of the analyzed lecture hall, the survey has been carried out. There were 107 participants of the survey (52 women 55 men). The average age was 21.8 years. Most of the respondents were characterized by a mediocre body build (sevenfold scale where 0 is average value). No one had chosen the „very fat” option. Only three people have declared that they are corpulent and five, that they are very thin. During the test everyone was sitting (metabolic rate about 70 W/m^2, 1.2 met). 35% of participants has been wearing clothes with high thermal insulation (clo 1.10; panties, stockings, blouse, long skirt, jacket, shoes). 28% of respondents has been wearing clothes with thermal insulation clo 1.00. During examination, occupants were staying in the lecture hall from 30 minutes. The average indoor air temperature was 20.4°C. Respondents were sitting evenly in all rows. Between the next seated person there was an empty seat. According to sevenfold scale where 0 is the optimal value (PN-EN 15251:2012): 9% chose the value -3 – cold; 21% pick the -2 value – cool; 46% chose the value -1 – slightly cool; 18% chose the value 0 – neutral; 3% indicated option +1 – slightly warm; 1% chose the value +2 – warm and 2 respondents pick the +3 value – hot.

Surveys, as well as CFD simulations, indicate that users complain about too low temperature in analyzed lecture hall. Experimental results are even more disadvantageous; during numerical investigation. In worst case about 10% of users should be dissatisfied because of thermal conditions meanwhile questionnaire shows 30% dissatisfied.

However, the precise, experimental investigation of the distributions of velocity, temperature and humidity are required for CFD model validation.

References

CHLUDZIŃSKA M. 2010. *Komfort cieplny człowieka w warunkach wentylacji indywidualnej w pomieszczeniach biurowych*. Politechnika Warszawska, Warszawa.

DJONGYANG N., TCHINDA R., NJOMO D. 2010. *Thermal comfort: A review paper*. Renewable and Sustainable Energy Reviews, 14: 2626–2640.

FANGER P.O. 1974. *Komfort cieplny*. Arkady, Warszawa.

FloVent User Guid, Software Version 10.1, On line: https://supportnet.mentor.com/docs/201406004/docs/pdfdocs/fv_user.pdf.

FRONTCZAK M., WARGOCKI P. 2011. *Literature survey on how different factors influence human comfort in indoor environments*. Building and Environment, 46: 922–937.

KAVGIC M., MUMOVIC D., STEVANOVIC Z., YOUNG A. 2008. *Analysis of thermal comfort and indoor air quality in a mechanically ventilated theatre*. Energy and Buildings, 40: 1334–1343.

MUHIELDEEN M.W., ADAM N.M., SALMAN B.H. 2015. *Experimental and numerical studies of reducing cooling load oflecture hall*. Energy and Buildings, 89: 163–169.

NIELSEN P.V. 2015. *Fifty years of CFD for room air distribution*. Building and Environment, 91: 78–90.

PN-EN 12831 Heating systems in buildings. Method for calculation of the design heat load.

PN-EN 15251:2012 Indoor Environmental Input Parameters for Design and Assessment of Energy Performance of Buildings Addressing Indoor Air Quality, Thermal Environment, Lighting and Acoustics.

PN-EN ISO 7726 Ergonomics of the Thermal Environment – Instruments for Measuring Physical Quantities.

PN-EN ISO 7730:2006 Ergonomics of the Thermal Environment – Analytical Determination and Interpretation of Thermal Comfort Using Calculation of the PMV and PPD Indices and Local Thermal Comfort Criteria.

RUPP R.F., VÁSQUEZ N.G., LAMBERTS R. 2015. *A review of human thermal comfort in the built environment*. Energy and Buildings, 105: 178–205.

STAMOU A., KATSIRIS I. 2006. *Verification of a CFD model for indoor airflow and heat transfer*. Building and Environment, 41: 1171–1181.

ŚLIWOWSKI L. 2000. *Mikroklimat wnętrz i komfort cieplny ludzi w pomieszczeniach*. Oficyna Wydawnicza Politechniki Wrocławskiej.

WANG Y., WONG K.K.L., DU H., QING J., TU J. 2014. *Design configuration for a higher efficiency air conditioning system inlarge space building*. Energy and Buildings, 72: 167–176.

YONGSON O., BADRUDDIN I.A., ZAINAL Z.A., NARAYANA P.A.A. 2007. *Airflow analysis in an air conditioning room*. Building and Environment, 42: 1531–1537.

ZAGROBA M. 2008. *Projekt budowlany budynku Wydziału Nauk Technicznych UWM w Olsztynie*. Constans Biuro Projektowo-Usługowe dr n. techn. inż. Zenon Drabowicz.

Technical Sciences, 2016, 19(1), 59–70

Quarterly peer-reviewed scientific journal
ISSN 1505-4675
e-ISSN 2083-4527
TECHNICAL SCIENCES
Homepage: www.uwm.edu.pl/techsci/

METHODS OF IDENTIFICATION AND DELIMITATION OF CONCAVE TERRAIN FEATURES BASED ON ISOK-NMT DATA

Tomasz Oberski

Department of Civil and Environmental Engineering, Division of Geoinformatics
Koszalin's University of Technology

Received 29 October 2015; accepted 17 January 2016; available online 18 January 2016.

Key words: DTM, ISOK, terrain, concave features, GIS.

Abstract

Airborne Laser Scanning (ALS) products are now often used to study the terrain due to their numerous advantages such as relatively low cost and ease of data collection. The ISOK project (pl: Informatyczny System Osłony Kraju – national hazard protection information system) developed elevation data for about 65% of the Polish territory. Parallel to the airborne laser scanning point cloud collection, additional products, such as orthophotomaps, digital terrain models (DTM), and digital surface models (DSM) were created. This resource is not only a reference material for the project, but also a valuable source of the analysis used in various fields of economy and science. Important features of the ISOK-data are the availability and their standardized format based on uniform technical conditions. The article presents the results of an experiment in which an attempt was made to use the digital elevation model with a resolution of 1 m based on airborne laser scanning data to determine concave terrain features using GIS tools. The ISOK-DTM has a height accuracy of 0.15 m for the outdoor areas, which makes it a better representation of small terrain forms than previous products. The research area is located at an undeveloped open ground with comparatively little variation of its shape for a long period. Several methods were tested to classify the terrain shape based of topographic attributes. Those methods led to similar locations of the concave features and further on coincide with results of the pre-analysis. Also, attention was drawn to the selection of the analysis parameters and their influence on the result. The results show the usefulness of ISOK's DTM for locating field concave terrain shapes.

Correspondence: Tomasz Oberski, Katedra Geoinformatyki, Wydział Inżynierii Lądowej, Środowiska i Geodezji, Politechnika Koszalińska, ul. Śniadeckich 2, 75-453 Koszalin, phone: +48 94 348 67 20, e-mail: tomasz.oberski@tu.koszalin.pl

Introduction

The shape of the terrain has a significant impact on the phenomena on its surface. The characteristics of the topographic surface and the presence of certain land forms determine the development and the usage of the area. Identification of particular landforms based on measured elevation data facilitates land use planning and the better understanding of land cover and phenomena occurring on it. Concave terrain forms, i.e. sinks, are one of the very important ones as they may be suitable as water catchments. Regardless of the terrain's inclination forms such as local depressions, sinks, wells or other synclinal forms interferes with the surface water runoff (Fig. 1). This may cause permanent or periodic wetness accumulation.

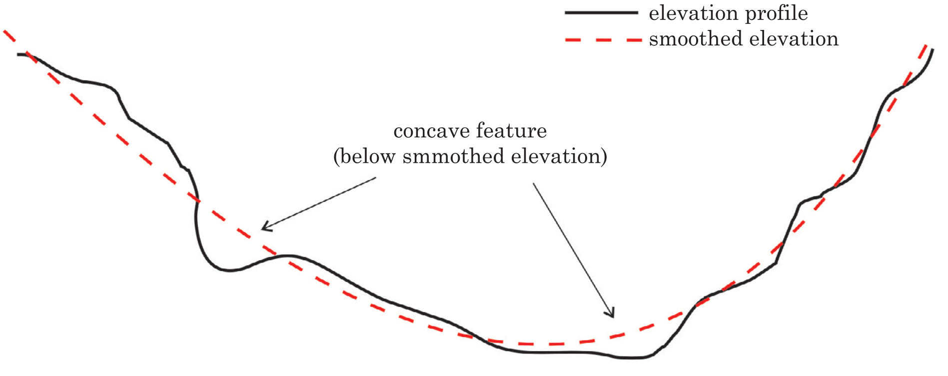

Fig. 1. Sample of concave features

Under some conditions the presence of concave forms can be a reason of accumulating material transported with the runoff of surface water. After a long period the accumulated material can change the surface characteristic for example by filling up the concave sites. This happens in areas covered with loose materials and high runoff intensity. Another case occurring in rural areas is filling sinks with organic matter derived from the decomposition of plants, and sometimes chemicals such as residuals of fertilizers and herbicides. Concave areas promote the accumulation of the water and due to the increased humidity may give an unfavourable environment for the growth of crops. As a result of excessive moisture at these sites anaerobic conditions may temporarily or permanently support decomposition processes. They are usually formed at local, mild synclinal forms, e.g. concave parts of the slopes. A dense measurement of the topographic surface is required to identify such features. Airborne Laser Scanning technology due to its ability to pass through openings in the canopy and to detect the underlying surface of the Earth can provide fairly dense data in forested or inaccessible areas. Measured points of the ground in areas usually obscured by vegetation support analytical methods of wetland delineation (UDWIG 2015) or channel networks mapping (KLADZYK 2015). This kind of measurement has been made recently by airborne laser scanning (ALS) in Poland in the frame of the ISOK (pl: Informatyczny System Osłony Kraju, national hazard protection information system) project. Airborne laser scanning (ALS) is now a widely used method of spatial data collection. With a combination of techniques for determining the position and the inclination of the measuring instrument (GPS, INS) and a system for measuring the flight time of a laser beam from its point of generation to the point of reflection and back it is possible to generate a point cloud representing the shape of the scanned surface. The scan frequency, and thus the density of the point cloud obtained is selected according to the needs and costs. The higher the frequency the more points are saved and thus the scanned object is mapped in a more detailed way. However, this increases the cost of data acquisition and generates larger files, and requires more resources during post processing. Laser scanning technology has been used already in Poland for a few years. Several domestic companies offer services in laser scanning. So far, studies were made locally and globally. Local studies include commercial tasks, e.g. the modernization of the rail network, or research and development for scientific institutions. The global studies include the ISOK-project as a part of an efficient system of the country protection against extreme hazards. The scanning was performed in years 2011–2013 during spring and autumn. In order to adapt to different terrain types scanning was done with two different setups. The first setup was defined for urban areas with a high point density of 12 points/m^2 while the second setup with a density of 4–6 points/m^2 was defined for the remaining area (KURCZYŃSKI, BAKUŁA 2012). After quality control the ISOK datasets have been made available as a part of National Geodetic and Cartographic Resource. Data such as point clouds in LAS format, orthophotos, digital terrain models and digital surface models are available for many applications. Now, high accuracy photogrammetric data are covering about 65% of the Polish territory. It is a good reference for comparative studies in different regions of the country because of its standardized data capture and processing, as well as the high up-to-dateness. The whole data was collected in relatively short time period so topographic situation shows same land use level. A digital terrain model (DTM) is one of the ISOK products. It was interpolated as a square grid based on the LIDaR point cloud. The best available resolution of the resulting gridded DTM is 1.0 m × 1.0 m. It is prepared on the basis of the point clouds obtained by the specification of the first and the second setup. According to the standard rules the DTM accuracy defined as the mean height error is assumed as 0.15 m for well defined uncovered area, and 0.25 m – 0.30 m for forested areas. The error of steep, hilly and forested slopes may be larger. The DTM has been saved as a text file containing the x, y, z coordinates. It is not associated with any specific software. Thus, it is possible to load the data into any GIS/CAD environment.

Methods

The topic of identifying and delineating concave forms was repeatedly addressed in scientific research. It is a very important issue regarding crisis management, natural disasters like floods, and other. The automatic methods of the localization of such sites by using a DTM could be applicable in many areas. The automatic methods are very helpful for some types of simulations based on the terrain shape, e.g. to determine the extent of the floods, to estimate probable losses and to plan preventive actions. A similar situation can happen in areas not covered by permanent flood monitoring, i.e. where no hazard maps are developed. There, problems of water management may happen due to the shape of the topographic surface. In such situations an overview of the DTM in conjunction with other available hydrographic survey materials helps to understand these phenomena and develop possible solutions, for example insulation or drainage (OBERSKI, SZCZEPANIAK 2013). Using GIS tools with DTM data on land use planning helps to find those areas which periodically collect water due to depressions. Such places inconvenient for several usages should be excluded from becoming construction sites (BIELSKA, OBERSKI 2014). Research carried out by the author showed the usefulness of GIS analysis using DTM data in locating natural bodies of water for undeveloped areas as methods to support landscaping (OBERSKI, ZARNOWSKI 2013).

An experiment was conducted in an area of an undeveloped agricultural region with comparatively little variation in the terrain shape over a long time. Due to the land use type (agricultural crops) it is possible to observe phenomena on the surface characteristic for different seasons, under different stages of plant growth, and „bare" earth. The location of the test area is shown on Figure 2.

It is located in the municipality of Stawiguda, district Olsztyn in Warmia-Mazury. The area has an undulated terrain. Glacier erosion as well as runoff, snowmelt and river water activities has formed the relief. The area is mostly plateau originating from the accumulation of moraines reaching up to a height of 120 m – 140 m above sea level. This upland has an early glacial terrain relief. The terrain's shape is undulating with convex forms (eskers, moraine hills) and concave forms as parts of river valleys and glacial. A characteristic feature

Fig. 2. Location of test area

of this area is the presence of numerous septic sinks and wells. Moraines have the form of individual, irregularly spaced hills (GLIŃSKA-LEWCZUK 2012). The detection of significant concave forms in the rural area can be done in-situ quite easily. However, this depends on periodically occurring factors such as time of year, hydrological conditions and vegetation cover. In the case of an impossible site's inspection archived photogrammetric materials can be used. The best and most independent data source is a DTM. The quality of the points of interest based on a DTM depends on its density and the height accuracy. If the DMT's grid is not dense, it is still possible to identify concave forms in regions of clearly distinguishable landforms such as saddles, sinks, and depression. However, due to a lack of visual comparison with surrounding points the boundaries of the concave areas are more difficult to determine in that way.

Of course, this method is not perfect and not suited for minor concave forms, especially those which define the characteristics of the terrain. Small discrete concave forms are not always found at the lowest parts of the study area. Due to irregularities of the terrain undulations they are often included in other landforms which do not exactly correspond to depressions. They may be located in a slightly concave parts of slopes or on hill tops. The examination of neighbouring cross sections is one of the primary method to determine recessed areas. This leads to the identification of barriers blocking superficial water runoff according to its average slope (OBERSKI, ZARNOWSKI 2012). Automatic or semi-automatic comparison of cross-sectional shapes allows the identification of concave forms. However, due to the two-dimensional nature of the analysis the delineation of those areas is only approximate.

The identification and the delineation of concave field forms is also possible with GIS tools. Software environments such as SAGA-GIS or ArcMap offer many opportunities to solve that task. Especially the Spatial Analyst Tools are very useful. By using several terrain analyst tools it is possible to find regions where surrounding points are higher and the slope is always directed to the inside. This phenomenon can occur anywhere on topographical surface, regardless of the height above sea level and its occurrence may not be related to the general direction of terrain slope. By applying a combination of ArcMap's Spatial Analyst functions Focal Flow, Flow Direction, Sink, Watershed, and Zonal Fill it is possible to recondition the DTM in order to create a „hydrologically correct" elevation model. A hydrologically correct elevation model is one in which every pixel in the surface slopes continually down gradient and out the edges of the elevation model boundaries. In this way concave terrain forms are filled in and equalized. Once they are filled, it is easy to locate differences between the original DTM and the corrected one. There are also several ways to find concave terrain features based on a DTM grid. The Topographic Position Index (TPI) is useful for landform classification which includes concave features. TPI is the difference between the cell elevation value and the average elevation of the neighbourhood (KOZIOŁ 2009).

$$\mathrm{TPI}(D)_i = h_i - \frac{\Sigma h_j}{n} \tag{1}$$

where:
h_i – height level in analysed cell,
h_j – height of cells that surrounds analysed cell,
n – number of surrounding cells.

The neighbourhood defines the extent of the area around the centre cell by defining a number of elevation points. Commonly used neighbourhood shapes are circle, rectangle or ring (circle with a circular hole). Usually, the type of the neighbourhood is selected empirically. Some researchers have used other shapes to distinguish specific forms. However, for this project a circular neighbourhood was used. Positive values of the TPI indicate a cell higher than its surroundings. Negative values indicate lower cells. TPI values around zero could either mean a flat area or a regularly sloped area.

The landforms classification needs more input data to give satisfactory results. Especially when TPI values are near zero it is necessary to check the terrain slope. Combination of slope and TPI values helps to distinguish between flat and constantly sloped areas. The size of the neighbourhood which determines the number of cells for computing the average elevation is crucial for the TPI values. It depends on the size of the neighbourhood, i.e. the radius of the circular area, the size of the rectangle, or the ring's radii. Therefore, TPI values depend on the scale factor describing the neighbourhood's size. The TPI is very scale dependent. In practice it is necessary to use several scale factors to choose the most convenient for a specific area. It is important because the TPI based landform classification may find a flat plain, convex forms or concave forms in the same location (JENNESS 2006). An example is shown in Figure 3.

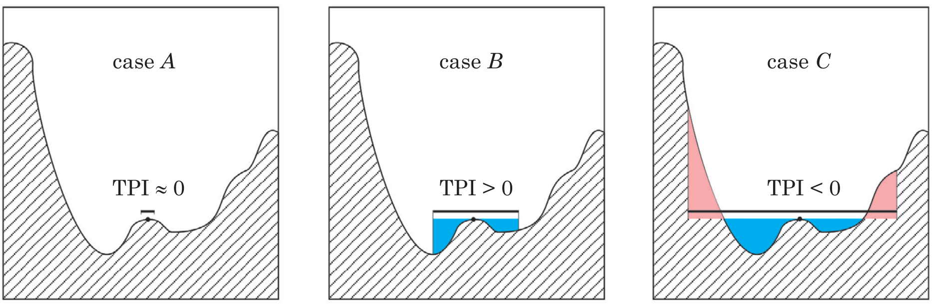

Fig. 3. TPI values for one location at three different scales (cases: *A* – small scale makes no difference between elevation of cell and neighbourhood, so TPI value is approximately 0; *B* – analyzed cell is distinctly higher then neighbourhood so TPI value is greater than 0; *C* – the neighbourhood includes the hills on either side of the valley, therefore, the analysed cell is lower than its neighbours and thus the TPI value is negative

Source: http://www.jennessent.com/downloads/TPI_Documentation_online.pdf, 2015.08.25.

The correct understanding of the scale as one of the main factors influencing the TPI values allows a precise analyses of the results. In general the TPI for the small scale enables the delineation of local hills and pits while the large scale helps to locate larger forms like valleys and mountains. Finally, the combination of two different scale factors (small and large) combined with slopes lead to the identification of 10 types of landform classification (WEISS 2001, JENESS 2006).

The Topographic Wetness Index (TWI) is another helpful analyst which is one of the quantitative measures describing the effect of topography on hydrological processes. The TWI indicates the relationship between the size of the area involved in surface water collection, and the value of its slope according to equation:

$$\mathrm{TWI} = \ln\left(\frac{\alpha}{\tan\beta}\right) \tag{2}$$

where:
α – catchment area,
β – slope measured in local cell.

The TWI shows the spatial distribution of moisture in the soil. Also, it shows the level of water saturation in soil based on topographic conditions (SØERSEN at al. 2006). The greatest values of the TWI are reached in areas of large surface water catchment and small slope. Topographically such places are usually very wet, so it could indicate the existence of concave forms (URBAŃSKI 2012).

Results and Discussion

The GIS software (ArcMap, SAGA-GIS) was used for the identification and delineation of concave forms in the test area. The ISOK DTM was the source data. This DTM is derived from ALS data. The scan density was in range of 6 to 12 points/m^2. The final DTM resolution is 1 metre. Declared by the manufacturer the height accuracy of the DTM is 15 cm. So this value has been adopted as the threshold below which all found locations are treated as concave terrain forms. The map with delineated concave forms was developed using tools for the surface terrain analysis (Fig. 4).

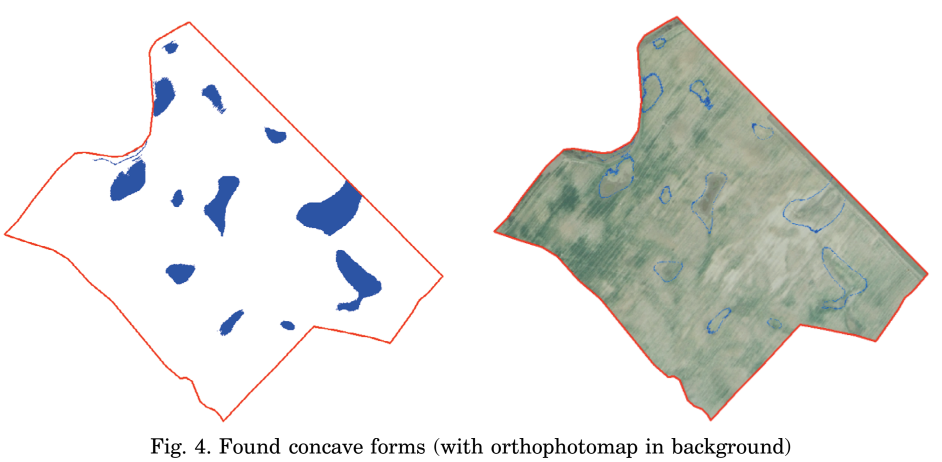

Fig. 4. Found concave forms (with orthophotomap in background)

At first, the TPI index was calculated. The circular shape was used to determine the neighbourhood's average terrain elevation of each DTM cell. Several sizes of radii (scale factor) of the neighbourhood were tested. The large scale (large radius) gave a few large concave features while using a small scale generated a lot of various small forms. An example of different scaled TPI maps is shown in Figure 5.

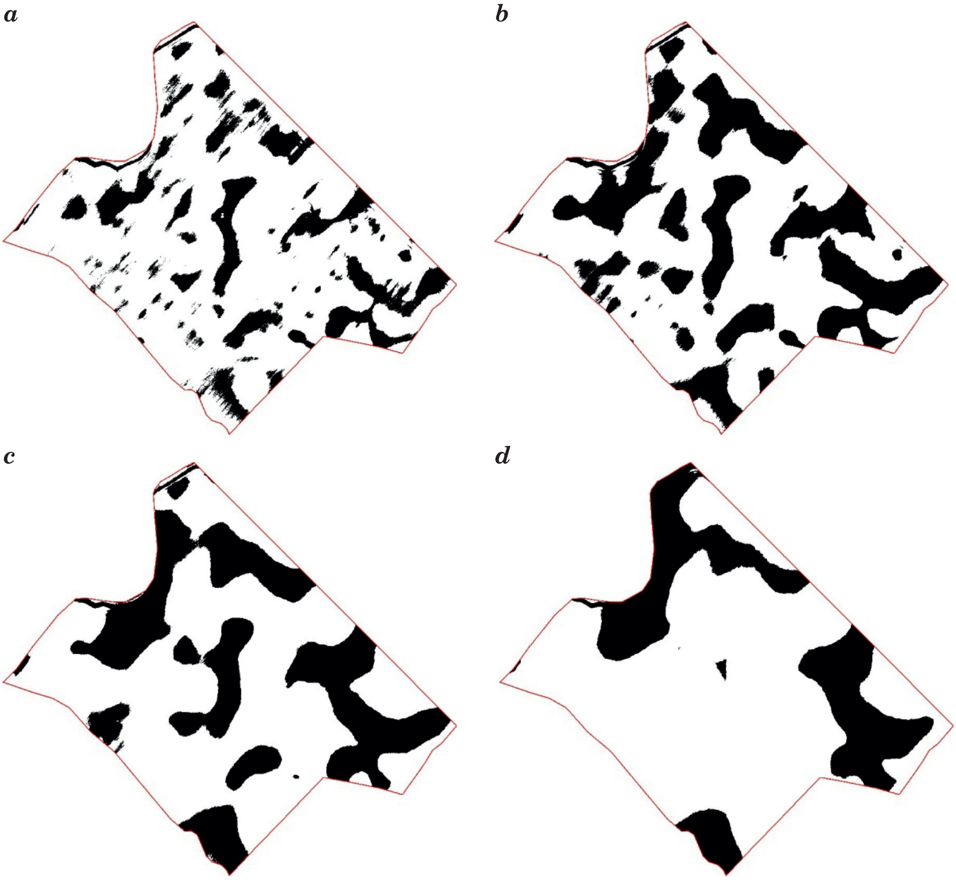

Fig. 5. Low values of TPI index at 4 different scales: *a* – 25 m, *b* – 50 m, *c* – 100 m, *d* – 300 m

Two most appropriate scales (radii) were selected (radius 25 m and 100 m). Using such TPI maps allows to combine small and large forms. In a second step the classification of the land forms were done. The combination of small and large scales gives 10 different types of the landform (WEISS 2001). The main topic of the experiment was finding concave forms. Thus, only such forms were analysed. The previous classification was reduced to forms which are naturally lower than their surroundings. Finally 5 different landforms were qualified as representative. There were: canyons, deeply incised streams, drainages mid-slope, shallow valleys and u-shaped valley. Figure 6 presents chosen landforms combined with previously delineated concave forms.

In additional the TWI index map for the test area was created. Large TWI values could indicate wetness in specific regions which is usually positively

Fig. 6. Selected landforms and delineated sinks

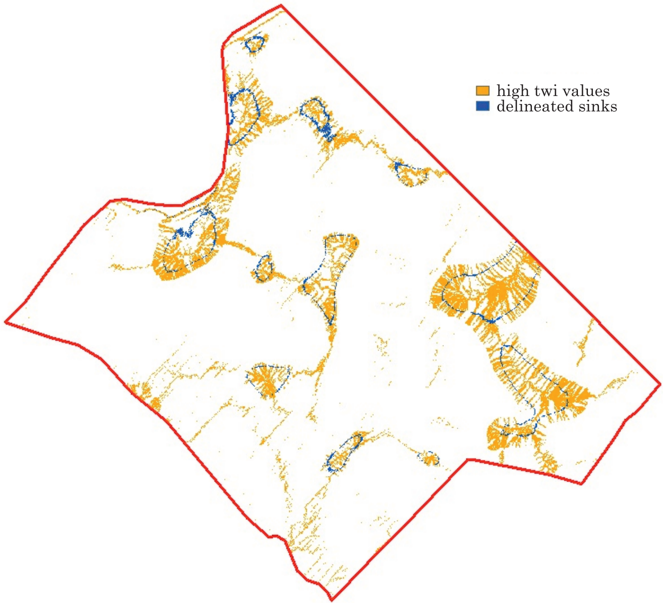

Fig. 7. The TWI highest values and delineated sinks

correlated to the shape of the analysed terrain, a concave form and its higher neighbourhood. The slope around such a depression is always directed inside. In the vast majority of cases such locations are concave forms. If they have a longish shape it often coincides with the direction of the water flow. In this experiment the highest values of the TWI have a similar location as the previously delineated concave objects and concave forms found using the TPI classification. The results are shown in Figure 7.

Conclusion

The precise delineation of concave forms is not an easy task, both in-situ and in the laboratory based on an DTM. We should remember that the correctness of the findings based on a DTM not only depends on its height precision but also on its resolution. The ISOK's DTM is interpolated from a point cloud captured by ALS. Obviously, filtering and classification of the ALS points led to a lower point density as declared by the data distributor. In fact, the density of 4–6 points/m^2 is probably not guaranteed everywhere. The grid is the result of an interpolation. It always approximates the shape of the topographic surface. Accordingly, small landforms could be smoothed. Consequently, they are impossible to be identified on the basis of this data. The results of the experiment show that the DTM of the ISOK project allows finding the boundaries of the concave forms in the tested area. Generally, in most cases the found concave forms have the correct location. However, their borders differ from those found by the TPI landform classifier. Attention should paid to the fact that TPI and TWI classified some regions as concave while the ArcGIS functions did not give any indications. This may mean that the forms are shallower (less than 0.15 m below the surrounding) and thus omitted due to the threshold of the height accuracy of the DTM. The method of searching concave forms based on the DTM can be very useful for every kind of terrain, especially difficult and non-accessible regions. The method has some limitations, among others a not fully reliable border detection. However, it showed that the analysis of the DTM data regarding small and larger land forms can be performed successfully. The ISOK DTM is currently the most reliable and quite accurate data source on the topographic surface of the majority of the Polish territory. It is a good foundation for various analyses. We can expect that through the development of new measurement techniques, hardware and software the DTM will in the future be even more precise which certainly will lead to even better analytical results.

References

BIELSKA A., OBERSKI T. 2014. *Wyłączenie spod zabudowy gruntów nadmiernie uwilgotnionych klasyfikowanych za pomocą narzędzi GIS*. Infrastruktura i Ekologia Terenów Wiejskich, II(2): 411–421.

GLIŃSKA-LEWCZUK K. 2011. *Mapa hydrograficzna w skali 1:50000, arkusz N-34-77-D Olsztyn*. *Komentarz do mapy hydrograficznej w skali 1:50000, arkusz N-34-77-D Olsztyn*. Główny Urząd Geodezji i Kartografii, Warszawa.

JENNESS J. 2006. *Topographic Position Index (TPI) v. 1.2*. http://www.jennessent.com/downloads/TPI_Documentation_online.pdf (access: 25.08.2015).

KLADZYK A.G. 2013. *GIS feature extraction tools in diverse landscapes.* Department of Environmental and Water Resources Engineering, University of Texas at Austin. http://www.caee.utexas.edu/prof/maidment/giswr2013/Reports/Kladzyk.pdf (access: 30.12.2015).

KOZIOŁ K. 2009. *Numeryczny model terenu dla wielorozdzielczej/wieloprezentacyjnej bazy danych przestrzennych*. Geomatics and Environmental Engineering, 3(1/1): 69–80.

KURCZYŃSKI Z., BAKUŁA K. 2012. *Generation of countrywide reference digital terrain model from airborne laser scannig in isok project.* Archiwum Fotogrametrii, Kartografii i Teledetekcji, Warszawa, p. 59–68.

OBERSKI T., SZCZEPANIAK-KOŁTUN Z. 2013. *Określania obszarów lokalnych podtopień na podstawie nmt i bazy hydro*. Roczniki Geomatyki, 11[2(59)]: 79–85.

OBERSKI T., ZARNOWSKI A. 2013. *Analiza wpływu rzeźby terenu na kształtowanie krajobrazu przyrodniczego i jego zagospodarowanie.* Inżynieria Ekologiczna, 33: 86–95.

OBERSKI T., ZARNOWSKI A. 2012. *Pozyskiwanie naturalnych zbiorników wodnych na podstawie numerycznego modelu rzeźby terenu i narzędzi GIS.* Infrastruktura i Ekologia Terenów Wiejskich, 1(3): 151–164.

SØRENSEN R., ZINKO U., SEIBERT J. 2006. *On the calculation of the topographic wetness index: evaluation of different methods based on field observations.* Hydrology Earth Systems Science, 10: 101–112.

UDVIG T. 2015. *Use of a Lidar Based Model for Remote Sensing of Ephemeral Wetlands in Anoka County, Minnesota USA*. Papers in Resource Analysis, 17: 12.

URBAŃSKI J. 2012. *GIS w badaniach przyrodniczych*. http://ocean.ug.edu.pl/~oceju/CentrumGIS/dane/GIS_w_badaniach_przyrodniczych_12_2.pdf (access: 31.08.2015).

WEISS A. 2001. *Topographic position and landforms analysis*. Poster Presentation, ESRI User Conference, San Diego, CA.

Technical Sciences, 2016, 19(1), 71–81

Quarterly peer-reviewed scientific journal
ISSN 1505-4675
e-ISSN 2083-4527
TECHNICAL SCIENCES
Homepage: www.uwm.edu.pl/techsci/

CONTROL OF MINDSTORMS NXT ROBOT USING XTION PRO CAMERA SKELETAL TRACKING

***Łukasz Żmudziński*[1], *Adam Augustyniak*[1], *Piotr Artiemjew*[2]**

[1] Robotic Circle
University of Warmia and Mazury in Olsztyn
[2] Department of Mathematics and Computer Science
University of Warmia and Mazury in Olsztyn

Received 28 July 2015; accepted 1 December 2015; available online 7 December 2015.

Key words: skeletal tracking, robot control, multi-user control, openGL.

Abstract

This paper focuses on the topic of creating a gesture-oriented user control system for robotic agents. For testing purposes we have used a Lego Mindstorm NXT self-designed robot and a Xtion Pro camera. Our construction consists of a NXT brick and three motors (two used for movement and one for the clutch mechanism). Our software is developed using C++ with NXT++ and OpenNi/NiTe libraries. System tests were performed in a real environment.

Introduction

In this work we present our gesture-oriented robot control system using C++ and the opensource libraries: NXT++ and OpenNi/NiTe. We explain the process of gathering user skeletal data (*OpenNi library for C++*. 2014) and transferring it into robotic movement (WALKER et al. 2014). The project was made as a part of (*OpenNi library for C++*. 2014). Lego Mindstorm acts only as a transmitter and all the calculations are done on a different machine.

The paper is divided in the following sections: section 2 presents information on the used libraries, section 3 describes the algorithm, section 4 shows

Correspondence: Piotr Artiemjew, Katedra Metod Matematycznych Informatyki, Uniwersytet Wrmińsko-Mazurski, ul. Słoneczna 54, 10-710 Olsztyn, phone: 89 524 60 82, e-mail: artem@matman.uwm.edu.pl

real life usage of the system and section 5 concludes the paper and shows future possibilities. Now we will show you, what are the reasons that motivated us in creating the project.

Motivation

Our main goal in creating the system is allowing the user to perform robotic movement with simple gestures; alone or in a team. We wanted to gather data on how well it performs compared to other steering methods and what possible use such a system could have in real world. Apart from that this is the first use of the connection between the provided libraries and making them work together. With that in mind, we would like to present some similar works by other authors.

Related Works

There are a few papers on the subject, but some of them especially caught our interest. The first one shows a mobile robot with Kinect on-board that tracks human movement and tries to keep the user in view of the camera (MACHIDA et al. 2012). Next paper (KOENEMANN, BENNEWITZ 2012) tracks human movement with a kinect-like device and transfers the data so that the robot agent mimics the moves. Third system focuses on usage of hidden Markov models (HMMs) to spot and recognize gestures captured with a data glove (IBA et al. 1999).

Library information

In this section we will show short information about the core libraries we used in our project – NXT++ (WALKER et al. 2014) and OpenNi/NiTe (*OpenNi library for C++*. 2014).

NXT++

In our project we use NXT++ for the sole purpose of accessing and steering our robotic agent. The library contains methods, that allow connection to the brick and motor movement invoked as follows:
‖ NXT: :OpenBT(&comm)

Opens the bluetooth communication with the Lego NXT brick.

```
NXT: : Close(&comm);
```

Closes bluetooth communication.

```
NXT: : Motor : : Stop(&comm, port, brake);
```

Stops the motor at a specified port and sets, if the motor should use brakes.

```
NXT: : Motor : : SetForward(&comm, port, speed);
```

Sets the forward movement speed of a motor at a specified port.

```
NXT: : Motor : : SetReverse(&comm, port, speed);
```

Sets reverse movement speed of a motor at a specified port.

OpenNi/NiTe

OpenNi is a framework for natural interfaces (human-machine interface that is invisible to the user, who continuously learns increasingly complex interactions). NiTe is a module for OpenNi which focuses on seeing gestures and user limb movement.

The NiTe module allows us to assign each limb that we have interest in with a single method and then read the position values in three-dimensional space. Here is an example taken from our project that manages the right hand skeletal point movement of the application user:

```
joints . insert
(
pair<string , const nite : : SkeletonJoint>
(
''right hand'' , user . getSkeleton (). getJoint ( nite : :JOINT RIGHT HAND)
)
);
if ( joints [ ''righthand'' ] . getPositionConfidence () > .5)
{ positions [ ''righthand'' ] [ ;x ; ] = joints [ ''righthand'' ] . getPosition (). x;
positions [ ''righthand'' ] [ 'y '] = joints [ ''righthand'' ] . getPosition (). y;
positions [ ''righthand'' ] [ 'z '] = joints [ ''righthand'' ] . getPosition (). z ; }
```

Firstly we add the right hand of the tracked user to the *joints* table and call it "right-hand". Then we read the x, y and z values of the joint (only if the confidence is higher than 50%, lower values can lead to corrupted results) and assign it to the added pair. This segment is looped in time so that we always get current position values.

Algorithm

Before we start going deep into the algorithm, we show the pseudocode below, which explains roughly how the whole process happens. We can divide it in three parts: initialization, data gathering and sending output commands depending on user selection and gestures. If the connection fails, the user is notified about the problem and the application stops.

```
IF connection to NXT established AND camera working
    User selects steering method
REPEAT ( Infinite )
Read camera data
    Find user skeleton
Assign joints
    Read three–dimensionaląpositions of joints
SWITCH steering mode
    IF joint positions in steering mode specified position
Send specific commands to NXT
ELSE
OUTPUT no connection message
```

The first part of the algorithm focuses on connections with the hardware and setting user preferences when it comes to steering methods, that he will be using. We start with checking the connection with the camera by executing the following command: ‖openni : : Status rc = openni : : OpenNI : : i n i t i a l i z e ();

If the return value is true, we proceed to establishing communication with our Mindstorm NXT robot. To achieve this, we need to call the OpenBT method as follows:

```
if (NXT: :OpenBT(&comm))
{
mindstrom _connection _open = true ;
} else
{ printf (’’Can ’ t_ _connect to
Mindstorm’ );
return openni : :STATUS ERROR;
}
```

Just like before, if the value is true we continue to the user interface communication screen. In both cases if the value turns out to be false the program exits with an error message.

Now is the time that the user can select the steering method of his choice. He has three possible inputs:

1. Simple steering
2. Depth steering
3. Steering with clutches support

The methods vary in complexity of the gestures that the user can perform to steer the robot. *Simple steering* operates only within the X and Y axes. *Depth steering* and *Steering with clutches support* both add the Z axis, with the second of them using additional motors.

When the user accepts his choice, we proceed to the second part of the algorithm, that focuses on gathering limb information and processing the data for future purposes.

We start with gathering the camera data through the OpenNi/Nite library. To check, if we can continue we compare the value of the skeleton state, that the NiTe library returns after using the following method: users [i] . getSkeleton (). getState ();

The possible states that are returned are:

– SKELETON_NONE
– SKELETON_CALIBRATING
– SKELETON_TRACKED

Of course to continue with the gesture system, the skeleton must be tracked (without this, the algorithm will come to a stop).

Now we assign the joints, just like it was explained in section 2.2 of this paper. The whole skeleton representation in NiTe consists of 15 elements (Fig. 1), each of them having an unique name and that allows us to track all of them in a manner that fits our needs.

Once we get the position of each joint it is time to move onto the third and last part of our application – steering the robotic agent using NXT++.

Considering that we are connected to our NXT brick, the only thing that is left is to send specified commands. We achieve this by using the methods that were introduced in section 2.1. Of course to move the robotic agent we will only use the *SetForward*, *SetReverse* and *Stop* functions. Each of the steering methods has a different gesture system, that is why we will only show how the gestures are tracked and the complete steering guide will be explained in the next section (Testing).

As we already know, the joint positions are updated every frame, so the only thing that is left is to compare the values and execute specific NXT++ commands as follows:

```
if ( positions [ joint name a ] [ 'z '] >
positions [ joint name b ] [ 'z ' ] +
precisionX
&& positions [ joint name c ] [ 'y ' ] >
```

```
 positions [ joint name d ] [ ’y ’ ] +
precisionY )
{
NXT: : Motor : : SetForward(&comm, port, speed );
   NXT: : Motor : : SetForward(&comm, port,
      speed ); }
```

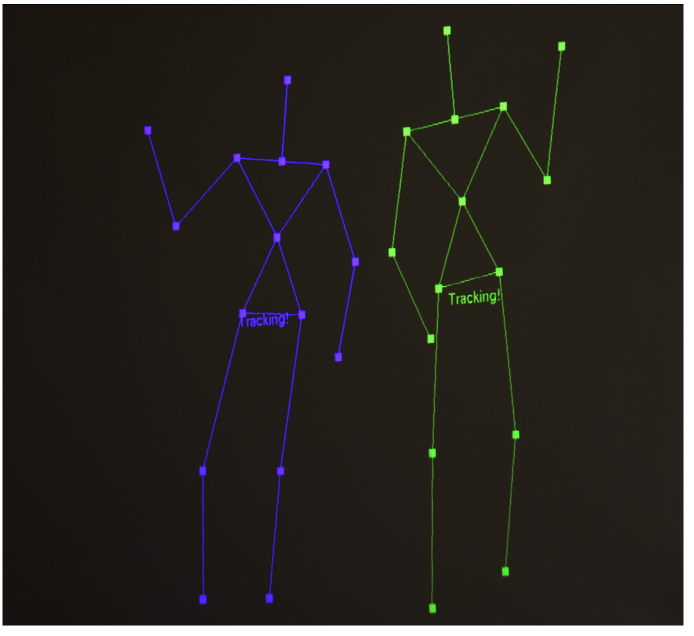

Fig. 1. Skeleton points

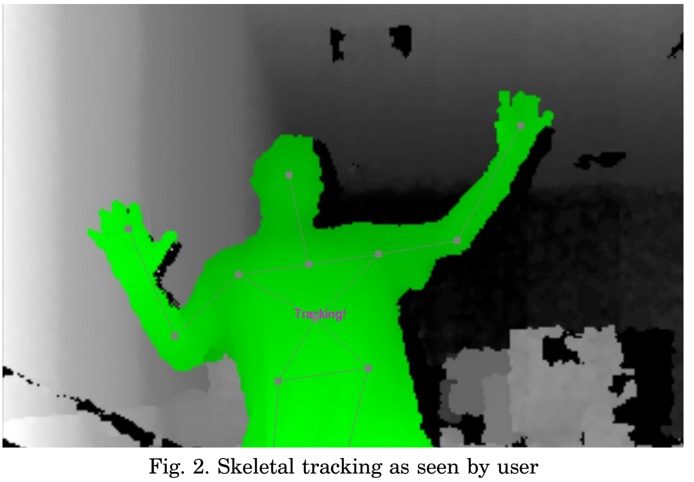

Fig. 2. Skeletal tracking as seen by user

As you can see, we introduced additional variables – precisionX and precisionY.

We use them to overcome the unwanted results with minimal movement of the users limbs. When none of the conditional statements are met, all the motors are stopped using the *Stop* method. The precision parameter was chosen in an experimental way, being highly dependent on the computer that was used. The parameter can be negative – but it's not recommended because we never encountered a situation where this would be needed.

When the user finished using the application, he can close the application by making a specific pose – crossing his arms on his chest for the time specified on the screen. It is explained in the following pseudocode:

```
IF user is detected
GET user pose status
IF pose entered
OUTPUT Show countdown message
Start timer
ELSE IF pose exited
Output Show interrupt message
Stop timer
    ELSE IF pose is held
IF countdown completes
      Finalize connections
```

Working copy of actual algorithm code with instructions can be found on *NXT-XTION project* (2015).

Testing

Testing was an important part of the whole process, focusing on working aspects of the code in real life situations using actual hardware (ŻMUDZIŃSKI, AUGUSTYNIAK 2015). We divided this operation into the following phases:
- Camera connection and usage,
- NXT brick bluetooth connection, – Getting it all: steering methods.

Robot construction

In our tests we are using two robots – Black Claw (a robot built specifically for this project based on the Tribot model, *LEGO NXT Tribotąbuilding instructions*) and the Silver Shadow (ARTIEMJEW 2015). Our robot is constructed from various NXT specific parts. The main processor is located in the NXT Intelligent Brick 2.0 which features a powerful 32-bit microprocessor and Flash memory. It also supports bluetooth that allows us to establish a connection. The brick is linked with motors and sensors. Black Claw is using three engines – two for steering and movement and one for clutching. Apart from the input devices it is also using a LEGO Ultrasonic Sensor, which measures the distance to the closest object in front of the robot. All the parts are linked with connector cables with RJ12 plugs. The main frame is built from various LEGO parts.

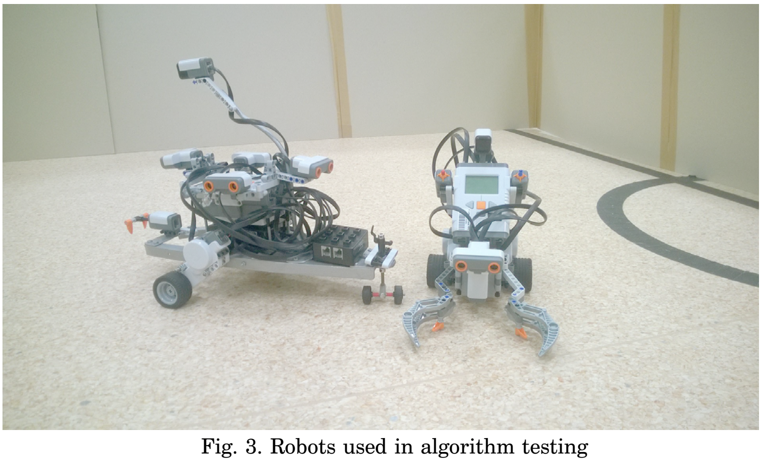

Fig. 3. Robots used in algorithm testing

Testing process

Camera connection and usage

First of all we started a self-written camera testing tool. The tool was written for the sole purpose of checking, if the camera works properly. When we finished installing all the drivers for XTion Pro camera we fired the mentioned application. We only encounter mediocre problems, that we corrected instantly within the code. After that we moved to the next step of our testing process.

NXT brick bluetooth connection

The main problem we met, was that the devices couldn;t find each other and then successfully pair (it was a hardware problem). After several tries and replacing bluetooth receivers, we finally managed to connect the robot with the main machine. After this, the connection was easily established and returned positive values in our code. Then we proceeded to testing the whole algorithm.

Getting it all: steering methods

To test the steering methods, we needed to run the application and get through all the previous steps. While testing, we got to the conclusion that the camera is not as accurate as we would want. Considering that fact, we had to add a precision parameter to all the gesture readings, to get the results within the minimal error margin. With three steering methods to pick, we had to test each of them respectfully. The testing resulted in making small amendments in all of them. Most changes were made to adjust the precision and the location collisions between joints. Moreover we modified the gesture system to make it easier for the user to transfer between different orders.

The final steering methods look as follows:

1. Simple steering
   - Forward movement
     Right hand directly above right shoulder (y-axis).
   - Reverse
     Left hand directly above left shoulder (y-axis).
   - Turn left
     Right hand above shoulder (y-axis) and left from right shoulder (x-axis).
   - Turn right
     Right hand above shoulder (y-axis) and right from right shoulder (x-axis).
2. Depth steering
   - Forward movement
     Right hand above shoulder (y-axis) and closer to the camera (z-axis).
   - Reverse
     Left hand above shoulder (y-axis) and closer to the camera (z-axis).
   - Turn left
     Left hand between shoulder and hip (y-axis), to the left of torso (x-axis).
   - Turn right
     Right hand between shoulder and hip (y-axis), to the right of torso (x-axis).
3. Steering with clutches support
   - Forward movement
     Right hand to the right of hip (x-axis).
   - Reverse
     Left hand to the left of hip (x-axis).
   - Turn left
     Left hand closer to the camera (z-axis).

– Turn right
  Right hand closer to the camera (z-axis).
– Open clutches
  Right hand directly above right shoulder (y-axis).
– Close clutches
  Left hand directly above left shoulder (y-axis).

The gesture system is constructed in the simplest possible way. Because of that, some gestures have a priority over others e.g. in the simple steering method lifting both hands over the shoulder will result in running the Forward movement method.

Additional testing

During the tests we checked how will the algorithm function when other users enter the scene as seen in Figure 4. Additional users are tracked and coloured respectfully in the process, but their movement doesn't affect the gesture system.

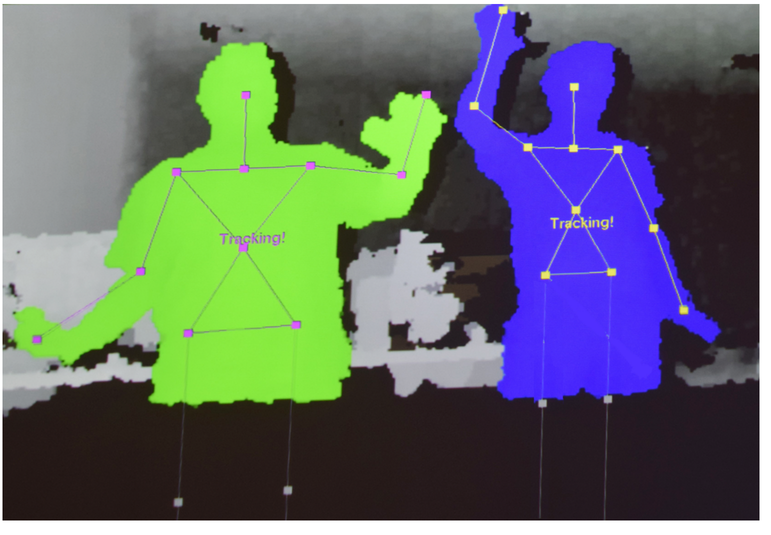

Fig. 4. Multi user test

Conclusions

The results of these experiments indicate that the combination of NXT++ with OpenNi/NiTE proved to be optimal. What is more its very easy and intuitive to add new kinds of steering methods. It comes from the fact that the whole process of assigning and reading joints and then transferring the gathered data through NXT++ to the agent is assimilable and fluid.

Focusing on understanding NiTE and OpenNI was the key to make the algorithm as simple as possible. This libraries enabled us to work freely with Xtion Pro camera and get the results fast from the very start.

Downloading data from Xtion Pro camera and skeletal tracking was necessary to give us the possibility to send various commands to the robot later. This part of the work is the most beneficial, because it creates a lot of future possibilities.

Thanks to the work of Piotr ARTIEMJEW (2015) we could use the NXT++ libraries which prove to be irreplaceable in making our robot controls. It was very comfortable to reconfigure data from the camera to create commands with NXT++.

Future works may develop more sophisticated usage of this kind of steering for example robot fights or delivering things without touching them. Of course gesture steering can be applied to other robots/machines like mechanical arms or humanoids (NAO) or even flying drones. Possibilities are nearly inexhaustible.

Acknowledgements

The research has been supported by grant 1309-802 from Ministry of Science and Higher Education of the Republic of Poland.

References

ARTIEMJEW P. 2015. *The localization of Mindstorms NXT in the magnetic unstable environment based on histogram filtering*. Conference: International Conference on Agents and Artificial Intelligence 2015 (ICAART2015), At Lisbon, Portugal, p. 341–348.

IBA S., WEGHE J.M.V., PAREDIS C.J.J., KHOSLA P.K. 1999. *An architecture for gesture-based control of mobile robots*. International Conference on ''Intelligent Robots and Systems'', IROS'99. Proceedings. IEEE/RSJ. Vol. 2.

KOENEMANN J., BENNEWITZ M. 2012. *Whole-body imitation of human motions with a Nao humanoid*. 7th ACM/IEEE International Conference on ''Human-Robot Interaction'' (HRI).

LEGO NXT Tribot building instructions. https://education.lego.com/dadk/lesi/support/product-support/mindstorms-education-nxt/nxt-base-set-9797/building-instructions.

MACHIDA E., CAO M., MURAO T., HASHIMOTO H. 2012. *Human motion tracking of mobile robot with Kinect 3D sensor*. Proceedings of SICE Annual Conference, Akita, p. 2207–2211.

NKR-UWM Robotic Circle of University of Warmia and Mazury. 2014. http://www.uwm.edu.pl/nkr/.

NXT-XTION project. 2015. https://github.com/nkruwm/nxt-xtion.

OpenNi library for C++. 2014. https://code.google.com/p/simple-openni/.

WALKER C., BUTTERWORTH D., ARTIEMJEW P. 2014. *NXT++ library*. https://github.com/cmwslw/nxt-plus-plus, http://wmii.uwm.edu.pl/~artem/downloads.html.

ŻMUDZIŃSKI Ł., AUGUSTYNIAK A. 2015. *Gesture system algorithm video presentation*. https://youtu.be/JppRyd3Vk1c.

Technical Sciences, 2016, 19(1), 83–92

Quarterly peer-reviewed scientific journal
ISSN 1505-4675
e-ISSN 2083-4527
TECHNICAL SCIENCES
Homepage: www.uwm.edu.pl/techsci/

INFLATION SIMULATION OF TRACTOR RADIAL TIRE

Józef Pelc

Department of Mechanical Engineering and Fundamentals of Machine Design
University of Warmia and Mazury in Olsztyn

Received 3 September 2015; accepted 28 December 2015; available on line 2 January 2016.

Key words: pneumatic tire, tractor, inflation, simulation, finite element modeling.

Abstract

The possibility of prediction of some parameters of large-size pneumatic tire was presented. Author's computer program based on the finite element method with the use of axisymmetric tire model was utilized. Material constants required for the tire analysis were determined experimentally. The procedure for obtaining a simplified axisymmetric tire tread was described. The method used for simulation of tire inflation process allows obtaining the shape of an inflated tire, forces in cords and elastic energy density distribution. A test tire overall dimensions obtained in this way are close to measured values.

Introduction

Until recently, the work of pneumatic tires designer was more like the work of a shoemaker than the engineer-designer. In his activity was something of craft and even of art. One had to put a lot of work, because it was necessary to design the tire profile in the vulcanization form in such a way, that after tire mounting on the rim and inflating, the required overall dimensions, i.e. diameter and width, were being obtained. To realize the difficult task nomograms by BIDERMAN et al. (1967) were helpful. This method of tire design was based on a net model of tire where the influence of rubber on the shape of inflated tire was neglected. The huge advances in computer technology made it possible to speed up tire designers' work. However, in Poland only in the

Correspondence: Józef Pelc, Katedra Mechaniki i Podstaw Konstrukcji Maszyn, Uniwersytet Warmińsko-Mazurski, ul. M. Oczapowskiego 11, 10-719 Olsztyn, phone: +48 89 523 49 31, e-mail: joseph@uwm.edu.pl

eighties there were attempts to automate this task (KONDEJ 1982). In the area of engineering activities, works by PELC and PETZ (1988, 1994) have provided effective, industry-verified design tools.

The finite element method enabled more advanced modeling of pneumatic tire deformation. Although its origins date back to the 1950s, in the field of pneumatic tires it has been applied only in the 70s (DUNN, ZOROWSKI 1970), while in Poland in the 90s (PELC 1992). This is due to the fact that from the view of the mechanics of deformable body, the pneumatic tire is a very complicated structure.

Today, the large-scale farms are being supplied with ever-larger power tractors. Pneumatic tires play a significant role in the effective use of these powers, determining the agriculture equipment productivity. Tire engineers have made a significant contribution to the process of increasing the efficiency of agricultural tractors through the development of radial tires. Compared to conventional tires, i.e. bias tires, radial ones are characterized by greater tread durability, less pressure on soil, more pulling power and a higher ride comfort (SKOCZEK 1995). Bearing in mind the reliability of the machines fitted with tires, tire manufacturers have been incorporated latest calculation methods into the tire design process. Due to the high efficiency in modeling of complex structures, the finite element method was mostly used (DEESKINAZI, RIDHA 1982, HEISE 1987, NANKALI et al. 2012).

The aim of the study is to examine the possibility of predicting some of the parameters of large-size tire using own computer program based on the finite element method and axisymmetric tire model. The way of the inflation process simulation for tractor radial tire is shown. A manner of simplified presentation of the geometrically complex actual tire tread, consisting of tread lugs smearing was proposed. The obtained results in the form of inflated tire shape, forces in cords, elastic energy density distribution are valuable for the tire designer allowing him to improve the structure. Overall dimensions of the test tire obtained from the simulation show good agreement with measurement results.

Characteristic of the modeled tire

Figure 1 shows a view of the actual tire for which the calculation model will be built and inflation simulation will be performed. This is the 14.9R28 radial agricultural tire, designed for rear drive wheels of tractors. The tire is a product of Stomil Olsztyn tire manufacturer. Tire parts within its profile are depicted in Figure 2. Nominal inflation pressure for the tire is equal to 160 kPa.

An inner tire profile in a mould and profile of the tire mounted on W12×28 rim are shown in Figure 3. It was assumed that, in the latter case, there was a pressure equal to zero in the tire. In fact, in this state, the pressure was equal to 10% of nominal one for the tire to ensure contact between the tire bead and the rim flange. During the simulation process the shape of tire profile was treated as its reference (initial) configuration.

Measurements of the overall dimensions of the tire, i.e. outer diameter and width, were performed on the randomly selected two prototype tractor tires. The diameter of the tire was determined by measuring its circumference. The

Fig. 1. Tractor radial tire 14.9R28

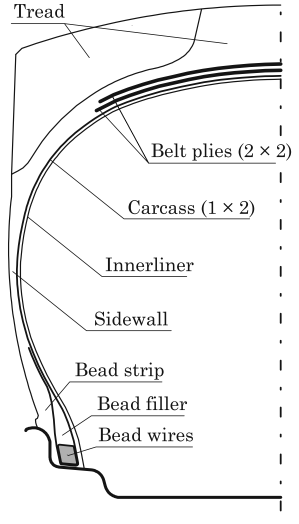

Fig. 2. Tire constituent elements within its cross-section

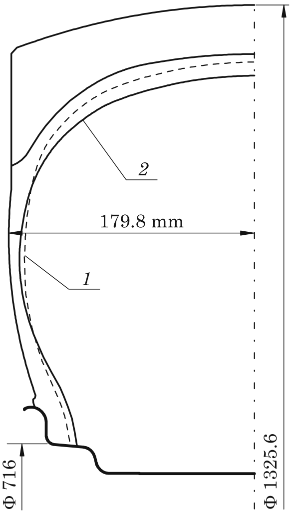

Fig. 3. Tire profile: *1* – in form (inner), *2* – after mounting on rim

Table 1

Measurement results of tire overall dimensions

Tire No.	Pressure kPa	Perimeter mm	Diameter mm	Width mm	Results of width measurement mm			
1	0	4161	1324.5	360.2	360.1	363.0	358.8	358.8
2	0	4168	1326.7	359.1	363.0	358.6	354.8	360.0
Average			1325.6	359.6				
1	160	4211	1340.4	364.6	364.7	365.0	364.6	364.2
2	160	4206	1338.8	369.1	367.5	369.5	369.7	369.8
Average			1339.6	366.8				
Changes in overall dimensions			14.0	7.2				

width of each tire was calculated as average value of the widths measured in four locations determined by quadrant points of the tire equator. The measurement results for the inflation pressure equal to zero and for the nominal pressure p = 160 kPa are shown in Table 1.

The tire carcass is made of two layers of polyamide cord, belts – four layers of rayon cord and the bead – 56 coils of steel wires. Young moduli of cord materials were determined on the basis of tensile tests:

– polyamide cord – E_p = 4428.8 MPa for effective yarn diameter d_p = 0.5 mm,

– rayon cord – E_r = 8383.6 MPa for effective yarn diameter d_r = 0.7 mm.

Shear moduli of purely rubber materials were determined by measuring their hardness. The relationship between hardness and Kirchhoff modulus has the form (PĘKALAK, RADKOWSKI 1989):

$$\mathrm{G} = 0.086 \cdot 1.045^{\mathrm{HSh}} \text{ [MPa]} \tag{1}$$

were HSh – rubber hardness measured by Shore durometer (scale A).

The results of measurements and calculations are shown in Table 2.

Table 2

Hardness and shear modulus for tire rubbers

Tire part	Shore A hardness (HSh)	Kirchhoff modulus [MPa]
Tread	65	1.50
Sidewall	53	0.89
Bead strip	75	2.33
Bead filler	70	1.87
Innerliner	65	1.50

Computational tire model

Deformation of pneumatic tire treated as a deformable continuum is described by differential equations of mechanics of continuous media:

$$\mathrm{div}\ {}_0^t\mathbf{T}({}^0\mathbf{X}, {}_0^t\mathbf{X}) - {}_0^t\mathbf{f} = \mathbf{0} \tag{2}$$

where:

${}^t\mathbf{T}$ – the first Piola-Kirchhoff stress tensor in configuration t with respect to configuration 0 (initial configuration),

${}^{0}\mathbf{X}$ – a material particle coordinate in initial configuration,
${}^{t}\mathbf{X}$ – deformation gradient,
${}^{t}\mathbf{f}$ – body force vector.

To obtain stresses and deformation of an elastic body the equations (2) is supplemented with strains-displacements and constitutive relations.

In the presented analysis of tire inflation by the use of the finite element method, an important role play a weak form of the problem:

$$\int_{{}^{0}V} \delta\, {}^{t+\Delta t}_{0}\mathbf{E} \cdot {}^{t+\Delta t}_{0}\mathbf{S}\, {}^{0}dV = {}^{t+\Delta t}L \tag{3}$$

where:
$\delta\, {}^{t+\Delta t}_{0}\mathbf{E}$ – variation of Green-Lagrange strain tensor,
${}^{t+\Delta t}_{0}\mathbf{S}$ – the second Piola-Kirchhoff stress tensor,
${}^{0}V$ – volume of the body in configuration 0,
${}^{t+\Delta t}L$ – virtual work of externally applied loads.

From (3) it follows FEM equation for determining the locations of model nodes in the consecutive states of balance for tire being inflated (BATHE 1982).

The main load carrying constituent elements of the pneumatic radial tire are shown in Figure 2. The deformation of the tire caused by internal pressure is characterized by moderate strains in its materials, and therefore a linear relationship between stresses and strains was assumed. Constitutive relationship for such a material written in the principal orthotropy axes has the form:

$$\mathbf{S}=\frac{1}{V}\begin{bmatrix} E_1(1-v_{23}v_{32}) & E_2(v_{12}+v_{13}v_{32}) & 0 & E_3(v_{13}+v_{12}v_{23}) & 0 & 0 \\ & E_2(1-v_{13}v_{31}) & 0 & E_3(v_{23}+v_{21}v_{13}) & 0 & 0 \\ & & V\cdot G_{12} & 0 & 0 & 0 \\ & & & E_3(1-v_{12}v_{21}) & 0 & 0 \\ & sym. & & & V\cdot G_{13} & 0 \\ & & & & & V\cdot G_{23} \end{bmatrix}\cdot\mathbf{E} \tag{4}$$

where:

$V = (1-v_{12}v_{21}-v_{13}v_{31}-v_{23}v_{32}-v_{12}v_{23}v_{31}-v_{21}v_{13}v_{32}$
S – vector of the second Piola-Kirchhoff stresses,
E – Green-Lagrange strains vector,
v_{ij} – Poisson ratio in ij plane: $i, j = 1, 2, 3$.

Indices 1, 2, 3 denote: the cord direction, axis perpendicular to the cord lying in the plane of the ply, the vector product of the unit vectors of 1 and 2 axes, respectively. Because the calculations are performed in a (x, y, φ) coordinate system, a constitutive matrix (4) is subject to appropriate transformations (cf. PELC 2007). The effective material constants for single ply E_1, E_2, G_{12} and υ_{12} is calculated using the HALPIN-TSAI (1969) equations. In addition, $\upsilon_{ij}E_j = \upsilon_{ji}E_i$, and it was admitted for the calculations that $E_3 = E_2$, $\upsilon_{13} = \upsilon_{12}$, $G_{13} = G_{12}$ and $G_{23} = 2G_{12}$. The determination method of constants takes into account the variability of cord volume fraction in cord-rubber composite, which is a result of tire forming process. Originally cord-rubber layers are arranged on a cylindrical building drum, wherein the cord density in each green layer remains constant (PELC 2009).

It should be noted that such a composite material model can be used to deformation analyses of tires with low inflation pressure (up to 250 kPa). At higher pressures, the tire model becomes numerically unstable.

The assumption was made that the material of rubber elements is homogeneous and isotropic, and almost incompressible (Poisson ratio $\upsilon = 0.48$).

The tractor tire tread possesses a fairly regular pattern of lugs in the circumferential direction, but complex geometry in general. Having the shape of the raw tread profile (Fig. 4) it is possible to smear the tire tread lugs both in the circumferential and meridional directions. Comparing the volume of rubber corresponding to the elementary increments of the arc coordinate s in the raw and cured treads, an outer contour line of the smeared tread can be obtained. Incompressibility of rubber was assumed, and therefore the treads are of equal volume.

With the smearing of the tread lugs in the circumferential direction henceforth the tire inflation problem can be treated as rotationally symmetrical. It was also assumed that the plane xz is the plane of symmetry of the tire model. To solve the problem, the finite element method was used. Taking into account the stratified nature of the tire its cross-section model has been discretized (Fig. 4.)

In order to reduce the number of elements in the model each of two adjacent layers were connected, i.e. adjacent belt plies with the cord angles $+\theta$ and $-\theta$ were modeled with one finite element in ply thickness direction. The innerliner was incorporated into the composite material of carcass. In result three orthotropic materials ($+\theta$ and $-\theta$ belts, carcass+innerliner and carcass turnup) and four homogeneous isotropic materials were specified.

On the axis of symmetry of the tire model the y-displacements of the nodes were blocked, and the nodes being in contact with the rim were fixed.

Due to the existence of geometric nonlinearity in the problem (large displacements) FEM equilibrium equations were written in Total Lagrangian

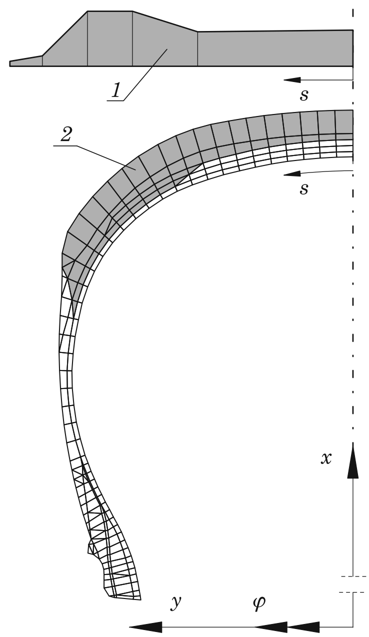

Fig. 4. Finite element mesh in reference tire configuration: *1* – raw tread profile, *2* – smeared tread profile of tractor tire

(TL) frame. (cf. PELC 2009). The nonlinear equilibrium path for the system was determined by modified Newton-Raphson method. To control the load increments, the modified constant arc length method suggested by CRISFIELD (1981) was utilized. The algorithm automatically increases the load increment if it is only possible due to the convergence rate of the iteration.

Results of simulation of tire inflation process

The tire model being in the initial configuration was loaded with an internal pressure equal to the nominal value p = 160 kPa. The procedure for automatic selection of load increment assured that in twelve steps the load has reached the final value. In each load step about three iterations have been performed.

The tire profile after deformation is shown in Figure 5. As a result of inflation the tire has increased both its width and diameter. It can be seen quite uniform displacements of the internal contour points of the tire toward the outside. This is the result of elongation of the carcass cords under the action of internal pressure.

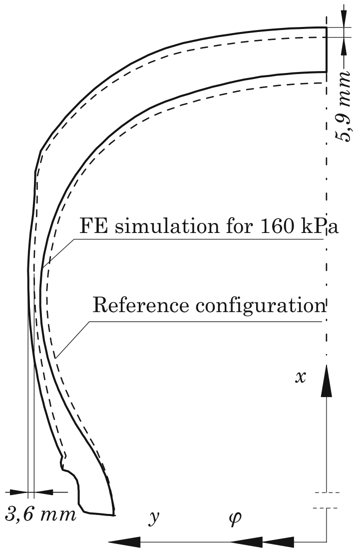

Fig. 5. Inflated tire profile

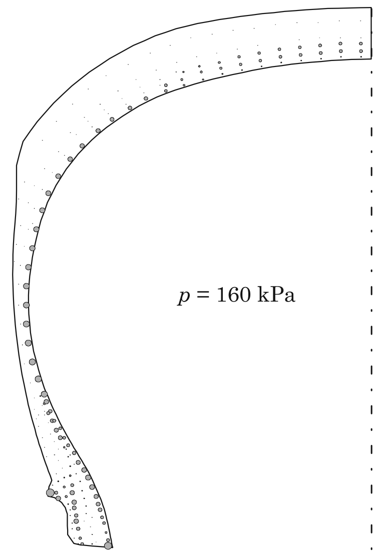

Fig. 6. Map of strain energy density in tire elements

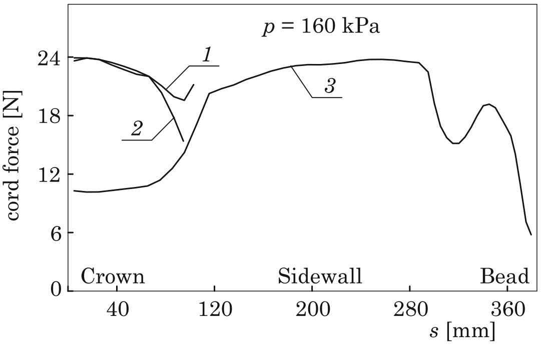

Fig. 7. Tensile forces in tire cords: *1* – 1st & 2nd belt, *2* – 3rd & 4th belt, *3* – carcass

The calculated increase in tire width is 7.2 mm and agrees well with the result of measurement equal to 7.2 mm. The measured increase in the tire diameter was 14.0 mm and the calculated – 11.8 mm and varies by 16%. The difference may be due to the fact that the smeared tread has greater circumferential stiffness than the tread built of lugs, and thus limits the radial displacements in tire.

Figure 6 shows the map of distribution of the elastic strain energy density within the inflated tire. The center points of circles are located in centroids of each finite element. Their diameters are proportional to the stored energy determined as the average of the sum of energies being occurred in Gauss

Points. It can be noticed high values of strain energy density in the layered materials, in particular within carcass ply below the largest width of the tire, also within the bead area as a result of the occurrence of considerable shear strains there.

Changes in cord forces of layered materials as a function of arc coordinate s running along the plies from the tire crown to the bead are shown in Figure 7. In the belt area the greater part of load is bearing by cords of belt plies. According to physics of the problem belt cord tensile force decreases towards the edges of the layer, because they ends are not stiffly fixed but embedded in a flexible rubber. The force does not fall to zero, as during the curing process the belts and the carcass plies are joined together with rubber. When the tensile force in the belt ply cord is decreasing the tensile force in the carcass cord is increasing, so that, within sidewall it is reaching twice the value occurred at the crown of the tire. Further, a local minimum can be seen resulting from the influence of the carcass layers turn-up. The existence of subsequent local maximum can be explained by the effect of cord-rubber layers bending around the edge of the rim. A further decline in the force value is due to increase in cord volume fraction of carcass and the impact of a rigid bead wires.

Conclusions

The proposed method of smearing of tractor tire tread lugs enables simulating of tire inflation by the use of axisymmetric model. Owing to this, obtained overall tire dimensions are in good agreement with the measurement results. This indicates a small influence of tread lugs on the overall shape of the inflated tire profile. Use of axisymmetric model in the tire inflation problem therefore has justification.

Finite element tire model makes it possible to determine the tensile force distribution between the carcass and the belt within belt zone of tire, which is not possible to achieve using the net tire model.

The simulation of pumping process results, especially information about the degree of effort of tire structural elements, can be utilized by designers of tires for their improvement.

References

BATHE K.J. 1982. *Finite element procedures in engineering analysis*. Prentice-Hall, Englewood Cliffs, N.Y.

BIDERMAN W.L. et al. 1967. *Atlas nomogramm rawnowesnych konfiguracii pnewmaticzeskih szin*. Chimija, Moscow.

CRISFIELD M.A. 1981. *A fast incremental/iterative solution procedure that handles "snapthrough"*. Computers and Structures, 13: 55–62.

DEESKINAZI J., RIDHA R.A. 1982. *Finite element analysis of giant earthmover tires*. Rubber Chemistry and Technology, 55(4): 1044–1054.

DUNN S.E., ZOROWSKI C.F. 1970. *A study of internal stresses in statically deformed pneumatic tires*. Office of Vehicle Systems Research Contract CST-376, U.S. National Bureau of Standards, Washington DC.

HALPIN J.C., TSAI S.W. 1969. *Effects of environmental factors on composite materials*. AFML-TR-67-423.

HEISE D.L. 1987. *Finite element modeling of tractor tire deformation*. MSc Thesis, Kansas State University.

NANKALI N., NAMJOO M., MALEKI M.R. 2012. *Stress analysis of tractor tire interacting with soil using 2D Finite Element Method*. Int. J. Advanced Design and Manufacturing Technology, 5(3): 107–111.

PĘKALAK M., RADKOWSKI S. 1989. *Rubber elastic elements*. PWN, Warszawa.

PELC J. 1992. *Large displacements in tire inflation problem*. Engineering Transactions, 40(1): 103–113.

PELC J. 2007. *Towards realistic simulation of deformations and stresses in pneumatic tyres*. Applied Mathematical Modelling, 31(3): 530–540.

PELC J. 2009. *Numerical aspects of a pneumatic tyre model analysis*. Technical Sciences. 12: 190–203.

PELC J., PETZ E. 1988. *Computer aid in inner tire profile design*. Polimery, 33(10): 381–383.

PELC J., PETZ E. 1994. *Pneumatic tyre designing by CAD/CAE technique*. Polimery, 39(11–12): 718–725.

SKOCZEK Z. 1995. *Tractor drive wheel tyres*. Auto – Technika Motoryzacyjna, 1: XIII–XV.

Guide for Autors

Introduction

Technical Sciences is a peer-reviewed research Journal published in English by the Publishing House of the University of Warmia and Mazury in Olsztyn (Poland). Journal is published continually since 1998. Until 2010 Journal was published as a yearbook, in 2011 and 2012 it was published semiyearly. From 2013, the Journal is published quarterly in the spring, summer, fall, and winter.

The Journal covers basic and applied researches in the field of engineering and the physical sciences that represent advances in understanding or modeling of the performance of technical and/or biological systems. The Journal covers most branches of engineering science including biosystems engineering, civil engineering, environmental engineering, food engineering, geodesy and cartography, information technology, mechanical engineering, materials science, production engineering etc.

Papers may report the results of experiments, theoretical analyses, design of machines and mechanization systems, processes or processing methods, new materials, new measurements methods or new ideas in information technology.

The submitted manuscripts should have clear science content in methodology, results and discussion. Appropriate scientific and statistically sound experimental designs must be included in methodology and statistics must be employed in analyzing data to discuss the impact of test variables. Moreover there should be clear evidence provided on how the given results advance the area of engineering science. Mere confirmation of existing published data is not acceptable. Manuscripts should present results of completed works.

There are three types of papers: a) research papers (full length articles); b) short communications; c) review papers.

The Journal is published in the printed and electronic version. The electronic version is published on the website ahead of printed version of Technical Sciences.

Technical Sciences does not charge submission or page fees.

Types of paper

The following articles are accepted for publication:

Reviews

Reviews should present a focused aspect on a topic of current interest in the area of biosystems engineering, civil engineering, environmental engineering, food engineering, geodesy and cartography, information technology, mechanical engineering, materials science, production engineering etc. They should include all major findings and bring together reports from a number of sources. These critical reviews should draw out comparisons and conflicts between work, and provide an overview of the 'state of the art'. They should give objective assessments of the topic by citing relevant published work, and not merely present the opinions of individual authors or summarize only work carried out by the authors or by those with whom the authors agree. Undue speculations should also be avoided. Reviews generally should not exceed 6,000 words.

Research Papers

Research Papers are reports of complete, scientifically sound, original research which contributes new knowledge to its field. Papers should not exceed 5,000 words, including figures and tables.

Short Communications

Short Communications are research papers constituting a concise description of a limited investigation. They should be completely documented, both by reference list, and description of the experimental procedures. Short Communications should not occupy more than 2,000 words, including figures and tables.

Letters to the Editor

Letters to the Editor should concern with issues raised by articles recently published in scientific journals or by recent developments in the engineering area.

Contact details for submission

The paper should be sent to the Editorial Office, as a Microsoft Word file, by e-mail: techsci@uwm.edu.pl

Referees

Author/authors should suggest, the names, addresses and e-mail addresses of at least three potential referees. The editor retains the sole right to decide whether or not the suggested reviewers are used.

Submission declaration

After final acceptance of the manuscript, the corresponding author should send to the Editorial Office the author's declaration. Submission of an article implies that the work has not been published previously (except in the form of an abstract or as part of a published lecture or academic thesis or as an electronic preprint), that it is not under consideration for publication elsewhere, that publication is approved by all authors and tacitly or explicitly by the responsible authorities where the work was carried out, and that, if accepted, it will not be published elsewhere in the same form, in English or in any other language.

To prevent cases of ghostwriting and guest authorship, the author/authors of manuscripts is/are obliged to: (i) disclose the input of each author to the text (specifying their affiliations and contributions, i.e. who is the author of the concept, assumptions, methods, protocol, etc. used during the preparation of the text); (ii) disclose information about the funding sources for the article, the contribution of research institutions, associations and other entities.

Language

Authors should prepare the full manuscript i.e. title, abstract and the main text in English (American or British usage is accepted). Polish version of the manuscript is not required.

The file type

Text should be prepared in a word processor and saved in doc or docx file (MS Office).

Article structure

Suggested structure of the manuscript is as follows:

Title
Authors and affiliations
Corresponding author
Abstract
Keywords
Introduction
Material and Methods
Results and Discussion
Conclusions

Acknowledgements (*optional*)
References
Tables
Figures

Subdivision – numbered sections

Text should be organized into clearly defined and numbered sections and subsections (optionally). Sections and subsections should be numbered as 1. 2. 3. then 1.1 1.2 1.3 (then 1.1.1, 1.1.2, ...). The abstract should not be included in numbering section. A brief heading may be given to any subsection. Each heading should appear on its own separate line. A single line should separate paragraphs. Indentation should be used in each paragraph.

Font guidelines are as follows:
- Title: 14 pt. Times New Roman, bold, centered, with caps
- Author names and affiliations:12 pt. Times New Roman, bold, centered, italic, two blank line above
- Abstract: 10 pt. Times New Roman, full justified, one and a half space. Abstract should begin with the word Abstract immediately following the title block with one blank line in between. The word Abstract: 10 pt. Times New Roman, centered, indentation should be used
- Section Headings: Not numbered, 12 pt. Times New Roman, bold, centered; one blank line above
- Section Sub-headings: Numbered, 12 pt. Times New Roman, bold, italic, centered; one blank line above
- Regular text: 12 pt. Times New Roman, one and a half space,full justified, indentation should be used in each paragraph

Title page information

The following information should be placed at the first page:

Title

Concise and informative. If possible, authors should not use abbreviations and formulae.

Authors and affiliations

Author/authors' names should be presented below the title. The authors' affiliation addresses (department or college; university or company; city, state and zip code, country) should be placed below the names. Authors with the same affiliation must be grouped together on the same line with affiliation information following in a single block. Authors should indicate all affiliations with a lower-case superscript letter immediately after the author's name and in front of the appropriate address.

Corresponding author

It should be clearly indicated who will handle correspondence at all stages of refereeing and publication, also post-publication process. The e-mail address should be provided (footer, first page). Contact details must be kept up to date by the corresponding author.

Abstract

The abstract should have up to 100-150 words in length. A concise abstract is required. The abstract should state briefly the aim of the research, the principal results and major conclusions. Abstract must be able to stand alone. Only abbreviations firmly established in the field may be eligible. Non-standard or uncommon abbreviations should be avoided, but if essential they must be defined at their first mention in the abstract itself.

Keywords

Immediately after the abstract, author/authors should provide a maximum of 6 keywords avoiding general, plural terms and multiple concepts (avoid, for example, 'and', 'of'). Author/authors should be sparing with abbreviations: only abbreviations firmly established in the field may be eligible.

Abbreviations

Author/authors should define abbreviations that are not standard in this field. Abbreviations must be defined at their first mention there. Author/authors should ensure consistency of abbreviations throughout the article.

Units

All units used in the paper should be consistent with the SI system of measurement. If other units are mentioned, author/authors should give their equivalent in SI.

Introduction

Literature sources should be appropriately selected and cited. A literature review should discuss published information in a particular subject area. Introduction should identify, describe and analyze related research that has already been done and summarize the state of art in the topic area. Author/authors should state clearly the objectives of the work and provide an adequate background.

Material and Methods

Author/authors should provide sufficient details to allow the work to be reproduced by other researchers. Methods already published should be indicated by a reference. A theory should extend, not repeat, the background to the article already dealt within the Introduction and lay the foundation for further work. Calculations should represent a practical development from a theoretical basis.

Results and Discussion

Results should be clear and concise. Discussion should explore the significance of the results of the work, not repeat them. A combined Results and Discussion section is often appropriate.

Conclusions

The main conclusions of the study may be presented in a Conclusions section, which may stand alone or form a subsection of a Results and Discussion section.

Acknowledgements

Author/authors should include acknowledgements in a separate section at the end of the manuscript before the references. Author/authors should not include them on the title page, as a footnote to the title or otherwise. Individuals who provided help during the research study should be listed in this section.

Artwork
General points

– Make sure you use uniform lettering and sizing of your original artwork
– Embed the used fonts if the application provides that option

– Aim to use the following fonts in your illustrations: Arial, Courier, Times New Roman, Symbol
– Number equations, tables and figures according to their sequence in the text
– Size the illustrations close to the desired dimensions of the printed version

Formats

If your electronic artwork is created in a Microsoft Office application (Word, PowerPoint, Excel) then please supply 'as is' in the native document format

Regardless of the application used other than Microsoft Office, when your electronic artwork is finalized, please 'Save as' or convert the images to one of the following formats (note the resolution requirements given below):

EPS (or PDF): Vector drawings, embed all used fonts

JPEG: Color or grayscale photographs (halftones), keep to a minimum of 300 dpi

JPEG: Bitmapped (pure black & white pixels) line drawings, keep to a minimum of 1000 dpi or combinations bitmapped line/half-tone (color or grayscale), keep to a minimum of 500 dpi

Please **do not**:
– Supply files that are optimized for screen use (e.g., GIF, BMP, PICT, WPG); these typically have a low number of pixels and limited set of colors
– Supply files that are too low in resolution
– Submit graphics that are disproportionately large for the content

Color artwork

Author/authors should make sure that artwork files are in an acceptable format (JPEG, EPS PDF, or MS Office files) and with the correct resolution. If, together with manuscript, author/authors submit color figures then Technical Sciences will ensure that these figures will appear in color on the web as well as in the printed version at no additional charge.

Tables, figures, and equations

Tables, figures, and equations/formulae should be identified and numbered consecutively in accordance with their appearance in the text.

Equations/mathematical and physical formulae should be presented in the main text, while tables and figures should be presented at the end of file (after References section). Mathematical and physical formulae should be presented in the MS Word formula editor.

All types of figures can be black/white or color. Author/authors should ensure that each figure is numbered and has a caption. A caption should be placed below the figure. Figure must be able to stand alone (explanation of all symbols and abbreviations used in figure is required). Units must be always included. It is noted that figure and table numbering should be independent.

Tables should be numbered consecutively in accordance with their appearance in the text. Table caption should be placed above the table. Footnotes to tables should be placed below the table body and indicated with superscript lowercase letters. Vertical rules should be avoided. Author/authors should ensure that the data presented in tables do not duplicate results described in figures, diagrams, schemes, etc. Table must be able to stand alone (explanation of all symbols and abbreviations used in table is required). Units must be always included. As above, figure and table numbering should be independent.

References

References: All publications cited in the text should be presented in a list of references following the text of the manuscript. The manuscript should be carefully checked to ensure that the spelling of authors' names and dates of publications are exactly the same in the text as in the reference list. Authors should ensure that each reference cited in the text is also present in the reference list (and vice versa).

Citations may be made directly (or parenthetically). All citations in the text should refer to:

1. Single author

The author's name (without initials, with caps, unless there is ambiguity) and the year of publication should appear in the text

2. Two authors

Both authors' names (without initials, with caps) and the year of publication should appear in the text

3. Three or more authors

First author's name followed by et al. and the year of publication should appear in the text

Groups of references should be listed first alphabetically, then chronologically.

Examples:

"... have been reported recently (ALLAN, 1996a, 1996b, 1999; ALLAN and JONES, 1995). KRAMER et al. (2000) have recently shown..."

The list of references should be arranged alphabetically by authors' names, then further sorted chronologically if necessary. More than once reference from the same author(s) in the same year must be identified by the letters "a", "b", "c" etc., placed after the year of publication.

References should be given in the following form:

KUMBHAR B.K., AGARVAL R.S., DAS K. 1981. *Thermal properties of fresh and frozen fish*. International Journal of Refrigeration, 4(3), 143–146.

MACHADO M.F., OLIVEIRA F.A.R., GEKAS V. 1997. *Modelling water uptake and soluble solids losses by puffed breakfast cereal immersed in water or milk*. In Proceedings of the Seventh International Congress on Engineering and Food, Brighton, UK.

NETER J., KUTNER M.H., NACHTSCHEIM C.J., WASSERMAN W. 1966. *Applied linear statistical models* (4th ed., pp. 1289–1293). Irwin, Chicago.

THOMSON F.M. 1984. *Storage of particulate solids*. In M. E. Fayed, L. Otten (Eds.), Handbook of Powder Science and Technology (pp. 365–463). Van Nostrand Reinhold, New York.

Citation of a reference as 'in press' implies that the item has been accepted for publication.

Note that the full names of Journals should appear in reference list.

Submission checklist

The following list will be useful during the final checking of an article prior to the submission. Before sending the manuscript to the Journal for review, author/authors should ensure that the following items are present:

– Text is prepared with a word processor and saved in DOC or DOCX file (MS Office). One author has been designated as the corresponding author with contact details: e-mail address

– Manuscript has been 'spell-checked' and 'grammar-checked'

– References are in the correct format for this Journal

– All references mentioned in the Reference list are cited in the text, and vice versa

– Author/authors does/do not supply files that are too low in resolution

– Author/authors does/do not submit graphics that are disproportionately large for the content